UCC
University College Cork, Ireland
Coláiste na hOllscoile Corcaigh
School of
Biological, Earth and
Environmental Sciences

Dr Chris Mays
School of Biological, Earth & Environmental Sciences
University College Cork
Distillery Fields, North Mall Campus
Cork T23 TK30, Ireland
cmays@ucc.ie
Ph.: +353 (0)85 761 9233

15th of October, 2024

RE: Submission of pre-print manuscript to *EarthArXiv*

To whom it may concern,

The following is a non-peer reviewed manuscript submitted for publication to the journal *Earth-Science Reviews*. The title of the manuscript is:

"**Measures of deep-time terrestrial net ecosystem productivity and carbon sink function**"

Please contact me if you have any further questions regarding the submission of this manuscript.

Yours sincerely,

Dr Chris Mays (corresponding author)

Measures of deep-time terrestrial net ecosystem productivity and carbon sink function

Chris Mays, Richard V. Tyson and Michael T. Hren

Abstract

Indicators of past biological productivity, or 'palaeoproductivity proxies', offer ways to indirectly measure Earth's deep-time ecosystem and carbon cycle functioning. Given that plants have been the principal primary producers on land for hundreds of millions of years, the abundances of fossil plants in the rock record can indicate past changes in net terrestrial ecosystem productivity (NTEP). This is the net carbon uptake or release by a terrestrial ecosystem, and a measure of whether the ecosystem is a carbon sink or source. When applied on a global scale, NTEP represents a major component of Earth's carbon cycle. Moreover, since plants are particularly sensitive to rapid climatic events, measuring NTEP with fossil plants should indicate how land carbon sinks are impacted by these climatic changes. Herein, we compare and contrast two proxies of NTEP changes in deep time: terrestrial organic microfossil concentrations (c_t) and terrestrial organic carbon (TrOC). However, the preservation pathways of terrestrial organic microfossils (hence, c_t and TrOC) are complex and poorly understood. In this review, we have: 1, summarized the factors that influence the preservation of land-derived organic carbon in the fossil record; 2, adapted and applied a framework of modern net ecosystem productivity (NEP) to prehistoric settings by incorporating post-burial effects; and 3, explored the conditions under which c_t and TrOC may provide valid estimates of relative changes in prehistoric NTEP. Lastly, we produce a roadmap towards refined proxy of deep-time NTEP, which would constrain biogeochemical models since the emergence of large land plants >360 million years ago.

Measures of deep-time terrestrial net ecosystem productivity and carbon sink function

Chris Mays[a,b,*], Richard V. Tyson[c] and Michael T. Hren[d]

[a] School of Biological, Earth & Environmental Sciences, Environmental Research Institute, University College Cork, Cork, T23 TK30, Ireland.

[b] Department of Geology and Palaeontology, Natural History Museum Vienna, Burgring 7, 1010 Vienna, Austria.

[c] School of Earth and Environment, University of Leeds, Woodhouse, Leeds LS2 9JT, United Kingdom.

[d] Department of Earth Sciences, University of Connecticut, Storrs, CT 06269, USA.

* Corresponding author at: School of Biological, Earth & Environmental Sciences, Environmental Research Institute, University College Cork, Cork, T23 TK30, Ireland. E-mail address: cmays@ucc.ie (C. Mays).

Keywords

Productivity, plant fossils, continental, palynology, concentrations, total organic carbon.

1. Introduction

Today, the rate of carbon sequestration on land and in the oceans is approximately equal (Canadell *et al.*, 2007), but terrestrial carbon sinks are far more susceptible to short-term disruptions to their efficiency (Friedlingstein *et al.*, 2022). The vast majority of net carbon sequestration in these land carbon sinks is the result of plant photosynthesis (Keenan & Williams, 2018). Hence, net carbon accumulation and burial on land tends to be highest in regions with dense vegetation, such as forests (Lorenz & Lal, 2010; Keenan & Williams, 2018) and peatlands (Loisel *et al.*, 2021). Since the emergence of large land plants in the Devonian Period (Maffre *et al.*, 2022), the relative contribution of terrestrial (vs marine) carbon sinks to the global carbon cycle was likely similar to today (Lenton *et al.*, 2018). Over long geological timeframes (e.g., 10^5–10^7 years), global changes in carbon burial rates have been largely driven by silicate weathering (Royer *et al.*, 2014; D'Antonio *et al.*, 2020) and associated carbonate deposition in the ocean (Planavsky *et al.*, 2022). While long-term climate trends and continental arrangements can cause broad changes in terrestrial biomass (Gurung *et al.*, 2022, 2024), biological events—like evolutionary innovations or climate-triggered ecosystem collapses—play the dominant role in changes in carbon burial rates on shorter intervals (Boyce *et al.*, 2023). Several biological innovations appear to have had major impacts on land productivity and burial, e.g., biosynthesis of the biopolymer lignin among plants (Niklas & Pratt, 1980, Weng & Chapple, 2010), fungal decomposition niches (Remy *et al.*, 1994, Nelsen *et al.*, 2016), or the emergence of trees (Algeo & Scheckler, 2010), flowering plants (Brodribb & Feild, 2010, Boyce & Zwieniecki, 2012; Zwieniecki & Boyce, 2014) and grasses (Strömberg, 2011, Linder *et al.*, 2018). Similarly, regional or global ecosystem changes can be expressed as dramatic changes in land plant productivity, such as anthropogenic (Mottl *et al.*, 2021) or climatic (Prentice *et al.*, 2011) deforestation, or the collapse of peat-forming ecosystems (Retallack *et al.*, 1996). Moreover, variations in land productivity are large contributors to the diversity of land faunas (e.g., Jetz & Fine, 2012; Myers *et al.*, 2012; Fritz *et al.*, 2016). Therefore, measuring fluctuations in continental carbon

burial, in the form of fossil primary producers, may serve as a proxy for net productivity and ecosystem function, particularly during key biological and climatic events. This, in turn, may improve the precision of biogeochemical climate models (e.g., Beerling, 2000; Berner, 2009; Lenton *et al.*, 2018) by constraining a principal component of Earth's deep-time carbon cycle since at least the Devonian Period.

Carbonate formation is relatively uncommon on the continents, compared to the oceans (Liu & Dreybrodt, 2015); hence, organic carbon (OC) constitutes almost the entirety of buried carbon in modern continental basins (Brett *et al.*, 2017; Drake *et al.*, 2018). Sedimentary OC concentrations are typically measured as total organic carbon (TOC). This has been used to inform prehistoric productivity (or 'palaeoproductivity'; e.g., Schwarzkopf, 1993; Tyson, 1995, 2001, 2005; Schoepfer *et al.*, 2015). TOC is measured from the organic residue following dissolution of a sample's non-organic mineral content, including inorganic carbon in the form of carbonate minerals (Schumacher, 2002). While additional geochemical proxies can provide constraints on palaeoproductivity, particularly for marine systems (Tribovillard *et al.*, 2006; Algeo *et al.*, 2013; Schoepfer *et al.*, 2015; Horner *et al.*, 2021; Lin *et al.*, 2024), TOC alone is incapable of determining carbon between organic carbon sources. This is particularly problematic during ecological disruptions, owing to the extreme fluctuations in abundances of different primary producers (e.g., microbial blooms, van de Schootbrugge & Gollner, 2013, Mays *et al.*, 2021; marine productivity collapse, Algeo *et al.*, 2013; deforestation, Vajda *et al.*, 2020; enhanced wildfire, Petersen & Lindström, 2012, Mays & McLoughlin, 2022, Zhang *et al.*, 2023).

1.1. Palaeoproductivity proxies

Although land plants constitute the vast majority of Earth's biomass (Bar-On *et al.*, 2018), and have an enormous impact on the global carbon cycle (Friedlingstein *et al.*, 2022), gauges of terrestrial palaeoproductivity are scarce (e.g., Wang *et al.*, 2023). Almost all

studies of palaeoproductivity have been conducted on marine systems. A variety of techniques have been employed to this end, including: 1, biomarker abundances (e.g., C_{37} alkenones: Bolton *et al.*, 2010; fatty acid $\delta^{13}C$: Ashley *et al.*, 2021); 2, TOC and inorganic geochemical proxies (e.g., Stein, 1986b; Felix, 2014; see review by Schoepfer *et al.*, 2015); 3, calcareous microfossil concentrations (e.g., nannofossils: Eshet & Almogi-Labin, 1996, Kinkel *et al.*, 2000); and 4, organic microfossil concentrations (e.g., dinoflagellate cysts: Zonneveld *et al.*, 2001, Reichart & Brinkhuis, 2003, Pearce *et al.*, 2009, Frieling *et al.*, 2018; algae or probable algal acritarchs: Head *et al.*, 1989; van Soelen & Kürschner, 2018; Lei *et al.*, 2019).

In contrast to the emphasis on palaeoproductivity from marine microfossil records, absolute organic microfossil abundances from continental records tend to focus on floristic population changes (Mander & Punyasena, 2018). Studies utilizing continental fossils (or subfossils) typically focus on pollen and plant spores (e.g., Bonny, 1972; Haberle & Maslin, 1999; Hardy & Wrenn, 2009; Mays *et al.*, 2020) or, less commonly, fungal spores (e.g., Etienne & Jouffroy-Bapicot, 2014; Perrotti *et al.*, 2022) or non-marine algal cysts/acritarchs (e.g., Head, 1992; Bonis *et al.*, 2010; Gravendyck *et al.*, 2020; Mays *et al.*, 2021). The abundance changes in these fossils can provide precise records of palaeoclimate changes, especially in Quaternary assemblages where the climate tolerances of fossil organisms can be directly inferred from their extant counterparts (Chevalier *et al.*, 2020). When applied to continental successions, concentrations of terrestrial microfossils (here defined as the microscopic organic remains of past terrestrial organisms, whether fragmentary or whole) have been used to constrain local palaeoenvironmental conditions (e.g., Goldring *et al.*, 1999). To our knowledge, no study has yet utilized the concentrations of terrestrial organic microfossils to infer the net terrestrial ecosystem productivity of the past.

The purpose of this review is three-fold. Firstly, we critically assess our present state of knowledge regarding the primary pre- and post-burial influences on terrestrial organic matter in the geosphere. Secondly, we employ a simple and commonly used framework of modern

net ecosystem productivity (NEP; = the amount of post-respiration carbon in an ecosystem), and consider how each of the key parameters might be accounted for to estimate trends in NEP of deep-time terrestrial ecosystems. Thirdly, we compare the utility of three potential metrics of ancient terrestrial productivity: 1, total organic carbon (TOC); 2, terrestrial organic microfossil concentrations (c_t, *sensu* Mays *et al.*, *pre-print*); and 3, the fossil-based 'terrestrial organic carbon' (TrOC).

We predict that c_t and TrOC should provide a more accurate gauge of terrestrial productivity than TOC, in large part because these metrics can identify the specific contributors of buried organic carbon. If validated, we argue that time-series of c_t and/or TrOC may therefore: 1, quantify relative (if not absolute) changes in net ecosystem productivity of the past; 2, determine the contributions of specific organism groups (e.g., plants vs other terrestrial primary producers) to past NEP; 3, constrain total carbon flux estimates in carbonate-poor continental successions; 4, detect and quantify changes in terrestrial organic matter export (when applied in marine systems); and 5, test hypotheses about past ecosystem community dynamics (e.g., co-occurrence vs competition).

1.2. Net terrestrial ecosystem productivity (NTEP) in Earth's history

1.2.1. Conceptual framework

Net ecosystem productivity (NEP) represents the net carbon gain or loss mediated through an ecosystem in a given timeframe (Chapin *et al.*, 2006). If the ecosystem is functioning as a carbon sink, NEP will be positive and is the amount of carbon stored in an ecosystem after accounting for all respiratory losses. In the most widely accepted form, it is calculated simply as the total amount of carbon assimilated via photosynthesis (gross primary productivity; GPP) minus the carbon released through respiration of all organisms within the ecosystem (total ecosystem respiration, TER; Woodwell & Whittaker, 1968; Keenan & Williams, 2018).

Here, we adopt the framework for calculating NEP proposed by Lovett et al. (2006; see review by Pace & Lovett, 2021):

$$NEP = GPP - TER = \Delta C_{org} + Ox_{nb} + E - I \quad (1)$$

where I is the imported (=allochthonous) organic carbon, E is the export of organic carbon, and Ox_{nb} is the non-biological oxidation of organic carbon (expelled as inorganic carbon, primarily CO_2). All terms above (excepting ΔC_{org}) are discussed at length in the context of prehistoric microfossil assemblages in their relevant sections below.

The term ΔC_{org} represents the change in organic carbon storage in the ecosystem. When this framework is applied to (pre)historic estimates of palaeoproductivity, we are typically examining time-averaged samples from past ecosystems that: 1, are isolated 'snapshots' in time; or 2, comprise a series of isolated, discontinuous data to build broad temporal trends. Hence, rather than estimating continuous changes in carbon in- and outputs over time, this factor would be better expressed as instantaneous carbon content when applied to ancient ecosystems; hence, TOC (total organic carbon) rather than ΔC_{org}. Eqn 1 can then be transposed as:

$$TOC = NEP - Ox_{nb} - E + I \quad (2)$$

Within the above formulation, TOC is the sum of NEP (i.e., post-respiration GPP) and the non-respired carbon in- and outputs for a given ecosystem. Accurate estimates of organic microfossil concentration (c) and TOC can be measured from strata, both of which are measured per unit weight of dried sediment or sedimentary rock (wt%). The use of fossil concentrations or TOC in this context requires that sedimentation rates should be measured and/or held consistent between samples; the methods and assumptions of this approach are explored further in see Section 3.1.6 and Table 1.

Following Eqn 2, NEP might be inferred from a potential proxy only if the sum of other factors is negligible ($Ox_{nb} + E + I \approx 0$) or if these can be accurately calculated. Here, we

define net terrestrial ecosystem productivity (NTEP) simply as the NEP of a terrestrial ecosystem.

NEP contributes to the two forms organic carbon in the hydrosphere and geosphere: particulate organic carbon (POC) and dissolved organic carbon (DOC). The difference between these is based solely on organic matter size, whereby DOC includes the carbon of all organic matter below a certain mesh size (typically 0.22–0.7 μm), and POC is the carbon of all organic matter larger than this (Kolka *et al.*, 2008; Repeta, 2015). Collectively, these constitute an ecosystem's TOC (= DOC + POC). Terrestrial ecosystem-derived DOC comprises a complex mixture of organic compounds dissolved in rivers, lakes and groundwater (Perdue & Ritchie, 2003), and represents a major carbon reservoir on modern continents (Hedges, 1992; Cole & Caraco, 2001). The majority (c. 70%) of exported total organic carbon in global catchments today is in the form of DOC (Alvarez-Cobelas *et al.*, 2012; Raymond & Spencer, 2015) and DOC is approximately equivalent to POC in global riverine carbon flux (Li *et al.*, 2017). However, owing to the high lability and reactivity of DOC, >40% of DOC in modern catchments is 'lost' within one year (Cole *et al.*, 2007; Moody & Worrall, 2017). This loss of terrestrial DOC is largely due to mineralisation (oxidation) by photochemical processes (Massicotte & Frenette, 2011; see sections 1.2.5 and 3.2.4) or respiration (Cole *et al.*, 2006), the latter of which can occur very rapidly (Demars, 2019). Subsequently, DOC seems to contribute a negligible amount of TOC to the rock record, where the vast majority (c. 95%) of TOC is in the form of solid, fossil-derived, insoluble 'kerogen' (Hunt, 1972; Vandenbroucke & Largeau, 2007). At present, there is no direct, empirical means of estimating absolute abundances of prehistoric, ecosystem-derived DOC from the continental rock record. Moreover, metrics derived from a sediment or sedimentary rock—such as c and TOC—represent only tiny portions of the productivity of entire prehistoric ecosystems. Hence, c and TOC will always provide underestimates of NEP.

With these limitations in mind, an alternative use for c or TOC is for inferring relative (rather than absolute) changes in NEP over time. For this, the values of carbon export,

import and oxidation should be accurately estimated, or held constant (if not eliminated), across a time-series of deep-time samples. For palaeoproductivity estimates using TOC, we have identified the primary contributors to NEP (Eqn 1) to reformulate the calculation of TOC (Eqn 2) as follows:

$$TOC = NEP - (Ox_{Ph} + Ox_{Py} + Ox_{T}) - (E_{DOC} + E_{POC} + E_{EOC}) + (I_{POC} + I_{EOC}) \quad (3)$$

where Ox_{Ph} is the amount of photo-oxidised carbon (via photodegradation); Ox_{Py} is the amount of pyrogenically oxidised carbon (via fires); Ox_{T} is the amount of thermogenically oxidised carbon (via thermal maturation); E_{DOC} is the amount of exported dissolved organic carbon (DOC); E_{POC} is the amount of exported particulate organic carbon (POC), which—when from the continents—is primarily in the form of plant debris; E_{EOC} is the amount of exported extractable organic carbon (EOC) in the form of soluble hydrocarbons (e.g., oil and natural gas), or insoluble solid bitumen; I_{POC} is the amount of imported particulate organic carbon (POC); and I_{EOC} is the amount of imported EOC. By discussing each of the terms that contribute to this formulation of TOC (Figs 1 & 2), and the relationship between TOC and terrestrial organic microfossil concentrations (c_t), we explore how this framework might apply to the fossil record for inferring relative changes in NTEP in Earth's past.

<INSERT FIG. 1>

1.2.2. Respiration of terrestrial organic matter

The first major barrier to long-term organic carbon burial is respiration. Following Eqn 1, net ecosystem productivity (NEP) is calculated as the gross primary productivity (GPP) minus total ecosystem respiration (TER); this latter term is the sum of respiration by two broad organism groups differentiated by their metabolism: autotrophic respiration (R_a) primarily by plants, algae and photosynthetic bacteria (i.e., the supporting energy costs of the autotrophs), and heterotrophic respiration (R_h) by their consumers or decomposers (Keenan & Williams, 2018). After autotrophic respiration, the majority of organic carbon in a terrestrial

ecosystem is respired by fungi, animals and microbes (Xu & Shang, 2016), even in areas with high potential for large, long-term carbon storage (e.g., peats; Clymo, 1984; Kuhry & Vitt, 1996). This causes differential degradation between types of organic matter (Zonneveld *et al.*, 1997; Versteegh & Zonneveld, 2002, Versteegh *et al.*, 2010). The terrestrial biomass that survives respiration, therefore, consists almost entirely of durable substances, like chitin and its derivatives (Graham *et al.*, 2017; Nuñez Otaño *et al.*, 2021), and plant biopolymers: lignin (the primary structural component of wood; Hatcher & Clifford, 1997; Prescott, 2010), cutan and/or cutin (waxy components of leaf tissues; Gupta *et al.*, 2006) and sporopollenin (found in the outer walls of plant spores and pollen; Li *et al.*, 2019). While many of these appear to be less recalcitrant in soils than previously thought (e.g., lignin; Klotzbücher *et al.*, 2011; Schmidt *et al.*, 2011), all of the organic microfossil categories that comprise c_t are principally composed of these relatively durable constituents (Baldock *et al.*, 2004; Feng *et al.*, 2008). Hence, prehistoric accumulations of these terrestrial fossils on the continents (e.g., organic-rich lake/river sediments, coal measures) represent areas in which, or near where, long-term (gross) primary productivity was necessarily greater than ecosystem respiration; hence, positive NTEP.

These durable plant- and fungus-derived components, and their associated organic microfossils, have deep evolutionary roots. Plant lignin first emerged in the Silurian (Niklas & Pratt, 1980; Weng & Chapple, 2010), chitin-like fungal remains in the late Ordovician–early Silurian (Taylor *et al.*, 2015, and references therein), plant cuticles in the late Ordovician–Silurian (Wellman & Ball, 2021, and references therein) and sporopollenin in the Ordovician (Wellman *et al.*, 2023, and references therein). Hence, all primary constituents of terrestrial organic microfossil assemblages had evolved by the Early Devonian (c. 420 Ma). Moreover, the Devonian Period marks the earliest records of the primary constituents of terrestrial GPP (arborescent plants; Algeo & Scheckler, 2010; Weng & Chapple, 2010) and terrestrial TER. For instance, mycorrhizal and saprotrophic fungi are major contributors to modern terrestrial ecosystem respiration (Cooke & Rayner, 1984; Frey, 2019; Han *et al.*, 2021), and both of

these fungal niches have been agents of terrestrial biomass decay (*sensu* Zak *et al.*, 2019) and therefore, TER, since at least the Late Devonian (c. 360 Ma; Remy *et al.*, 1994; Nelsen *et al.*, 2016). Relatively consistent primary biomass producers and consumers/decomposers (and their fossil counterparts) suggest that fossil-based metrics, such as c_t or TrOC, should be useful for detecting trends in net ecosystem productivity throughout most of the Phanerozoic.

Very little organic carbon is preserved in forest soils over the long term (Richter *et al.*, 1999; Shi *et al.*, 2020). Instead, most terrestrial organic fossil assemblages can be found in aquatic palaeoenvironments (e.g., lakes, rivers, deltas, nearshore marine areas). These are regions where the efficiency of long-term organic carbon burial is higher (Middelburg, 1989; Hartnett *et al.*, 1998; Hedges *et al.*, 1999). This is considered largely owing to the increased rate of respiration by animals and aerobic microbes—principal agents of organic carbon mineralisation in aquatic systems (primarily into CO_2; Burdige, 2005)—in soils, while anaerobic metabolism of organic carbon typically occurs at a slower rate (Canfield, 1994). Once buried, the key role seems to be the duration of O_2 exposure (e.g., Hartnett *et al.*, 1998, Sobek *et al.*, 2009), the primary controls of which are: 1, the O_2 penetration depth in the sediment (Meyers, 1997; Keiluweit *et al.*, 2016; i.e., thickness of the “oxic layer”); and 2, sediment burial rate (Middelburg *et al.*, 1993; Katsev & Crowe, 2015). However, the long-term degradation rate in marine sediments is a function of carbon age, independent of oxygen availability (Rothman, 2024). Another key factor is composition, whereby organic compounds are oxidized in relation to their reactivity (e.g., Arndt *et al.*, 2013; Rothman, 2024). Early estimates of carbon ‘burial (or transfer) efficiency’ (= the percentage of organic carbon deposited in a basin that becomes buried to a specified depth; Bradley *et al.*, 2022) in marine settings were c. 20% (Berner, 1982). However, the complexity of ocean systems have revealed major heterogeneities in organic matter degradation and carbon burial rates across the world (Arndt *et al.*, 2013; Bianchi *et al.*, 2018; LaRowe *et al.*, 2020; Jørgensen *et al.*, 2022). Contributing to these uncertainties are changes in aquatic settings that can

deepen the sediment oxic layer, leading to a ‘burn-down’ effect in previously carbonaceous sediments (Jung *et al.*, 1997; Kodrans-Nsiah *et al.*, 2009), reducing the preserved TOC by up to c. 90% in deep marine conditions (Prahl *et al.*, 2003). Moreover, recent investigations of the microbial ‘deep biosphere’ have revealed that this respiration can continue at great depths in the crust (up to c. 2.4 km, Fang *et al.*, 2017; see review by Colwell & D'Hondt, 2013), albeit at much slower rates than aquatic or oxic sediment respiration (Price & Sowers, 2004) which are characterized by younger and more labile carbon pools.

On the continents, the rates and degrees of organic carbon respiration tend to be greater than in the oceans, but highly variable (Catalán *et al.*, 2016). In most lakes, the upper layer of sediment on the lake floor tends to be oxic, promoted by animal bioturbation which can reduce the long-term storage of TOC to c. 10–20%, and POC to c. 35% (Thomsen *et al.*, 2004; Li *et al.*, 2012). However, burial efficiency is much higher for eutrophic lakes (e.g., >60%; Radbourne *et al.*, 2017) or those with higher terrestrial matter influx (e.g., c. 45–80%; Sobek *et al.*, 2009; Gudasz *et al.*, 2017). Moreover, terrestrial organic matter appears to be more likely buried in lakes than autochthonous (lake-derived) organic matter (Gudasz *et al.*, 2012; Guillemette *et al.*, 2017). While burial rates on river floodplains are typically much faster than lakes, these deposits suffer from greater durations of oxidation during temporary storage in floodplain deposits (Scheingross *et al.*, 2019; Repasch *et al.*, 2021). As such, the long-term burial efficiencies of POC in river floodplains are typically 20–50% (Scheingross *et al.*, 2021). With these losses of terrestrial organic carbon during the burial phase in continental settings, we should expect to see disproportionate abundances of organic remains that are resistant to decay by microbes (e.g., lignin-rich and lipid-poor fossils; Meyers *et al.*, 1995; Prescott, 2010) preserved in the fossil record.

The anatomy of fossil plants can provide independent clues to deep-time terrestrial plant productivity estimates. Since these fossils are the remains of plants following respiration (R_a), such anatomy-based productivity estimates are most closely linked to net primary productivity (= post-autotrophic respiration productivity, or $NPP = GPP - R_a$). Several plant

functional traits that are preservable in fossils have demonstrable potential to constrain past NPP, including leaf vein density (Brodribb *et al.*, 2007; Boyce *et al.*, 2009; Zwieniecki & Boyce, 2014; Westbrook & McAdam, 2021) and leaf mass per area (Poorter & Bongers, 2006; Poorter *et al.*, 2009); see the recent review by McElwain *et al.* (2024). While these proxies provide evidence of carbon assimilation rates by land plants (Boyce & Zwieniecki, 2019), they say nothing about heterotrophic respiration. Moreover, they are incapable of providing direct estimates of NTEP, since they endeavour to answer different but related questions. However, we predict that fossil plant anatomy-based productivity could provide a crucial complement to proxies of NTEP; following Eqn 1, fossil-based NTEP estimates could, in principle, be subtracted from the plant anatomy-based NPP estimates to gauge terrestrial heterotrophic respiration.

<INSERT FIG. 2>

1.2.3. Pre-burial exported organic carbon (E_{DOC}, E_{POC})

A full accounting of NTEP must include organic carbon that has been exported from the terrestrial ecosystem (term 'E' in Eqns 1–3). Exported organic carbon comprises three factors: E_{DOC} and E_{POC} pertain to pre-burial processes and will be discussed in this section, while E_{EOC} is considered in Section 1.2.6. In rare cases, the *in situ* remains of terrestrial ecosystems can be found in the form of prehistoric soils (or 'palaeosols'; Tabor & Myers, 2015). Such soils provide not only indications of aboveground terrestrial biomass (e.g., Williams *et al.*, 2003; Miller *et al.*, 2016) but also belowground biomass, the latter of which can be greater in some terrestrial ecosystems (e.g., tundra, grasslands; see Robinson, 2007). Palaeosols can be sites of major peat deposits (Retallack, 2001). Modern peats are the principal land carbon sinks and, thus, are areas where overall NTEP has been necessarily greater than the sum of respiration, non-biological oxidation and export (Worrall *et al.*, 2003, 2009; Worrall & Evans, 2008). It is far more common, however, to find terrestrial

organic microfossil assemblages that have undergone a degree of transport into aquatic conditions, owing to their preferential preservation in water (Traverse, 2007). In such cases, entire assemblages of terrestrial organic remains have been exported from their original ecosystems, precluding clear inferences of productivity from many specific past environments.

A pragmatic approach is to broaden the 'ecosystem' to encompass the terrestrial biota of the entire drainage basin area, comprising a variety of coeval environments and associated biotas (Fig. 2). Given that most soils at any given time in Earth's history will not be preserved and are regularly subjected to physical erosion, these dispersed assemblages likely represent a mix of both above- and belowground biomass. Studies of Quaternary continental basins have shown that the microfossil assemblages derived from rivers (Moss *et al.*, 2005), lakes (Hjelle & Sugita, 2011) and upper deltas (Hardy & Wrenn, 2009; Gastaldo, 2012; Pandey & Holt, 2018) are remarkably representative of the proportions of plants in the drainage basin, but with a bias towards riverine/riparian taxa. Models of modern pollen dispersal (e.g., Sugita, 2007; Broström *et al.*, 2008; Theuerkauf *et al.*, 2016) provide an increasingly accurate means to reconstruct past floristics, vegetation cover and distributions. These are constrained by parameters that are testable by comparison to extant taxa—e.g., pollen productivity and dispersal range—but such parameters are rarely available from the fossil record, particularly for pre-Quaternary assemblages. Hence, there is little control on expected pollen abundances between plant groups for deep-time assemblages.

A path forward lies on relying less on specific fossil types, and more on the full suite of terrestrial biomass (plant spores, pollen, fungi, leaves, wood, and other terrestrial organic debris). Because these tend to behave as sedimentary clasts in a basin, their dispersal is almost entirely driven by gravity and fluid dynamics (e.g., Fall, 1987; Tyson, 1995; Batten, 1996; Martín-Closas *et al.*, 2005). The contributions of grains that do not behave clastically (e.g., zoochorous pollen) will tend to be overwhelmed by the rest of the assemblage. Moreover, these total terrestrial assemblages represent the majority of organic matter in

continental deposits (Tyson, 1995) and, as fossilised terrestrial POC, are representative of a major component of past NTEP (Li *et al.*, 2017). Hence, the concentrations of total terrestrial organic microfossil assemblages (c_t) can be considered parautochthonous (=regionally sourced) and may provide valid approximations of relative terrestrial productivity for a given drainage basin.

If we utilise the broader, drainage basin-scale perspective outlined above, then terrestrial ecosystem export is equivalent to the terrestrial carbon, both dissolved and particulate (E_{DOC} and E_{POC}, respectively), that ends up in contemporaneous marine basins. While photodegradation of plant matter contributes to E_{DOC} (see sections 1.2.5 and 3.2.4) terrestrial DOC is extremely labile (Cole *et al.*, 2006; Massicotte & Frenette, 2011; Demars, 2019) and, as noted above, seems to contribute very little to long-term sedimentary TOC. Another potential driver of organic carbon export is wildfire. While there is increasing evidence of wildfires as a vehicle of long-distance dispersal of (non-mineralised) organic matter, particularly during ‘megafire’ events (Tang *et al.*, 2021), the abundances of this ‘pyrogenic’ exported organic matter are not well constrained (Clark *et al.*, 1998; Santín *et al.*, 2015). In contrast, it is clear that the vast majority of exported organic carbon is via river and delta transport, which can result in enormous terrestrial organic matter deposits in marine, primarily nearshore, environments (Schlünz & Schneider, 2000; Hage *et al.*, 2022). These can be larger than *in situ* marine organic matter (up to 70–80% of total buried organic matter in deltas; Burdige, 2007; Blair & Aller, 2012). As a measure of exported particulate organic carbon (E_{POC}), fossil plant debris concentrations in nearshore marine environments have successfully provided measures of cyclic environmental changes by estimating shoreline migrations (Waterhouse, 1995, 1999; Ruf *et al.*, 2005; Pross *et al.*, 2006). Owing to the considerable sorting, winnowing and recycling during pre-burial transport (Gastaldo, 2012), such marine deposits are unlikely to provide valid estimates of terrestrial palaeoproductivity. However, we argue that they can provide a gauge of relative, if not absolute, E_{POC}.

A supplementary approach for accurate organic carbon export estimates in deep-time contexts are biogeochemical models based on modern analogue basins. Studies of modern basin carbon cycling demonstrate the key role that regional tectonism/magmatism (e.g., France-Lanord & Derry, 1997; Blair & Aller, 2012) plays in determining carbon cycle functioning, including organic carbon export (see review by Hilton & West, 2020). For instance, tectonically active regions tend to export a greater proportion of continental organic carbon to the oceans than passive margin basins (see Blair & Aller, 2012 and references therein). The stratigraphic and sedimentologic records provide a wealth of data on regional tectonic and magmatic influence, which can inform basin-wide carbon cycle models. Sedimentological characters, combined with relative abundances of organic microfossil components (Duringer & Doubinger, 1985; Tyson, 1995), can help determine distance and direction from a source of terrestrial organic remains. In ideal cases, where contiguous prehistoric continental and marine basins are preserved, lateral transects of c_t and/or TrOC should be estimated, greatly constraining gradients of E_{POC}.

Not only will more accurate estimates of terrestrial organic carbon export provide a more comprehensive picture of prehistoric NTEP, but will reveal export fluctuations in Earth's past. Changes in terrestrial organic carbon export can be driven by changes in regional topography (Anell *et al.*, 2009), and have been triggered by global biotic crises events. This has been indicated by enhanced soil run-off during mass extinctions events, such as the Frasnian–Famennian (Kaiho *et al.*, 2013), end-Devonian (Smart *et al.*, 2023), end-Permian (Algeo & Twitchett, 2010; Algeo *et al.*, 2013; Shen *et al.*, 2015; van Soelen *et al.*, 2018) and end-Triassic (Steinthorsdottir *et al.*, 2012; van de Schootbrugge *et al.*, 2020). Such events would be prime targets for terrestrial palaeoproductivity proxies.

1.2.4. Organic carbon import (I_{POC} and I_{EOC})

For valid estimates of NEP, allochthonous carbon that contributes to the examined buried organic carbon ('I' in Eqns 1–3) needs to be excluded. This includes both pre-burial (imported particulate organic carbon, I_{POC}) and post-burial (imported extractable organic carbon, I_{EOC}) sources. For many microfossil-bearing *in situ* terrestrial sites, such as prehistoric organic soils or peat deposits, import of exogenous carbon was likely a minor component relative to copious amounts of particulate and dissolved organic carbon export (Worrall *et al.*, 2009; Alvarez-Cobelas *et al.*, 2012; Moody & Worrall, 2017). However, the most common terrestrial biomass accumulations found in the continental records are deposited in lakes, rivers or deltas, where terrestrial microfossils are necessarily considered imported organic carbon. In these contexts, *in situ* (aquatic) microfossil absolute abundances can serve as a proxy for aquatic TOC while the imported (terrestrial) microfossil concentrations can indicate the imported carbon. Conversely, as noted above (see Section 1.2.3), we recommend that the terrestrial microfossil assemblages in these prehistoric waterbodies can be utilised as representing the terrestrial ecosystem in the drainage basin. Hence, changes in c_t from continental waterbodies should reflect changes in buried organic matter from the regional terrestrial ecosystem.

In our expanded drainage basin-scale terrestrial ecosystem, the sole source of imported organic carbon comes from the exposure and erosion of 'old' carbon within the basement rock (or petrogenic organic carbon, OC_{petro}). The contribution of OC_{petro} to a basin's TOC can be substantial, and a principal determinant of imported OC_{petro} is the exposure of hydrocarbon-rich rocks in the region (Blattmann, 2022). For basins in or near active tectonic regions, recycled particulate OC_{petro} (= I_{POC} herein) can comprise a major proportion of TOC (e.g., 30–40% in the Waipaoa watershed, New Zealand; Blair *et al.*, 2010). Although this rate is much lower for passive margin drainage basins (e.g., <15% for the lower Amazon Basin; Bouchez *et al.*, 2010), I_{POC} is considered relatively non-reactive, so it tends to accumulate in continental sediments for extensive durations (Blair & Aller, 2012; Kalks *et al.*, 2021). In contrast, drainage basins in volcanic regions (e.g., 'hotspot' islands) have negligible

basement-hosted organic carbon (Lloret *et al.*, 2013; see review by Hilton & West, 2020). Given this variability in imported OC_{petro}, determining the tectonic and/or magmatic contexts of a basin will assist in constraining past NTEP estimates.

A wide array of methods can be utilized to quantify the proportions of recycled (basement-derived, i.e., OC_{petro}) and contemporaneous (ecosystem-derived) organic carbon in a sediment, such as isotopic (e.g., $\delta^{13}C$, radiocarbon), geochemical (e.g., Rock-Eval pyrolysis) or optical (see below) analyses. These methods have been most successful for Quaternary samples, where the relative ages and thermal maturity of OC sources can be easily distinguished (e.g., Graz *et al.*, 2011; Kalks *et al.*, 2021 and references therein). A key strength of organic microfossil assemblages as potential palaeoproductivity proxies is that they can be used to quantify recycled organic matter (hence, I_{POC}). Fossil palynomorphs (e.g., spores, pollen, algae/acritarchs) can enter the continental carbon cycle by erosion of exposed basement rocks, where they are treated as petrogenic POC (Blattmann *et al.*, 2018). The abundances of these ‘reworked’ or ‘exogenous’ palynomorphs can be extreme (up to 95% of a palynomorph assemblage; Lopes *et al.*, 2014). Since a similar degree of reworking is likely reflected for the whole organic microfossil assemblage, it can be essential to quantify the abundances of reworked palynomorphs for accurate palaeoproductivity estimates. Fortunately, there are several ways to discern reworked palynomorphs from *in situ* or ‘indigenous’ microfossils (i.e., those contemporaneous with deposition; Fig. 3), including discrepancies in their: 1, thermally induced colours (Combaz, 1980; Batten, 1981; Yule *et al.*, 1998; Strother *et al.*, 2017); 2, autofluorescence responses (Phillips, 1972; Waterhouse, 1998; Strother et al., 2017); 3, degrees of morphological degradation (Neves & Sullivan, 1964; Elsik, 1966; Wilmshurst & McGlone, 2005); 4, susceptibilities to staining (Stanley, 1965); 5, taxon age ranges (e.g., Mildenhall, 1994; Mays & Stilwell, 2013; van de Schootbrugge *et al.*, 2020; see review by Batten, 1991); and 6, palaeoenvironmental affinities (e.g., marine fossils in continental deposits; Lopes *et al.*, 2014). The identification of reworked palynomorphs has been utilised for detecting regional tectonic uplift (e.g., Streel &

Bless, 1980; Lopes *et al.*, 2014) and intervals of enhanced continental run-off (e.g., van de Schootbrugge *et al.*, 2020).

In water or air, palynomorphs act as other sedimentary clasts (Traverse & Ginsburg, 1966; Holmes, 1994). Although there is a greater degree of sorting between different organic matter grains with increasing transport distance—especially when transported into marine conditions (Shepard, 1956; Boulter & Riddick, 1986)—they tend to behave similarly to other terrestrial particulate organic matter of similar size (see review by Tyson, 1995). Hence, we argue that recycled palynomorphs can provide a gauge of the relative contribution of imported particulate organic matter. A key assumption in this argument is that the abundance ratios of exogenous-to-indigenous non-palynomorph microfossils (e.g., wood fragments) are similar to those for the palynomorphs. To test this, maturation measurements of other microfossils (e.g., vitrinite reflectance of fossil wood; see sections 1.2.6 and 3.2.5) would provide additional support for the proportions of *in situ* vs reworked organic matter. I_{POC} values can then be inferred from these reworked microfossil concentrations by estimating their carbon concentrations; this can be achieved by utilising reasonable concentrations from modern analogues and experimentally matured terrestrial organic matter (see Section 3.1 and Table 1). Finally, the resulting I_{POC} values can then be subtracted from TOC, terrestrial OC (TrOC) or c_t, thus generating more accurate values of prehistoric NTEP. While reworked palynomorphs have long been considered a problem to solve (Johnson & Thomas, 1884; Iversen, 1936), they present a solution for more accurate palaeoproductivity estimates.

An additional source of allochthonous organic carbon that needs to be accounted for is imported extractable organic carbon (I_{EOC}), typically occurring as oil, bitumen or gas. Based on the stage during which they contribute to the TOC of a sediment or sedimentary rock, two types of EOC can be differentiated: 1, syn-burial EOC; and 2, post-burial EOC. Syn-burial EOC is incorporated into a sediment from surface exposure of hydrocarbon-rich rocks in the region (Wang *et al.*, 2001; Feng *et al.*, 2021). However, the contribution of syn-burial EOC to the TOC of continental basins is likely minimal owing to the instability of these hydrocarbons

at the Earth's surface (Blattmann, 2022). In contrast, the contribution of post-burial EOC to a sedimentary rock can be substantial; our modern civilisation largely depends on this fact. Owing to the propensity of liquid or gaseous hydrocarbons—petroleum or natural gas—to migrate through rock, continental rocks may serve as reservoirs of mobile hydrocarbons (Hunt, 1996). While these exogenous hydrocarbons can be a major source of a rock's TOC, particularly for porous, reservoir strata (Steiner *et al.*, 2016), they typically comprise <1% of the TOC within a fine-grained sedimentary rock (Jarvie, 1991). For this reason, among several others, fine-grained facies are preferred for TOC- and organic microfossil-based proxies of net ecosystem productivity. The remaining organic matter in a sedimentary rock consists of kerogen, which is largely represented by the indigenous organic microfossil assemblage. One exception to this is the EOC that has been adsorbed by mineral matter, which, after processing for microfossils, contributes to the amorphous organic matter (AOM) content of an assemblage (Tyson, 1995). However, AOM (except for resin) is excluded from the terrestrial microfossil counts. So, in contrast to TOC, both forms of I_{EOC} are excluded from terrestrial organic microfossil-based metrics (c_t and TrOC; see Section 3.1 and Table 1). These microfossil metrics, therefore, provide a far more direct estimate of ecologically relevant organic carbon divorced from the influence of I_{EOC}.

<INSERT FIG. 3>

1.2.5. Non-biological oxidation of organic carbon: pre-burial (Ox_{Py} and Ox_{Ph})

Net ecosystem productivity includes the organic carbon sequestered by an ecosystem that has subsequently been oxidised and liberated into the atmosphere, hydrosphere or geosphere (primarily as CO_2 or CO) via non-biological processes (Ox_{nb} in Eqns 1–3). These will always result in reductions of the measured organic carbon accumulations. Hence, NEP trends from microfossil- and OC-based metrics will be biased by changes in non-biological (abiogenic) oxidation sources. These sources occur in two stages: 1, pre-burial (Ox_{pre}); and

2, post-burial (Ox_T). Thus, an expanded accounting of all non-biological oxidation would consist of:

$$Ox_{nb} = Ox_{pre} + Ox_T = \left(Ox_{Py} + Ox_{Ph}\right) + Ox_T \quad (4)$$

where Ox_{pre} is the sum of pyrogenic oxidised carbon (Ox_{Py}) and photo-oxidised carbon (Ox_{Ph}; see Chapin *et al.*, 2006; Pace & Lovett, 2021), while Ox_T consists solely of post-burial, thermogenically oxidised carbon (see Section 1.2.6). Given that these factors vary considerably under different past environmental conditions (Ox_{Py} and Ox_{Ph}) and different basin histories (Ox_T), NTEP estimates should account for these non-biological sources of organic carbon oxidation. The pre-burial factors, Ox_{Py} and Ox_{Ph}, are expanded below.

Wildfires are an extremely efficient means of rapid biomass oxidation over large areas. Fires can cause the loss of as much as 25% of annual net primary productivity in tropical to subtropical savannahs (van der Werf *et al.*, 2003) and contribute a major part of global greenhouse gas emissions (Levine *et al.*, 1995; Beringer *et al.*, 2007). Average annual global emissions of greenhouse gas—primarily CO_2—from wildfires was equivalent to 6% of 2014 fossil fuel CO_2 emissions (van der Werf *et al.*, 2017), and recent megafire events have demonstrated carbon emissions far greater than previous models predicted (van der Werf *et al.*, 2017; van der Velde et al., 2021; Zheng et al., 2023). In the wake of wildfires, large volumes of recalcitrant particulate organic matter ('black carbon', consisting largely of soot and charcoal) can accumulate in soils and continental waterbodies (González-Pérez *et al.*, 2004). These incompletely combusted remains of vegetation and hydrocarbons can remain nearly unaltered in the geological record for hundreds of millions of years as fossil charcoal (Scott, 2010) or microscopic 'inertinite' (Scott & Glasspool, 2007; Mays & McLoughlin, 2022). The resistance of charcoal to further oxidation or biodegradation (Tilston *et al.*, 2016), means that charcoal accumulations may be effective carbon sinks (e.g., Lehmann *et al.*, 2006), although the longevity of charcoal in the geosphere has been questioned (Wardle *et al.*, 2008; Bird *et al.*, 2015). Regardless, in intervals of high fire prevalence, charcoal can form the dominant components of organic microfossil assemblages (Mays & McLoughlin, 2022),

and its high preservation potential provides records of long-term changes in wildfire activity, hence biomass oxidation, for most of the Phanerozoic (Glasspool & Scott, 2010; Glasspool & Gastaldo, 2023). Estimating concentrations of fossil charcoal—for instance, as a proportion of c_t—would inform the degree of fire-driven terrestrial biomass oxidation (Ox_{Py}) in prehistoric environments.

Additional precision for Ox_{Py} might be obtained by estimating burn temperatures. While there is considerable debate over the longevity of charcoal on geologic timescales (Singh *et al.*, 2012; Bird *et al.*, 2015), the recalcitrance of charcoal is directly proportion to its carbon concentration (Ascough *et al.*, 2010; Kasin & Ohlson, 2013), which, in turn, increases with temperature since this process preferentially expels hydrogen and oxygen (Almendrosa *et al.*, 2003; Wolf *et al.*, 2013). As temperatures rise, the proportional weight of carbon in charred wood increases from c. 50% to >80% at >600°C (Braadbaart & Poole, 2008; Ascough *et al.*, 2010). Despite its high density in the resultant charcoal, the total amount of retained carbon is small compared to the carbon lost to the atmosphere during a fire: only c. 30% of carbon in dead vegetation was retained following prescribed fires (Alexis *et al.*, 2007). Precise burn temperature estimates can be gleaned from fossil charcoal with a range of complementary techniques, e.g., carbon concentrations (e.g., Ascough *et al.*, 2010), optical reflectance (Braadbaart & Poole, 2008; Hudspith *et al.*, 2015; Belcher *et al.*, 2018), stable carbon isotopes (see review by Bird & Ascough, 2012) and/or spectroscopy (e.g., Wiedemeier *et al.*, 2015; Gosling *et al.*, 2019). By revealing the amount of carbon liberated during combustion, these temperatures will further constrain estimates of non-biological oxidation of organic carbon during the pre-burial stage (Ox_{pre}).

While the impacts of UV photo-oxidation on aquatic ecosystems have long been recognized (Geller, 1986; Kieber *et al.*, 1989), it has since been implicated as a major agent of soil and plant litter decomposition in terrestrial ecosystems (e.g., Moorhead & Callaghan, 1994; Pancotto *et al.*, 2005; Austin *et al.*, 2016). The majority of products from the degradation of plant biomass are indicative of oxidation (e.g., CO_2), but non-oxidative

processes have been implicated as contributors to ecosystem DOC (Vigano *et al.*, 2008, 2009; Day *et al.*, 2019). Hence, the broader term 'photodegradation' should be used in this context, as it describes the abiotic liberation of all carbon from terrestrial biomass owing to surface exposure to electromagnetic radiation (Lee *et al.*, 2012). Photodegradation, therefore, contributes to both Ox_{Ph} and DOC.

Initially, photodegrading radiation was considered largely within the UV spectrum; however, the combination of UV and blue light radiation alone can contribute >40% of total carbon loss in dryland areas in less than two years (Austin & Vivanco, 2006; Day & Bliss, 2020), and blue-green light has a particularly large impact on lignin (Austin *et al.*, 2016). As this effect is a function of insolation, photodegradation is enhanced at lower latitudes (King *et al.*, 2012) and in areas where tree cover has been lost (Gliksman *et al.*, 2018). Within these low latitude regions, the effects of photodegradation are significant in both dryland (Adair *et al.*, 2017; Grünzweig *et al.*, 2022) and (sub)tropical (Marinho *et al.*, 2020; Jiang *et al.*, 2022) conditions; in drylands, it can account for c. 60% of biomass loss in <2 years (Austin & Vivanco, 2006). The quantification of photochemical oxidation is complicated by DOC byproducts, the generation of which promotes microbial metabolism (Wang *et al.*, 2015; Austin *et al.*, 2016; Day *et al.*, 2018; Berenstecher *et al.*, 2020; Jiang *et al.*, 2022) and contributes to the sum of exported organic carbon (E_{DOC}). Thus, photodegradation not only directly contributes to non-biological carbon loss (Ox_{Ph}), but indirectly to TER and E_{DOC}.

Limited attempts have been made to model photodegradation on a global scale (Foereid *et al.*, 2011), but this phenomenon has not yet been incorporated into long-term carbon cycle models of the Phanerozoic, nor on a smaller, palaeoecosystem scale. For a given latitude and terrestrial biome type, changes in photodegradation are likely modest. However, it may have played a large role on the broadest temporal and spatial scales, since latitudinal vegetation cover has undergone dramatic shifts over the Phanerozoic (Gurung *et al.*, 2022), thus significantly changing the abundances of terrestrial biomass in regions of maximum photodegradation. On shorter timescales, recent studies have also indicated that the

radiation intensity at the Earth's surface may have undergone major fluctuations. UV radiation may have increased in response to ozone depletion during magmatically triggered environmental changes (e.g., end-Devonian event, Marshall *et al.*, 2020; end-Permian event, Black *et al.*, 2014, Liu *et al.*, 2023). Hence, we predict that increased rates of photodegradation would have enhanced Ox_{Ph} (and DOC) during such biotic collapse events.

1.2.6. Non-biological oxidation of organic carbon: post-burial (Ox_T and E_{EOC})

While the original formulation of NEP followed here included only surface processes (Lovett *et al.*, 2006; Pace & Lovett, 2021), a full accounting of prehistoric NEP entails the contributions of post-burial factors, specifically: thermogenically oxidised carbon (Ox_T) and exported extractable organic carbon (E_{EOC}). Since both factors will deplete the amount of organic carbon preserved in a given sedimentary stratum, failing to account for them will lead to an underestimate of NEP. While the deep biosphere plays a role in microbial respiration of late-stage buried organic matter (see sections 1.2.2 and 3.2.1), almost all post-burial oxidation and export is due to thermal decomposition, or 'kerogen cracking'.

This multi-stage process involves the successive breakdown of complex organic molecules into simpler components, resulting in the predictable transformation of buried accumulations of insoluble organic matter, or 'kerogen', into light hydrocarbons (see review by Helgeson *et al.*, 2009). Kerogen is the most abundant form of organic matter in the Earth's crust (Durand, 1980; Hunt, 1996), and its maturation has been extensively studied, largely owing to the central role this process plays in the generation of economic hydrocarbon reserves (White, 1915; Trager, 1924; Cooles *et al.*, 1986). The degree of this kerogen decomposition is principally a function of: 1, organic matter composition (typically categorised as broad 'kerogen types' *sensu* Tissot & Welte, 1984); 2, burial conditions, specifically temperature (Price, 1983) and, to a lesser degree, pressure (Landais *et al.*, 1994; Carr, 1999); and 3, time (Sweeney & Burnham, 1990).

Terrestrial organic remains are uniquely suited for estimating the degree of carbon lost from a kerogen during maturation. Plant microfossils—the prime constituents of Type III kerogen (see review by Vandenbroucke & Largeau, 2007)—tend to be highly resistant to maturation, and remain identifiable at higher maturation than microfossils associated with other kerogen types (van Bergen *et al.*, 1995; Fraser *et al.*, 2014; see review by Tyson, 1995). For this and other reasons, the taphonomic signatures of plant microfossils have long been used as thermal maturation proxies (see review by Hartkopf-Fröder *et al.*, 2015). One such proxy relies on plant spore/pollen colour (e.g., Spore Colour Index, Thermal Alteration Index or Palynomorph Darkness Index; Collins, 1990; Marshall & Yule, 1999; Goodhue & Clayton, 2010; Tahoun *et al.*, 2018; Spina *et al.*, 2021) or fluorescence (e.g., Senftle *et al.*, 1993; Mao *et al.*, 1994). A second, widely used metric is vitrinite reflectance (VR), which relies on the optical reflectance of fossil wood (Price, 1983; Sweeney & Burnham, 1990; Petersen, 2002; Mählmann *et al.*, 2012; Mählmann & Le Bayon, 2016; Hackley, 2017) and is often expressed as the maximum reflectance (%R_{max}) or mean random reflectance (%R_O) of incident light. These fossil-based metrics provide well-established, independent gauges of post-burial carbon oxidation (Ox_T) and generation of fluid hydrocarbons (or 'extractable organic carbon', EOC) that can then be used to back-calculate the abundances of originally buried organic carbon (Raiswell & Berner, 1987; Peters *et al.*, 2006; Jarvie, 2012; Modica & Lapierre, 2012; Algeo *et al.*, 2013; Curiale, 2017; Xiao *et al.*, 2023). For instance, 4–28% of the original TOC for land plant-based (Type III) kerogens is considered 'generative organic carbon' (*sensu* Jarvie, 2012), which might be converted to oil, bitumen or gas at high maturation (Daly & Edman, 1987; Jarvie, 2014). Maturation estimates from fossil-based proxies can be reinforced by geochemical approaches, e.g., Rock-Eval pyrolysis (Behar *et al.*, 2001; Suárez-Ruiz *et al.*, 2012); however, fossil assemblages have the added benefit of providing productivity estimates of different biomes, and supplementary insights (e.g., biodiversity, biostratigraphy, biogeography, etc.).

Under even greater temperatures, kerogen continues to lose additional carbon, first via metagenesis then by metamorphism. Extreme thermal maturation of kerogen tends to occur in one of two primary ways. Firstly, contact metamorphism via magmatic intrusion. This results in the thermal devolatilization of buried organic matter, releasing mineralised carbon *en masse* primarily in the form of CO_2 (Aarnes *et al.*, 2011). Such magmatically driven outgassing of greenhouse gas has been implicated in major biotic turnovers (Svensen *et al.*, 2007, 2018; Self *et al.*, 2014). Secondly, kerogen can be decomposed in a regional metamorphic context under the heat and pressure generated by overburden. In extreme cases, this results in the formation of graphite and, eventually, diamond (Buseck & Bo-Jun, 1985; Buseck & Beyssac, 2014; Childress & Jacobsen, 2017; see review by Galvez *et al.*, 2020). Under both of these conditions of metamorphism, the utilisation of most fossil-based maturation proxies become problematic, with the possible exception of vitrinite reflectance (Mählmann *et al.*, 2012; Hartkopf-Fröder *et al.*, 2015; Mählmann & Le Bayon, 2016). However, under extreme metamorphism (%R_{max} >6–7), even the most resistant organic microfossil assemblages become difficult to validly discern; thus, kerogens become unsuitable for NEP estimation.

When we incorporate post-burial, thermal maturation processes into our formulation of NEP in Eqn 1, we see that it plays a role in all three of the factors contributing to a sedimentary sample's accumulated organic carbon (TOC; see Eqn 3): 1, import (I, as I_{EOC}); 2, export (E, as E_{EOC}); and 3, non-biological oxidation (Ox_{nb}, as Ox_T). As kerogens are 'cracked' into simpler components with increasing thermal maturation (Fig. 4), soluble hydrocarbon byproducts—such as oil and gas—can result in net carbon import to, or export from, a given sediment. These hydrocarbon components constitute a rock's extractable organic carbon (EOC). If the goal is to estimate palaeoproductivity, these hydrocarbon in- and outputs will obfuscate the signal if, for example, we solely use total organic carbon (TOC) as a proxy, which consists of both EOC and particulate organic carbon (POC). While TOC cannot differentiate these complex carbon fluxes, a thorough accounting may be

achieved by, for example, tracing the carbon provenance by their biomarker and/or stable isotope signatures (e.g., Bechtel *et al.*, 2008; Ankit *et al.*, 2022), or estimating the abundances of extractable vs kerogen from sample pyrolysis (Behar *et al.*, 2001; Lamoureux-Var *et al.*, 2023).

<INSERT FIG. 4>

A terrestrial organic microfossil-based metric, on the other hand, is typically impervious to imported post-burial hydrocarbons (I_{EOC}; see Section 1.2.4 and Table 1). This is because: 1, the fossils are indigenous to the sediment; 2, they include only solid, structured, insoluble remains; and 3, prior to data collection, EOC is either removed (via some combination of dissolution or dilution with organic solvents, followed by centrifugation, settling and/or filtration) or excluded by setting a minimum count grain size. (Note: Some post-burial hydrocarbons are non-extractable, solid and insoluble, e.g., pyrobitumen [Mastalerz *et al.*, 2018, Misch *et al.*, 2019]; however, the amorphous forms of these bitumens would contribute to a kerogen sample's 'amorphous organic matter', and thus excluded from counts of terrestrial microfossil assemblages, which typically have identifiable structures.)

The oxidised carbon (Ox_T) and exported extractable organic carbon (E_{EOC}) generated from an ecosystem's organic matter during the post-burial phase will tend to be in gas or liquid forms; these will not be directly measurable by the organic microfossil record. Hence, terrestrial microfossil- and OC-based proxies of NEP may be severely biased, unless the Ox_T and E_{EOC} are estimated and subsequently added. Fortunately, the abundances of kerogen cracking byproducts (Ox_T and E_{EOC}) have long been estimated for assessing hydrocarbon source rock potential (e.g., Behar *et al.*, 1995 Lorant & Behar, 2002; Vandenbroucke & Largeau, 2007). Under increasing temperature, the process of organic matter maturation causes the preferential loss of oxygen (via diagenesis) followed by hydrogen (via catagenesis), as illustrated by the 'van Krevelen diagram' (Fig. 4; van Krevelen, 1950; Vandenbroucke *et al.*, 1993; Burnham, 2017; Rivas-Ubach *et al.*, 2018). While carbon is lost throughout this process, this loss occurs at a slower rate than other

elements, thus concentrating carbon in the decomposed residues (Hedges, 1988). Since buried (post-respiration) terrestrial organic matter consists of high proportions of C, O and H, it has a simpler maturation path than most marine organic matter, which typically has higher proportions of S and N (Pelet, 1983; Lorant & Behar, 2002). This results in the predictable loss of terrestrial C with increasing maturation, which can be estimated with high precision (Lorant & Behar, 2002; Behar *et al.*, 2003; Burnham, 2019). For example, experimentally matured low-grade coals lost >60% of their TOC at 500°C, principally as CO and CO_2 (the main contributions to Ox_T), in addition to CH_4 (Behar *et al.*, 1995), the latter of which is the main contribution to EOC (Fig. 5). Such estimates of Ox_T and E_{EOC} might be refined further with a combination of modern analogues and thermal maturation experiments, as outlined below.

While great steps have been made towards the quantification of post-burial kerogen carbon loss (Ox_T and E_{EOC}), the relationship between thermal maturity and carbon loss is not uniform for all organic matter types (van Krevelen, 1950; Vandenbroucke *et al.*, 1993). For example, charcoal-rich assemblages—like those typical of hyperthermal events (Petersen & Lindström, 2012; Mays & McLoughlin, 2022)—would be highly resistant to carbon loss compared to one dominated by non-charcoalified wood (Bird *et al.*, 2015). Constraining the 'maturation half-life' of each organic matter category (Fig. 4) would: 1, indicate the proportions of organic microfossils (and associated carbon) lost in a given kerogen sample; and 2, facilitate back-calculations of the original carbon concentrations from each of the microfossil populations, greatly improving estimates of prehistoric NTEP. Until that point, however, well-established carbon loss functions for each kerogen type (e.g., Daly & Edman, 1987; Jarvie, 2014), rather than precise kerogen components, could be utilized.

<INSERT FIG. 5>

2. Materials and methods

2.1. Sample details.

To test the relationships between the three examined metrics (total organic carbon [TOC], terrestrial organic microfossil concentrations [c_t] and terrestrial organic carbon [TrOC]), a case study was performed by collecting parallel data sets from the same samples. All new data analysed herein are from one drill-core succession (Bonneys Plain-1; 41° 46' 27.69"S, 147° 36' 13.35"E), which was extracted from the northern Tasmania Basin, southeastern Australia (Fig. 6). These samples derive from the upper Permian (Lopingian) to Lower Triassic strata of the upper Parmeener Supergroup (Reid *et al.*, 2014). These strata were deposited in non-marine alluvial or coastal plain palaeoenvironments (Reid *et al.*, 2014; C.R. Fielding, pers. comm.). To test variations in size sorting, reworking and distal transport, siliciclastic facies consisting either primarily of mudrock (i.e., silt- or clay-sized) or heterolithic sand/silt facies were included herein.

<INSERT FIG. 6>

2.2. Total organic carbon (TOC)

For total organic carbon (TOC) analyses, 23 samples were chosen from the Bonneys Plain-1 core (see Appendix A for sample details). Samples were crushed using an agate mortar and pestle and placed in a glass sample container. Powdered samples were reacted with 5% HCl until all carbonate was removed and rinsed with deionized water until neutralized. Samples were then centrifuged to remove excess water and dried at 50°C prior to isotopic analysis.

TOC was measured using a Costech Elemental Analyzer coupled to a Thermo Scientific MAT 253 plus in the Stable Isotope and Organic Molecular Biogeochemistry laboratory, University of Connecticut. Total organic carbon (TOC) content was determined through measurement of an internal laboratory standard (acetanilide) over a range of masses and carbon amounts. Typical analytical precision (expressed as standard error) is c. <1% for the quantification of total carbon in an unknown sample, but the TOC in natural samples is highly

variable. As a result, accurate estimates of total organic carbon in samples with low TOC requires large sample masses, whereas high TOC samples require small masses during measurement. Hence, precision for wt% C estimates varies from <0.02% for samples with <0.5 wt% TOC, to close to 1% for samples with TOC of >70%.

2.3. Microfossil processing

The same 23 sediment samples from Bonneys Plain-1 that were processed for total organic carbon (TOC) were also analysed for organic microfossils. Non-organic mineral content was removed by digestion with hydrochloric acid followed by hydrofluoric acid. Prior to acidification, a known quantity of exotic markers was added. The exotic markers utilised in this study were *Lycopodium clavatum* spores. Tablets of these spores were introduced into the processing prior to the acidification stage, following Price *et al.* (2016). Tablets were produced by the Department of Geology, University of Lund, Sweden; details of the tablets (including the number of tablets introduced to each sample, the means and uncertainty estimates of *Lycopodium* spores per tablet and their batch numbers provided by the manufacturer), are provided in Appendix A. No heavy-liquid separation or oxidation was performed. The resultant sedimentary organic matter residues were sieved with a mesh size of 250 μm. Coarser organic microfossils were removed; the remaining finer fraction were mounted onto glass coverslips and sealed onto glass slides with epoxy. These non-oxidised residues of sedimentary organic matter (*sensu* Hutton *et al.*, 1994) are the subjects of palynofacies analysis (*sensu* Combaz, 1964), and are reflective of the undissolved particulate organic carbon (POC, *sensu* Schlesinger & Melack, 1981, Li *et al.*, 2017) of a sample's total organic carbon (TOC). Estimating microfossil concentrations from sedimentary organic matter (or 'kerogen') assemblages avoids the potential biasing effects of sieving, oxidation and heavy liquid separation (Mertens *et al.*, 2009; see reviews by Wood *et al.*, 1996, and Riding, 2021).

These samples were processed at Global Geolab, Medicine Hat, Canada. Slides with prefix ‘S’ are housed at the Department of Palaeobiology, Naturhistoriska riksmuseet (NRM), Stockholm, Sweden; slides with prefix ‘L’ are housed at GNS Science, Lower Hutt, New Zealand.

2.4. Microfossil counts and concentration estimates

Estimating concentrations of a target population of organic microfossils is typically performed by comparing their estimated abundances to a known quantity of exotic spores, pollen or other microscopic markers (e.g., Kirkland, 1967; Stockmarr, 1971; Craig, 1972). While typically applied in palynological contexts (e.g., 1962; Mertens et al., 2009), variants of this technique have long been utilised in fields as disparate as agriculture and field ecology (see Mays *et al.*, *pre-print* and references therein). By adding a known quantity of these markers and measuring the original sample size (mass or volume), one can gauge the absolute concentrations of the microfossils of interest (or ‘targets’ herein) in a sediment sample by establishing the ratio of the fossil targets to the exotic markers (n). In this study, the targets were: 1, the total number of organic microfossils (x); or 2, the total number of terrestrial organic microfossils (x_t), which consisted of (in order of approximately decreasing abundance) wood (=’phytoclasts’, including charcoalified wood), leaves, plant spores, pollen and fungal remains; the abundances of fossil resins, animal-derived clasts and other terrestrial microfossils were negligible. Only microfossil ≥5 μm in diameter were counted, since specimens smaller than this could not be confidently identified and classified. To mitigate expectation biases, all counts followed the “blind protocol” outlined by Mays & McLoughlin (2022), whereby: slide labels were masked, then the order of slides was randomized before conducting counts. Organic microfossil count data were collected with a Zeiss Axioskop 2 transmitted light microscope.

The general formula for organic microfossil concentration (c) follows Benninghoff (1962), and terms follow Maher (1981):

$$c = \frac{x \times N_1 \times \overline{Y}_1}{n \times \overline{V}} \tag{5}$$

where x = total target microfossil grains counted, N_1 = number of exotic marker tablets, $\overline{Y}_1$ = mean number of exotic markers per tablet, n = exotic markers counted, and $\overline{V}$ = total mass of dried sediment. Concentrations of terrestrial organic microfossils (c_t) were calculated with Eqn 5, but with c_t in place of c and x_t (the counted number of terrestrial microfossils) in place of x. Both c and c_t are expressed in fossils per gram of dried sediment or sedimentary rock (f g^{-1}).

To gauge the precision of the concentration estimates, concentration total error values (σ) were calculated with the formula (from Stockmarr, 1971, updated with terms defined by Maher, 1981):

$$\sigma = 100\sqrt{\left(\frac{s_{1P}}{\sqrt{N_1}}\right)^2 + \left(\frac{\sqrt{x}}{x}\right)^2 + \left(\frac{\sqrt{n}}{n}\right)^2} \tag{6}$$

where σ is the total standard error of the concentration estimate (in %). In this formula, s_{P1} is the proportional sample standard deviation of the number of exotic markers per tablet; N_1 is the number of doses (e.g., tablets) of exotic markers added to the sample; and s_{1P} is the proportional sample standard deviation of the number of exotic markers per dose (see Appendix A). Total error of terrestrial organic microfossil concentration (σ_t) for each sample was calculated with Eqn 6 by substituting σ with σ_t and x with x_t.

Microfossil concentrations were estimated using two independent counting methods: the 'linear method' (*sensu* Mays *et al.*, *pre-print*) and the 'field-of-view subsampling method' (or FOVS method). The former count method has long been the standard approach for palynological concentrations (Benninghoff, 1962; Maher, 1981; Mertens *et al.*, 2009, Mertens *et al.*, 2012). It consists of a series of successive specimen counts until one or more count

criteria are reached; usually, this is a predetermined number of targets (x) or, less commonly, markers (n). In the present study, counting continued for each assemblage until both of the following count criteria were met: 1, at least 500 of all organic microfossils; and 2, at least five markers. In contrast, FOVS method counts are conducted by two successive data collection phases: a series of calibration counts (in which the means and standard deviations of targets per field of view are calculated) followed by extrapolation (or 'full') counts (whereby only the markers and fields of view are counted). In this way, large numbers of extrapolated targets ($\hat{x}$) can be counted, and concentrations calculated by substituting $\hat{x}$ for x in Eqn 5 (for calculation of FOVS method error, please see Appendix A). When applied to simulated and microfossil data sets, the FOVS method has demonstrated the same concentration results as the linear approach, but superior precision (=lower error), more accurate precision estimates and/or lower sampling effort (Mays *et al.*, *pre-print*). In the present study, the FOVS method count criteria were: 1, 15 calibration counts; and 2, total standard errors of <17%. In all assemblages, the target-to-marker ratio ($\hat{u}$) was >1, meaning that targets were always more common than markers. A paired *t*-test was conducted on the estimated concentrations from each count method to test for any systematic biasing (Appendix B).

Significance tests were conducted with PAST v. 4.13 (Hammer *et al.*, 2001). See the Glossary for descriptions of terms, abbreviations and initialisms used in this study.

3. Results and discussion

3.1. Comparing potential NTEP proxies

Total organic carbon (TOC) is perhaps the most widely utilised proxy for palaeoproductivity (e.g., Pedersen & Calvert, 1990; Tyson, 1995, 2005; Schoepfer *et al.*, 2015; Shen *et al.*, 2015), and represents the mass of covalently bound carbon per unit of dried sediment or sedimentary rock (Jarvie, 1991; Bisutti *et al.*, 2004). To test the contribution of the terrestrial organic microfossils to the TOC values, linear correlation tests were conducted; a similar

approach has been taken for specific palynomorph groups vs TOC (e.g., Hardy & Wrenn, 2009; Reichart & Brinkhuis, 2003) or between different organic microfossil groups (e.g., Heimhofer *et al.*, 2006). In this case, the abundances of coeval TOC (Appendix A) and total terrestrial organic microfossil concentrations (c_t) from the non-marine strata of Bonneys Plain-1 yielded a strong positive correlation (Pearson's $r = 0.7319$, $p < 0.0001$; Spearman's $\rho = 0.6392$, $p = 0.001$; $N = 23$; Fig. 7A). This is not surprising; it indicates that the primary contributors to the TOC in these continental samples consisted of terrestrial (specifically, land plant) remains. However, the residual variation ($1 - r^2 = 1 - 0.464 = 46.4\%$) is indicative of a substantial degree of influence from additional factors. Possible contributors to this variability have been identified and discussed below.

<INSERT FIG. 7>

3.1.1. Measurement uncertainty

Both TOC and c_t have their own inherent uncertainties that stem from imprecisions in instrumentation and count data collection method, respectively. While standard errors of TOC herein were quite low 0.015–0.182% wt (mean = 0.11% wt), the low TOC values of some of the samples (e.g., 0.37% wt for S090318) were approaching the instrument detection limits. The impact of this was the high 'proportional error' for some samples; specifically, when expressed as a proportion of TOC, error was high for low TOC samples (e.g., 35.9% for S090318, the sample with the lowest TOC).

Total standard errors (*sensu* Stockmarr, 1971) associated with microfossil concentrations were largely a function of the count method used. For the linear method, c_t error was 8.4–44.8% (mean: c. 30.7%; Appendix A). This total error alone could explain a major proportion of the discrepancy between TOC and linear method-derived c_t. However, the errors associated with the FOVS method counts were typically far lower than the linear method counts (7.7–16.9%; mean: 13.0%). These lower errors were achieved with a non-significant difference in concentration estimates (see Appendix B), suggesting no compromise in

accuracy for the FOVS method. For this reason, the correlations between TOC and c_t presented here (Fig. 7) only used data collected with the FOVS method.

Implications. Improved precisions in TOC can be achieved by using large sample masses where possible, particularly for samples with low organic carbon content, and increasing the number of replicate analyses. Additional precision in TOC can be achieved by utilizing carbonate mineral removal methods that minimize the loss of organic carbon (e.g., vapor fumigation). Regardless of the choice, the method should be consistent for all compared samples, to standardise the potential biasing effect of these methods (Note: both the microfossil and TOC data in this study utilized the same carbonate removal method [HCl acidification], thus enhancing the validity of comparisons between these data sets.)

Given that the data collection method for c_t (and c) can be a major source of statistical error, applying the most precise methods of microfossil concentrations available should be prioritized. Specific count and preparation techniques to improve precision have been proposed and tested (Regal & Cushing, 1979; Maher, 1981; Mertens *et al.*, 2009; Price *et al.*, 2016). More recently, the FOVS method—which utilizes random subsampling of slide surface areas—has demonstrated improved precision under almost all simulated and 'real world' conditions (Mays *et al.*, *pre-print*). As such, we recommend that the FOVS method be utilized to minimize errors associated with organic microfossil concentration estimates.

3.1.2. Non-terrestrial microfossils

The concentration of terrestrial organic microfossils, c_t, excludes non-terrestrial matter (e.g., aquatic algae) and any amorphous organic matter (AOM) not derived from plants (c_t includes one amorphous category: fossil tree resin [= amber]). A large proportion of AOM likely derives from aquatic algae and/or bacteria (Taylor *et al.*, 1998; Pacton *et al.*, 2009, 2011). Most continental organic microfossil assemblages—including those examined here—accumulated in continental aquatic conditions such as lakes, rivers and deltas where the

contribution of non-terrestrial remains may be substantial. This is especially true during intervals of terrestrial ecosystem stress when inputs from land plants are anomalously low and/or aquatic primary producers are anomalously high (Vajda *et al.*, 2020, Mays *et al.*, 2021). For the Tasmania Basin samples, terrestrial microfossils comprised an average of 68% of the total microfossil assemblages, but this was extremely variable (20–99%; Appendix A). Since both TOC and microfossil data were derived from the samples, the relative contributions of terrestrial vs non-terrestrial carbon will be similar in both data sets. Given the substantial and/or variable amount of non-terrestrial carbon in these continental samples (e.g., non-resin AOM, algal microfossils), TOC is, therefore, a less appropriate proxy for terrestrial productivity than c_t.

To test whether a more accurate OC-based proxy of net terrestrial ecosystem productivity could be achieved, we used the relative abundances of terrestrial microfossils (= x_t/x) and multiplied this by a sample's TOC to approximate the proportion of terrestrial organic carbon (TrOC %wt; see Glossary). TrOC is akin to other proportional metrics of a sediment's terrestrial organic carbon—sometimes called the 'terrestrial fraction' (Ft)—which have typically been derived isotopically (e.g., Newman *et al.*, 1973; Li *et al.*, 2016; Ghsoub *et al.*, 2020) or, as in the present study, palaeontologically (e.g., Wagner, 1999; Wagner *et al.*, 2003; Algeo *et al.*, 2004, Algeo *et al.*, 2007; Schnyder *et al.*, 2017). Since it encompasses all terrestrial fossilised organic matter, TrOC should represent a more appropriate metric of NTEP than other fossil-based metrics of proportional terrestrial OC, like the proportional organic carbon of fossil wood, or 'phytoclasts' (Wrenn & Beckman, 1981; Tyson, 1989).

We predicted that the correlation between TrOC and c_t should be greater than that between TOC and c_t (Fig. 7). The correlation was slightly stronger between TrOC and c_t (Pearson's r = 0.746, p <0.00005; N = 23; Fig. 7B) than between TOC and c_t (Pearson's r = 0.73192, p <0.0001; N = 23). This indicates that a modest improvement to an OC-based palaeoproductivity can be achieved by estimating the proportional contribution of terrestrial fossils in an assemblage.

Implications. The preferential preservation of organic carbon in aquatic conditions, even on the continents, means that metrics that can differentiate between aquatic and terrestrial organic remains—like c_t and TrOC—are distinctly suited as proxies of net terrestrial ecosystem palaeoproductivity. In contrast, the use of TOC for this purpose should be limited to continental successions, where assemblages tend to be dominated by terrestrial microfossils and, therefore, the primary contributors to TOC will be plants. The validity of an OC-based NTEP proxy can be improved by determining the proportions of terrestrial vs non-terrestrial organic remains (e.g., palynofacies analysis); the metric, terrestrial organic carbon (TrOC) described herein, demonstrates this. Despite this, only modest improvements might be achieved for TrOC, without controlling for the other variables (e.g., instrument error, grain sizes/densities, and the others discussed here).

3.1.3. Indigenous vs exogenous organics

Since c_t is derived solely from fossil-based kerogen assemblages, it measures only organic matter that is indigenous to the sample (i.e., accumulated during deposition). TOC, in contrast, also includes extractable organic carbon (EOC, *sensu* Jarvie, 1991), such as oil, gas and bitumen. Hence, TOC may comprise a mix of both indigenous organic carbon (kerogen) and imported EOC (I_{EOC}), owing to the extensive subsurface migration that EOC can undergo (Schowalter, 1979), even through low-porosity rocks (Slatt & O'Brien, 2011). Hence, metrics based on microfossil assemblages (e.g., c_t or TrOC) exclude these exogenous sources of organic carbon, thus providing a 'cleaner' gauge of NTEP. Moreover, as discussed above (see sections 1.2.4 and 3.2.3), organic microfossils might be utilized to detect and subtract the proportion of imported particulate organic matter (I_{POC}) in a sample, further refining calculations of NTEP.

Implications. Absolute microfossil abundances (e.g., concentration metrics like c or c_t) circumvent the effects of I_{EOC} and I_{POC} to which TOC is prone. In this regard, c_t is also likely

superior to fossil-based OC metrics, like TrOC; however, the influence of exogenous OC on TrOC is likely mitigated (compared to TOC), because large, identifiable reworked fossils (contributors to I_{POC}) can still be identified and eliminated from TrOC.

3.1.4. Carbon concentrations

NTEP is measured in carbon. While TOC is divorced from other elements, organic matter has diverse carbon concentrations (*δC*, herein, $0 \leq \delta C \leq 1$), owing to their complex compositions of (primarily) C, O, H, plus minor amounts of other elements such as N, S and P. (The symbol *δC* was chosen to represent the ratio between C and other elemental constituents.) The vast majority of terrestrial organic microfossils consist of plant remains, a commonly cited carbon concentration of which is c. 50% wt (i.e., $\delta C_{plant} \approx 0.5$), but there are substantial differences between plant groups, tissues and plant-derived compounds (Thomas & Martin, 2012). The carbon content of the durable, palaeontologically relevant compounds lignin, sporopollenin and cutin are c. 47–60% wt ($\delta C_{lignin} \approx 0.47$–$0.6$; Sarkanen & Ludwig, 1971; Cope, 1980), c. 60–73% wt ($\delta C_{sporopollenin} \approx 0.6$–$0.73$; Robert, 1988) and c. 71% wt ($\delta C_{cutin} \approx 0.71$; Goñi & Hedges, 1990), respectively (see review by Tyson, 1995, table 5.1). Reasonable modern analogues can then inform the original carbon concentrations of fossil materials. Changes in these components between samples will add to the residual variance between c_t and TOC (or TrOC) in a given sample.

Moreover, the concentrations of C in organic fossils are largely a factor of thermal maturation as (O- and H-rich) volatiles are progressively expelled (van Krevelen, 1950; Lorant & Behar, 2002). With increasing maturity, carbon concentration increases until it approaches 100% under extreme maturation during graphitization (Mählmann & Le Bayon, 2016; Galvez *et al.*, 2020). Hence, variations in sample thermal maturity will contribute to the variance between c_t and TOC (or TrOC).

Implications. Carbon concentrations of pre-burial terrestrial biomass can be estimated from modern analogues (e.g., plant tissues, algae, fungi). From these, maturation pathways of individual organic matter types might be estimated (see Section 1.2.6 and Table 1), thus reflecting more accurate contributions of each fossil population to a sample's TOC.

3.1.5. Grain dimensions

The sizes of organic fossils might be highly variable in the residues from which c_t are estimated. c_t does not discriminate between grain size, but variations in fossil sizes will affect how representative c_t is of a sample's terrestrial organic carbon. Consider two samples with the same c_t: the one with larger fossils will have a greater TOC than the sample with smaller mean fossil size. In the extreme case, samples of coals comprising large fossil wood fragments would have inordinately high OC levels, but tell us very little of NEP in a catchment area. Without quantifying a sample's grain dimensions, c_t may entail an unacceptable degree of uncertainty as a gauge of net ecosystem productivity.

Moreover, two competing biases will affect how representative c_t is of the 'true' total terrestrial organic carbon: 1, the minimum dimensions of identifiable microfossils (biased towards larger grains; minimum identifiable sizes in this study = 5 μm); and 2, the upper mesh sizes (biased towards smaller grains; upper mesh size in this study = 250 μm).

The first of these biases (minimum grain size) would be particularly problematic when examining samples from marine sediments. In marine systems, the exclusion of small microfossils would cause a major discrepancy between TOC and absolute abundances of microfossils, since TOC tends to increase with smaller (organic or non-organic) sediment grain sizes (Trask, 1939; Hennessee *et al.*, 1986). In samples with small grain sizes, a large proportion of TOC will comprise small organic matter particles that would be underrepresented by c_t. However, this relationship inverts for continental settings, where the primary contributors to TOC are coarse fragments of plant debris (Shepard, 1956; Hedges &

Parker, 1976; Silva *et al.*, 2014). Hence, the lack of small microfossil representation—and the influence of this first bias—should have a minimal effect on c_t for samples derived from continental environments.

The fact that large plant fragments are the primary contributions to TOC in continental environments, however, means that the second bias (maximum grain size) likely has a more significant effect on c_t. For instance, some high TOC samples may represent assemblages dominated by large organic fossils (e.g., coalified macroscopic wood fragments), even if the total number of such grains is low (i.e., low c_t but high TOC). Such large grains would not be detected during c_t data collection, except with upper sieves with very large mesh sizes or no upper sieve (hence, no upper size limit).

Dissolved organic carbon (DOC) is generally defined by mesh size (typically, DOC is <0.45 μm, although this varies between studies; Kolka *et al.*, 2008). Thus, if present, DOC would be represented in the TOC but not c_t, since the latter had a minimum grain size of 5 μm herein. Instead, c_t represents only a terrestrial ecosystem's particulate organic carbon (POC). However, the disproportionate contribution of pre-burial DOC to TOC was likely minimal, since pre-burial DOC is extremely labile and it seems likely that negligible amounts of DOC accumulate in the geosphere (see Section 1.2.2). For geological samples, other organic carbon in this size category will be derived from imported, fluid hydrocarbons (I_{EOC}); as noted above (see Section 3.1.3), contamination from I_{EOC} should have minimal impact on net ecosystem palaeoproductivity proxies based on microfossil concentrations.

An additional dimension that may contribute to the variance between c_t and TOC (or TrOC) is density. Organic microfossil density can be quite variable, with a major discrepancy between primary aquatic and terrestrial microfossil-dominated maceral groups: alginite: c. 0.96–1.12 g/cm^3 and vitrinite: c. 1.25–2.25 g/cm^3, respectively (see Tyson, 1995, appendix A). However, the variation in density is limited for the primary plant-derived terrestrial fossil groups (e.g., inertinite and vitrinite; Robl *et al.*, 1987, 1992; Mastalerz *et al.*, 2012). To further complicate this, the densities of these grains increase with maturity and/or combustion—

primarily owing to the loss of hydrogen as a function of temperature—but at different rates for the different fossil groups (Okiongbo *et al.*, 2005).

Implications. The impacts of hydraulically induced sorting of grain sizes between samples can be minimised, in large part, by targeting sedimentary samples of similar grain-size profiles (including means and distributions). Moreover, fossil- and OC-based proxies should come from continental palaeoenvironments, where organic carbon is disproportionately represented by large, indigenous particulate organic matter. In a palynological context, large upper sieve mesh sizes (or no upper sieve at all) should be preferred to ensure large fossil fragments are accounted for. Higher fidelity estimates of buried terrestrial organic carbon based on c_t would be achieved by the quantification of organic fossil grain sizes, possibly assisted by automated image analysis techniques.

Grain densities can be incorporated into fossil-based estimates of NEP by measuring the densities of the primary grain types in an assemblage, or substituting reasonable estimates from modern or fossil analogues. Moreover, the validity of inter-sample comparisons would be further strengthened by targeting samples of similar burial histories, thus minimizing the variations in grain densities caused by thermal maturation.

3.1.6. Accumulation rates and inorganic sediment dilution

Under oxic aquatic conditions, like those typical of continental deposits, organic remains are more likely to survive if buried quickly (Stein, 1986a; Tyson, 2005). However, since both OC and c_t are measured per unit mass, the amount of inorganic clastic sediment from which a sample is derived can severely impact these values (Tyson, 1995). This dilution effect can be a dominant determinant of TOC and, by extension, c_t in a sediment (Bustin, 1988; Ittekot, 1988; Tyson, 2005).

If the total sedimentation rate (=bulk accumulation rate, or BAR measured in g cm^{-2} kyr^{-1}) can be estimated, this enables the calculation of the total organic carbon accumulation rate (OCAR, in mg C cm^{-2} kyr^{-1}) with the following formula (updated from Schoepfer *et al.*, 2015):

$$OCAR = OMAR \times \delta C = TOC \times BAR \times 1000, \quad (7)$$

where, OMAR is the total organic matter accumulation rate measured in mg cm^{-2} kyr^{-1} and δC is the mean carbon concentration of the organic matter in a sample (note: x1000 factor is to account for difference in units between BAR and OCAR: g cm^{-2} kyr^{-1} and mg cm^{-2} kyr^{-1}, respectively). If we wish to focus on the terrestrial inputs only, we can do so by substituting TrOC or c_t into modified versions of Eqn 7. Firstly, terrestrial organic carbon accumulation rate (TrOCAR) can be estimated by

$$TrOCAR = TrOMAR \times \delta C_{Tr} = \left(\frac{x_t \times TOC}{x}\right) \times BAR \times 1000, \quad (8)$$

where TrOMAR is the accumulation rate of terrestrial organic matter in mg cm^{-2} kyr^{-1} and δC_{Tr} is the mean carbon concentration of the terrestrial organic matter in a sample. Lastly, we can utilise the concentrations of fossils (c) or, in this case, terrestrial fossils (c_t) from a sediment sample to estimate the rate of terrestrial organic fossil accumulation ($TrOFAR$):

$$TrOFAR = c_t \times BAR. \quad (9)$$

Since c_t (and c) are expressed in fossils (f) per gram of dried sediment or sedimentary rock (hence: f g^{-1}), and BAR accounts for sample weights, the units for TrOFAR are in fossils per cm^2 per kiloyear (f cm^{-2} kyr^{-1}). Note: Eqn 9 is not directly analogous to Eqns 7 and 8 because neither fossil masses nor their dimensions are typically well constrained; however, these might be achieved utilizing a variant of the method developed by Graz *et al.* (2010). In Eqns 7–9, sediment dilution has been estimated and mitigated; as such, net ecosystem productivity proxies that incorporate accumulation rates (e.g., OCAR, TrOCAR, TrOFAR) should be superior to the dimensionless values TOC, TrOC or c_t. This can be achieved with accurate absolute sedimentation rates.

For many prehistoric successions, sedimentation rates can be calibrated by some combination of precise radiogenic isotopic age controls (e.g., Burgess *et al.*, 2014; Fielding *et al.*, 2021), chemostratigraphic correlation (e.g., Widmann *et al.*, 2020), annual increment age estimation (e.g., lake varves; Anderson & Dean, 1988), astronomical tuning (e.g., Olsen, 1986; Ruhl *et al.*, 2016), or time-averaging over stratigraphic units (e.g., Algeo *et al.*, 2013; Mays *et al.*, 2020).

When absolute estimates of sedimentation rates are unavailable, efforts can be made to standardise sediment dilution effects, thus enabling the detection of relative (rather than absolute) changes in organic matter/carbon burial. Fluvial floodplains, for example, can experience large differences in interannual sedimentation rates (e.g., 2–7 mm/year in the Netherlands; Hobo *et al.*, 2010; 2–10 mm/year in southeastern Canada; Saint-Laurent *et al.*, 2010). However, time-averaging of samples (e.g., across several sediments of strata) can substantially reduce the variability both between samples of the same site, and between sites of the same environmental setting (Du & Walling, 2012). Samples of TOC (or TrOC) and c (or c_t) carried out with standardised stratigraphic thicknesses (e.g., across several centimetres) will provide time-averaged results that should limit intersample variability.

(Note: In the present case, however, the degree of organic carbon dilution by sedimentary lithogenic or biogenic components can be eliminated as contributing to the residual variance between TOC [or TrOC] and c_t. Both the OC-based metrics and c_t are proportional values: TOC [or TrOC] is the weight of carbon proportional to the total sediment weight [in %], while c_t is the number of identified terrestrial microfossils proportional to the total sediment weight. Since the OC and c_t data are from the same samples, and both measures have a common denominator [the mass of the sediment], the dilution would influence both values by the same degree.)

Implications. For estimating valid estimates of NTEP, non-organic sediment accumulation rates need be accounted for, owing to the impact this rate has on both OC-based NEP proxies (Schoepfer *et al.*, 2015) and c_t. Without this, these proxies might still serve as a

gauge of relative NTEP changes if comparisons are made between samples of consistent stratigraphic thicknesses and sedimentary facies, as this will limit the variation in sedimentation rates and durations. Lithofacies should be mud-dominated (claystone or siltstone) to reduce variations in sediment hydraulic sorting, while compositions and diagenetic histories should be standardised where possible to minimise variations in grain density and post-burial cementation. We predict that further improvements to OCAR (and analogous metrics, like TrOCAR) will be achieved if the carbon concentrations of the principle organic fossil types (see Section 3.1.4 above) and their proportions are measured and accounted for (Eqn 8).

Both OC-based metrics (e.g., TOC, TrOC) and fossil concentration-based metrics (e.g., c, c_t) hold potential for measuring net terrestrial ecosystem productivity, but both have important biases that should be considered (Averyt & Paytan, 2004; Tyson, 2005; Schoepfer *et al.*, 2015). Above, we have outlined specific strategies to mitigate their shared biases: measurement imprecision and inorganic sediment dilution. The confounding factors unique to TOC are: 1, non-terrestrial organic matter; and 2, exogenous organic carbon. Metrics that incorporate fossils only from the targeted ecosystem (e.g., c_t or TrOC) circumvent this issue, because they account for fossil provenance, and avoid specific sources (e.g., non-terrestrial). Moreover, c_t reduces the impact of exogenous organic matter, owing to its focus on larger, particulate organic matter of terrestrial origin. In contrast, since organic microfossils comprise a mix of non-carbon elements, c_t is influenced by variations in carbon concentration. Hence c_t would offer a more accurate measurement of past carbon burial when informed by modern analogues (for organic matter concentrations) and burial histories (to account for thermogenic C loss). We recommend that applications of c_t be utilised in conjunction with (semi-)independent proxies, such as TOC (or TrOC), to converge on the trends of deep-time net terrestrial ecosystem productivity.

NTEP factors	Considerations	Recommendations	Methods
Pre-burial export; sections 1.2.3 and 3.2.2	Local vs regional ecosystems	Compare only assemblages with similar local depositional conditions: e.g., *in situ* (palaeosols/peats) vs *ex situ* (dispersed)	(1) Terrestrial and (2) aquatic organic (micro)fossil analyses; (3) sedimentological analyses
		Reconstruct the regional tectonic regime to target similar drainage basin areas	(4) Sedimentary petrology/provenance analysis
	Production and dispersal biases	Collect dispersed assemblages only from continental deposits	(1) Terrestrial and (2) aquatic organic (micro)fossil analyses; (3) sedimentological analyses
		Measure total terrestrial organic microfossil assemblages rather than pollen-only assemblages	(1) Terrestrial organic (micro)fossil analyses (c_t; TrOC)
	Regional transport rates (E_{DOC} + E_{POC})	Reconstruct the regional tectonics and topography to infer export rates from analogous extant basins	(3) Sedimentogical analyses; (4) sedimentary petrology/provenance analysis; (5) basin evolution modelling
		Estimate concentrations of terrestrial microfossils in contiguous marine basins	(1) Terrestrial organic (micro)fossil analyses (c_t; TrOC); (3) sedimentological analyses

Import (I); sections 1.2.4 and 3.2.3	Terrestrial ecosystem scale	Examine continental aquatic settings (e.g., lakes, rivers) to infer terrestrial ecosystems on drainage basin-scale	(1) Terrestrial and (2) aquatic organic (micro)fossil analyses; (3) sedimentological analyses
	Petrogenic organic carbon (I_{POC})	Determine regional tectonic and/or magmatic conditions for basement rock composition	(4) Sedimentary petrology/provenance analysis
		Quantify and subtract the proportion of recycled organic matter	(1) Terrestrial organic (micro)fossil analyses (c_t; TrOC); (6) palynomorph-based maturation indices (e.g., PDI, SCI, TAI, degradation, autofluorescence); (7) vitrinite reflectance; (8) geochemical provenance analyses (e.g., $\delta^{13}C$, radiocarbon, Rock-Eval).
	Fluid hydrocarbons (I_{EOC})	Analyse organic matter that is indigenous to the sediment/ary rock, exclude liquid/gas organic matter	(1) Terrestrial organic (micro)fossil analyses (c_t; TrOC)
		Target low porosity, fine-grained facies	(3) Sedimentogical analyses
Pre-burial non-biological degradation (Ox_{pre});	Wildfire oxidation (Ox_{Py})	Measure absolute abundances of charcoal to test for wildfire prevalence	(9) (Micro)charcoal concentrations
		Analyse charcoal for wildfire burn temperatures; compare to modern analogues	(10) Burn temperature proxies of charcoal (e.g., optical reflectance, C concentrations, stable C isotope ratios, spectroscopy); (11) pyrogenic carbon loss experiments

sections 1.2.5 and 3.2.4		Estimate the abundances of molecular fossils (biomarkers) generated by wildfires in sedimentary organic matter	(12) Organic geochemical techniques (e.g., gas chromatography-mass spectrometry)
	Photodegradation (incl. photo-oxidation, Ox_{Ph})	Estimate incident solar radiation, and compare samples/basins of similar palaeolatitude	(13) Palaeogeographic reconstructions
		Calculate relative photodegradation susceptibility of terrestrial biomass components	(14) Photodegradation carbon loss experiments
		Test for anomalies in radiation intensity	(15) Fossil-based UV radiation intensity and/or canopy closure proxies
Post-burial non-biological degradation (Ox_T & E_{EOC}); sections 1.2.6 and 3.2.5	Thermal maturation	Gauge thermal maturation depth gradient of the basin to account for variable maturation across an assemblage time-series	(6) Palynomorph-based maturation indices (e.g., PDI, SCI, TAI, degradation, autofluorescence); (7) vitrinite reflectance; (16) geochemical proxies of maturation (e.g., hydrogen and oxygen indices)
		Identification of intrusive igneous bodies that may have enhanced post-burial thermal maturation	(6) Palynomorph-based maturation indices (e.g., PDI, SCI, TAI, degradation, autofluorescence); (7) vitrinite reflectance; (16) geochemical proxies of maturation (e.g., hydrogen and oxygen indices); (17) regional geological mapping and lithostratigraphy
		Calculate carbon loss vs maturation functions of individual kerogen constituents (if possible) or kerogen types (if not possible) for back-calculations of post-burial carbon loss	(1) Terrestrial organic (micro)fossil analyses (c_t; TrOC); (5) palynomorph-based maturation indices (e.g., PDI, SCI, TAI, degradation, autofluorescence); (6) vitrinite reflectance; (15) geochemical proxies of maturation (e.g., hydrogen

	and oxygen indices); (18) thermal maturation carbon loss experiments; (19) carbon concentrations of extant analogues

Table 1. Considerations, recommendations and suggested methods for deep-time studies of relative net terrestrial ecosystem palaeoproductivity (NTEP). The NTEP factors listed here have been updated from Pace & Lovett (2021). c_t = concentration of terrestrial organic microfossils; PDI = Palynomorph Darkness Index; SCI = Spore Colour Index; TAI = Thermal Alteration Index.

3.2. Microfossil-based proxies of net ecosystem productivity: considerations and recommendations

To maximise the accuracy of microfossil-based proxies of net ecosystem productivity, such as c_t and TrOC, one should consider several limitations. Crucially, the proxies discussed herein (c_t, TOC or TrOC) are not capable of providing direct, absolute estimates of net terrestrial ecosystem productivity (NTEP). However, we argue that these may be suitable for relative NTEP changes. Above, we have outlined practical considerations when using these metrics (see Section 3 and Table 1), specifically: measurement uncertainty, organic matter provenance, grain sizes, carbon concentrations, and inorganic sediment dilution. Below, we have compiled additional considerations and offer practical recommendations for each by relating these to the components of NEP and NTEP (Eqns 1–3); specific methods are summarised in Table 1.

3.2.1. Heterotrophic respiration

While this is not a factor of NEP (or NTEP; Eqn 1), targeting assemblages that have largely avoided respiration by heterotrophs (e.g., animals, fungi, bacteria) may provide a clearer signature of gross primary productivity (GPP), which may be more important for many research questions. In such cases, we recommend targeting:

- samples with minimal evidence of bioturbation or oxidation (Li *et al.*, 2012);
- consistent palaeoenvironmental conditions across samples, and emphasising conditions with thin oxic zones to reduce post-depositional degradation (e.g., deep or eutrophic lakes; Thomsen *et al.*, 2004; Radbourne *et al.*, 2017) and/or rapid burial (e.g., river floodplains; Scheingross *et al.*, 2021);
- microfossil assemblages that are resistant to decay and representative of most biomass in typical terrestrial biomes (i.e., lignin-, sporopollenin- and/or cutin-rich

components; Meyers *et al.*, 1995; Prescott, 2010), from which pre-burial organic matter abundances might be inferred; and

- fine-grained lithofacies.

With a mature proxy of NTEP, independent estimates of heterotrophic respiration (R_h) might be gleaned when combined with coeval anatomy-based rates carbon assimilation for fossil plants. Plant anatomy-based proxies are closely linked to terrestrial net primary productivity (NPP). Hence, the difference between these productivity estimates will likely shed light on relative (if not absolute) heterotrophic respiration rates; i.e., $R_h = NPP - NEP$.

3.2.2. Pre-burial organic carbon export (E)

Organic matter that has been produced in an ecosystem but subsequently exported from the local site of production is challenging to estimate in prehistoric settings. This is particularly challenging for allochthonous fossil assemblages, like those preserved in fluviodeltaic floodplains or lakes. To address these, we recommend:

- comparing assemblages of the same class of depositional conditions, namely: 1, *in situ* terrestrial conditions (e.g., palaeosols, peats), which might be used to inform local NTEP and export rates with constraints by modern analogues (e.g., Worrall & Evans, 2008; Worrall *et al.*, 2009); or 2, *ex situ* continental assemblages of similar drainage basin areas and depositional conditions (e.g., the same basin, or basinal region, over time) to infer relative productivity trends;
- targeting continental deposits for gauging terrestrial ecosystems within a drainage basin (in the case of *ex situ* assemblages), while coeval terrestrial organic matter assemblages in marine deposits can provide estimates of changing continental run-off (e.g., Waterhouse, 1995);

- interpreting the regional palaeotectonic and palaeoclimatic conditions for estimating drainage basin sizes (Blair & Aller, 2012) and constrain rates of export from continental regions (Schlünz & Schneider, 2000; Burdige, 2007); and
- utilising the total terrestrial microfossil assemblage to gauge changes across entire ecosystems, in contrast to pollen records, which can have disparate dispersal and production rates between species (Sugita, 2007; Theuerkauf & Couwenberg, 2021).

3.2.3. Organic carbon import (I)

The two primary sources of imported organic matter in a continental basin are: 1, organic matter-rich basement rock exposed and eroded upstream during the pre-burial phase (‘petrogenic organic matter’, OM_{petro}); and 2, the injection of fluid hydrocarbons (‘extractable organic matter’, EOM, such as oil or gas) during the post-burial phase. To mitigate these sources of imported organic carbon, we recommend:

- determining the regional tectonic or magmatic influences on a continental basin, from which analogous modern continental basins can constrain the expected estimates of imported OC_{petro} from uplifted basement or volcanogenic rocks (Hilton & West, 2020);
- quantifying the proportions of basement-derived vs contemporaneous organic carbon in a sediment by isotopic, geochemical or palynological analyses, thus facilitating corrected values of indigenous organic matter by subtracting the reworked fraction;
- utilizing kerogen-based proxies (e.g., organic microfossils) over TOC, the latter of which is prone to contamination from exogenous fluid hydrocarbons (I_{EOC}) and recycled particulate organic carbon (I_{POC}); and
- consistently targeting fine-grained, low-porosity lithofacies.

3.2.4. Pre-burial non-biological oxidation (Ox_{pre})

Two broad categories of pre-burial non-biological biomass oxidation have been considered herein: 1, oxidation via wildfires (Ox_{Py}); and 2, oxidation via photochemical processes (Ox_{Ph}). The microfossil record, in conjunction with experiments and modern analogues, offer the opportunity to estimate the influence of these two factors in prehistoric terrestrial ecosystems. To this end, we suggest that:

- relative changes in fossil charcoal abundances will provide long-term trends in wildfire prevalence (e.g., Glasspool & Scott, 2010; Mays & McLoughlin, 2022), while fossil charcoal concentrations will indicate their absolute carbon contributions to the atmosphere and geosphere;
- molecular markers of fire (e.g., polycyclic aromatic hydrocarbons, anhydrosugars, lignin oxidation products) can be utilized for past fire abundance/intensity and may also provide measures of the significance of fire in ecosystem processes (e.g., Bhattarai *et al.*, 2019; Karp *et al.*, 2020);
- burn temperature proxies from fossil charcoal—informed by pyrolysis experiments on modern plants (e.g., Braadbaart & Poole, 2008; Wolf *et al.*, 2013)—will further refine estimates of pyrogenic biomass oxidation;
- a first approximation of prehistoric photodegradation can be provided by insolation estimates, as a function of palaeolatitude;
- improvements in photodegradation estimates would be facilitated by experiments on the primary components of terrestrial biomass (e.g., lignin, cellulose, sporopollenin) at various radiation frequencies and intensities to measure differential carbon losses. In principle, such experiments would facilitate back-calculations of carbon for pre-photodegraded biomass—including degradation-

resistant and degradation-susceptible components—from the residual fossil record; and

- photodegradation estimates may be further constrained by fossil proxies of radiation (e.g., UV-B absorbing compounds in plant microfossils; Rozema *et al.*, 2001; Jardine *et al.*, 2016).

3.2.5. Post-burial non-biological carbon loss (Ox_T and E_{EOC})

Thermal degradation, or 'kerogen cracking', occurs via thermogenic oxidation (Ox_T) and the formation of simple, fluid hydrocarbons, which can subsequently be exported (E_{EOC}). This degradation is the primary means of organic matter carbon loss to organic matter during the post-burial phase. To control for the effects of thermal degradation on net ecosystem productivity proxies, we propose that:

- valid inter-sample comparisons can be made between stratigraphic intervals of similar maturity (e.g., short intervals within a single basin or between basins of similar burial histories);
- accurate calculations of post-burial organic carbon loss may be achieved by employing well-established geochemical and/or terrestrial fossil-based thermal maturation proxies (Suárez-Ruiz *et al.*, 2012; Hartkopf-Fröder *et al.*, 2015);
- further refinements of post-burial organic carbon losses (Ox_T + E_{EOC}) will be informed by maturation experiments, not only on kerogen types (Behar *et al.*, 1995; Lorant & Behar, 2002), but on different organic matter categories, thus establishing their carbon loss and preservation biases with burial temperature and (to a lesser extent) pressure; and
- an inspection for intrusive igneous bodies, in addition to signatures of anomalous thermal maturation, will indicate potential contact metamorphism, which may have devolatilized organic matter from the target samples (Aarnes *et al.*, 2011).

Even without accounting for all the above limitations, we propose that careful applications of microfossil concentrations (c, c_t) or fossil-based OC (e.g., TrOC) may indicate relative changes in terrestrial palaeoproductivity. We envisage that the most common application for the present formulations of c_t and TrOC would be to gauge relative changes in, rather than absolute, NTEP. In such cases, microfossil-based proxies will correlate, but not equate, to NEP. However, this can only be achieved if the variations in extraneous variables are minimized (or, ideally, their influences are measured and subtracted). For example, the impacts of changing climate on NTEP through time might be estimated if the following were largely consistent throughout a target interval: 1, sedimentary facies; 2, thermal maturity; 3, local palaeoenvironment; 4, regional tectonic regime; 5, latitude; and 6, drainage basin size. Constraining any or all of these would provide improvements in relative NTEP, and most might be controlled for simply by targeting samples of similar facies from narrow stratigraphic ranges within the same basin.

Ultimately, as our methods of estimating carbon flux at each step—from ecosystem to burial to maturation—are continually refined, we predict that fossil-based proxies will evolve from their present utility in identifying and quantifying relative changes in productivity to proxies of absolute, regional C flux. Such estimates would feed directly into high-resolution biogeochemical cycling models.

4. Conclusions

We echo the concerns expressed by Curiale & Curtis (2016) when they stated (p. 16): "...all approaches seeking to determine [net ecosystem palaeoproductivity] ... are heavily laden with assumptions, most of which are difficult or impossible to validate." Indeed, the preservation pathway of organic carbon from the ecosphere to the geosphere is long, complex and difficult to quantify. By adapting a widely accepted function of modern net ecosystem productivity (NEP), we have identified five primary factors that any net terrestrial

ecosystem productivity (NTEP) proxy must address: terrestrial organic carbon (or organic matter), carbon export, carbon import, and pre- and post-burial oxidation. Within this framework, we discuss how terrestrial organic microfossil-based proxies (c_t and TrOC) may be suitable metrics for addressing these factors. To this end, we offer suggestions—some readily applicable, others presently aspirational—on how sources of carbon in- and output may be quantified and/or eliminated, and potential sources of error circumvented.

With careful application, concentrations of terrestrial organic microfossils (c_t) or the fossil-based terrestrial organic carbon (TrOC) can provide a proxy for changes in relative, if not absolute, NTEP. Therefore, we argue that these metrics may reflect semi-quantitative, long- and short-term fluctuations in NTEP preserved in continental deposits since at least the emergence of large land plants during the Devonian Period. Moreover, the ability of c_t to discern primary carbon sources makes it superior to total organic carbon (TOC) for identifying and quantifying discontinuities in regional terrestrial primary production, such as land ecosystem disruptions and/or recovery events, or evolutionary innovations. Terrestrial organic carbon (TrOC)—a fossil-constrained alternative to TOC—combines key aspects of both fossil- and OC-based proxies. Lastly, we envisage that c_t and/or TrOC may yet form the basis for indirect measures of absolute NTEP, but only by accounting for exported organic carbon, measurement uncertainty, inorganic sedimentation rates, recycled organic matter and the unique carbon loss pathways of each type of terrestrial organic fossil. Such a standardised, generalised productivity proxy would greatly enhance biogeochemical models on regional and global scales.

Acknowledgements

We thank Vivi Vajda, Tracy Frank, Christopher Fielding & Steve McLoughlin for their thought-provoking comments and discussions regarding the utilisation of these methods. Artwork was produced by Victor O. Leshyk (https://victorleshyk.com), and we thank Aidan Sweeney

(University College Cork) for her graphical contributions. We also thank Jennifer McElwain and William Matthaeus for their perspectives on plant productivity. We are grateful to Bas van de Schootbrugge and Marcos Amores for sharing their palynomorph photomicrographs. We acknowledge the assistance of L. Unwin, S. Newett (Mineral Resources Tasmania) and M. Slodownik (University of Adelaide) for sample collection.

Data statement

All newly collected data are available in Appendix A.

Author contributions

CM: conceptualization, funding acquisition, methodology, visualization (with input from Victor O. Leshyk), project administration and synthesis; CM & MH: data collection, curation and analyses; CM, MH & RT: writing, reviewing and editing.

Funding sources

This project was funded by grants awarded to CM from the Science Foundation Ireland's Research Centre in Applied Geosciences (#13/RC/2092_P2) and Science Foundation Ireland's Frontiers for the Future Programme (#22/FFP-P/11448).

Glossary

List of abbreviations or initialisms used herein and their definitions; microfossil concentration terms follow Mays *et al.* (*pre-print*), updated from Maher (1981); (palaeo)productivity terms updated from Lovett *et al.* (2006).

Abbreviation	Expansion and definition
Microfossil concentration terms	
c **(and** σ**)**	**Total organic microfossil concentration**. This is an estimate of total organic microfossils per unit size. In this study, c is expressed as fossils per gram of dried sediment or sedimentary rock (f g^{-1}). For the 'linear method': c is calculated by Eqn 5 (following Benninghoff, 1962); σ is the total standard error for c and is calculated by Eqn 6 (following Stockmarr, 1971). For calculations of c and σ using the FOVS method, see Mays *et al.* (*pre-print*).
c_t **(and** σ_t**)**	**Terrestrial organic microfossil concentration**. This is an estimate of terrestrial organic microfossils per unit size. In this study, c is expressed as fossils per gram of dried sediment or sedimentary rock (f g^{-1}). It is calculated in the same way as c (see above), but the counted fossil targets (x) include only microfossils of wood, leaves, plant spores, pollen, resin and fungi. Animal remains were not included in this study, owing to their extreme scarcity and difficulty in determining provenance (terrestrial vs aquatic). σ_t is the total standard error for c_t and is calculated as for σ (see above).
x **(or** x_t**)**	**Number of counted organic microfossils in a sample**. The specific fossil group counted depends on the research question. For example, to calculate c_t, this value would be number of counted terrestrial microfossils in the sample, x_t.
n	**Number of counted exotic marker grains**. Most commonly, exotic spores or pollen of a known quantity are used (e.g., *Lycopodium* spores).
$\hat{u}$	**Target-to-marker ratio in a sample count.** $\hat{u}$ is equivalent to the total number of counted targets divided by the total number of counted markers in a sample $\left(\hat{u} = \frac{x}{n}\right)$.
N_1	**Number of doses (e.g., tablets or aliquots) of exotic marker grains**. For example, this is the number of tablets of *Lycopodium* spores introduced during sample processing.
$\overline{Y}_1$	**Mean number of exotic markers in one tablet (dose)**. The details of the *Lycopodium* spore tablets (doses) utilised in the empirical case study were provided by the manufacturer (Lund University, Sweden; see details in Appendix A).
$\overline{V}$	**Total sample size (e.g., mass, volume)**. For the present study, this was measured as total mass in grams.
s_1	**Standard error of the exotic markers for one tablet (dose).** Details of the *Lycopodium* tablets utilised in this study were provided by the manufacturer (Lund University, Sweden; see details in Appendix A).
s_{1P}	**Proportional sample standard deviation of the number of exotic markers per dose.** $\left(s_{1P} = \frac{s_1}{\overline{Y}_1}\right)$

s_3	**Sample standard deviation for the target specimens.** This is calculated from the calibration counts; FOVS method only.
s_{3P}	**Proportional sample standard deviation of the number of common specimens in the calibration counts.** This includes the unbiased estimator of the population standard deviation ($\hat{s}_3$), as calculated by Mays *et al.* (*pre-print*); FOVS method only.
N_{3C}	**Number of fields of view counted during the calibration counts.** FOVS method only.
N_{3F}	**Number of fields of view counted during the full counts.** FOVS method only.
$\overline{Y}_{3x}$	**Mean number of targets for each field of view.** This is a measure of target density; FOVS method only.
$\overline{Y}_{3n}$	**Mean number of markers for each field of view.** This is a measure of marker density; FOVS method only.
$\hat{x}$ **(or** $\hat{x}_t$**)**	**Extrapolated number of counted target specimens for the full counts**. This is calculated by: $\hat{x} = \overline{Y}_{3x} \times N_{3F}$. If the target specimens are terrestrial microfossils (x_t), this value would be the extrapolated number of terrestrial microfossils in the sample ($\hat{x}_t$). FOVS method only.
(Palaeo)productivity terms	
GPP	**Gross primary productivity**. Total amount of carbon assimilated by primary producers though carboxylation over a given time.
TER	**Total ecosystem respiration**. The sum of carbon loss by all living autotrophs (e.g., photosynthetic organisms such as plants, algae, cyanobacteria) and heterotrophs (e.g., animals, fungi, many prokaryote groups) in an ecosystem over a given time.
NEP	**Net ecosystem productivity**. Gross primary production minus total ecosystem respiration. Two formulations are used herein. Modern ecosystems (adapted from Lovett *et al.*, 2006): $NEP = GPP - TER = \Delta C_{org} + E + Ox_{nb} - I$ Past ecosystems: $NEP = GPP - TER = TOC + E + Ox_{nb} - I$ Note: for modern ecosystems, NEP, GPP and TER are expressed as rates, measured per unit time. This is impractical for most palaeoproductivity metrics, such as TOC and fossil-based proxies (like c_t), which measure organic matter per gram of dried sediment. For this reason, inorganic sedimentation rates should be accounted for and/or held consistent between samples; see Section 3.1.
NTEP	**Net terrestrial ecosystem productivity**. The net ecosystem productivity of a terrestrial ecosystem (see NEP).
OC	**Organic carbon**. Carbon bound in organic compounds.

OM	**Organic matter**. Any material composed of organic compounds derived from living organisms.
OC_{petro} (or OM_{petro})	**Petrogenic organic carbon (or matter)**. The amount of organic carbon (or matter) originally of biological origin that is found within sedimentary and metamorphic rocks. Typically, such organic matter is in a reduced state, and expressed per unit weight (%wt) of dried sediment or sedimentary rock.
DOC (or DOM)	**Dissolved organic carbon (or matter)**. The fraction of organic carbon (or matter) that passes through a submicron mesh; typically, the mesh size is between 0.22 and 0.7 µm (depending on the study).
POC (or POM)	**Particulate organic carbon (or matter)**. The fraction of organic carbon (or matter) that <u>does not</u> pass through a submicron mesh; typically, the mesh size is between 0.22 and 0.7 µm (depending on the study).
EOC (or EOM)	**Extractable organic carbon (or matter)**. The fraction of organic carbon in the form of fluid hydrocarbons (e.g., oil, gas, bitumen).
TOC	**Total organic carbon**. The total amount of organic carbon, and is calculated: $$TOC = DOC + POC + EOC$$ For (pre)historic samples, this is measured per unit weight (%wt) of dried sediment or sedimentary rock.
σ_{TOC}	**Standard error of total organic carbon.** Measured per unit weight (%wt).
TrOC	**Terrestrial organic carbon.** The total amount of organic carbon in a sample or region derived from terrestrial sources. In this study, the TrOC is measured per unit weight (%wt) of dried sediment or sedimentary rock, and estimated by: $$TrOC = \left(\frac{x_t}{x}\right) \times TOC$$
δC (or δC_{Tr})	**Carbon concentration of organic matter.** Mean carbon concentration of the total organic matter in a sample ($0 \leq \delta C \leq 1$). Variant: δC_{Tr} is the mean carbon concentration of the terrestrial organic matter in a sample (see Eqns 7 and 8).
BAR	**Bulk sediment accumulation rate.** Measured in grams of organic matter per square centimetre per millennium (g cm^{-2} kyr^{-1}).
OMAR	**Total organic matter accumulation rate.** Measured in milligrams of organic matter per square centimetre per millennium s (mg cm^{-2} kyr^{-1}).
OCAR	**Total organic carbon accumulation rate.** Measured in milligrams of carbon per square centimetre per millennium (mg C cm^{-2} kyr^{-1}; see Eqn 7).
TrOMAR	**Terrestrial organic matter accumulation rate.** Measured in milligrams of organic matter per square centimetre per millennium (mg cm^{-2} kyr^{-1}).

TrOCAR	**Terrestrial organic carbon accumulation rate.** Measured in milligrams of carbon per square centimetre per millennium (mg C cm^{-2} kyr^{-1}; see Eqn 8).
TrOFAR	**Terrestrial organic fossil accumulation rate.** Measured in number of fossils (f) per square centimetre per millennium (f cm^{-2} kyr^{-1}; see Eqn 9).
E (including E_{DOC}, E_{POC} and E_{EOC})	**Export (or exported organic carbon)**. The amount of organic carbon exported from an ecosystem and/or sediment/ary rock. Three types of exported organic carbon are differentiated herein, defined by their provenance and composition. These are indicated by subscript, specifically: exported dissolved organic carbon (E_{DOC}), exported particulate organic carbon (E_{POC}) and exported extractable organic carbon (E_{EOC}). Note: this does not include organic carbon that has undergone mineralisation and subsequently exported. For example, organic carbon converted to CO_2 in fire contributes instead to pyrogenically oxidised carbon (Ox_{py}).
I (including I_{POC} and I_{EOC})	**Import (or imported organic carbon)**. The amount of organic carbon imported into an ecosystem and/or sediment/ary rock. Two types of imported organic carbon are differentiated herein, defined by their provenance and composition. These are indicated by subscript, specifically: imported particulate organic carbon (I_{POC}) and imported extractable organic carbon (I_{EOC}). A third type of imported organic carbon (dissolved organic carbon, I_{DOC}) can constitute a major component of organic carbon in modern ecosystems, but very little of this is preserved in the geosphere (see Section 1.2). Given that this study focuses on deep-time contexts, I_{DOC} is not considered further herein.
Ox_{nb}	**Non-biological oxidised organic carbon**. The total amount of carbon converted from organic carbon to oxidised forms through non-biological processes (*sensu* Lovett *et al.*, 2006). These consist of: $$Ox_{nb} = Ox_{pre} + Ox_T = \left(Ox_{Py} + Ox_{Ph}\right) + Ox_T$$ The components of Ox_{nb} are expanded below.
Ox_{pre} (including Ox_{py} and Ox_{ph})	**Pre-burial non-biological oxidised organic carbon**. The total amount carbon converted from organic carbon to oxidised forms through non-biological processes on the Earth's surface. Ox_{pre} is the sum of pyrogenic oxidised carbon (Ox_{py}) and photo-oxidised carbon (Ox_{ph}): $$Ox_{pre} = Ox_{Py} + Ox_{Ph}$$
Ox_T	**Post-burial non-biological oxidised organic carbon**. Also known as thermogenically oxidised carbon, which is created through the process of post-burial 'kerogen cracking'. The byproducts of this process are primarily CO_2 and CO.
ΔC_{org}	**Change in an ecosystem's stored organic carbon**. For (pre)historic records where time-averaged samples preclude short-term ecosystem storage rates of change, the TOC (measured per unit of weight of sediment [%wt], rather than time) is utilised herein.

1324

References

Aarnes, I., Fristad, K., Planke, S., Svensen, H., 2011. The impact of host-rock composition on devolatilization of sedimentary rocks during contact metamorphism around mafic sheet intrusions. Geochemistry, Geophysics, Geosystems, 12, Q10019, 11 pp. doi: 10.1029/2011GC003636.

Adair, E.C., Parton, W.J., King, J.Y., Brandt, L.A., Lin, Y., 2017. Accounting for photodegradation dramatically improves prediction of carbon losses in dryland systems. Ecosphere, 8, e01892, 16 pp. doi: 10.1002/ecs2.1892.

Alexis, M.A., Rasse, D.P., Rumpel, C., Bardoux, G., Péchot, N., Schmalzer, P., Drake, B., Mariotti, A., 2007. Fire impact on C and N losses and charcoal production in a scrub oak ecosystem. Biogeochemistry 82, 201–216. doi: 10.1007/s10533-006-9063-1.

Algeo, T.J., Henderson, C.M., Tong, J., Feng, Q., Yin, H., Tyson, R.V., 2013. Plankton and productivity during the Permian–Triassic boundary crisis: An analysis of organic carbon fluxes. Global and Planetary Change 105, 52–67.

Algeo, T.J., Lyons, T.W., Blakey, R.C., Over, D.J., 2007. Hydrographic conditions of the Devono–Carboniferous North American Seaway inferred from sedimentary Mo–TOC relationships. Palaeogeography, Palaeoclimatology, Palaeoecology 256, 204–230.

Algeo, T.J., Scheckler, S.E., 2010. Land plant evolution and weathering rate changes in the Devonian. Journal of Earth Science 21, 75–78.

Algeo, T.J., Schwark, L., Hower, J.C., 2004. High-resolution geochemistry and sequence stratigraphy of the Hushpuckney Shale (Swope Formation, eastern Kansas): implications for climato-environmental dynamics of the Late Pennsylvanian Midcontinent Seaway. Chemical Geology 206, 259–288.

Algeo, T.J., Twitchett, R.J., 2010. Anomalous Early Triassic sediment fluxes due to elevated weathering rates and their biological consequences. Geology 38, 1023–1026.

Almendrosa, G., Knicker, H., González-Vila, F.J., 2003. Rearrangement of carbon and nitrogen forms in peat after progressive thermal oxidation as determined by solid-state ^{13}C- and ^{15}N-NMR spectroscopy. Organic Geochemistry 34, 1559–1568.

Alvarez-Cobelas, M., Angeler, D.G., Sánchez-Carrillo, S., Almendros, G., 2012. A worldwide view of organic carbon export from catchments. Biogeochemistry 107, 275–293.

Anderson, R.Y., Dean, W.E., 1988. Lacustrine varve formation through time. Palaeogeography, Palaeoclimatology, Palaeoecology 62, 215–235.

Anell, I., Thybo, H., Artemieva, I.M., 2009. Cenozoic uplift and subsidence in the North Atlantic region: Geological evidence revisited. Tectonophysics 474, 78–105.

Ankit, Y., Muneer, W., Gaye, B., Lahajnar, N., Bhattacharya, S., Bulbul, M., Jehangir, A., Anoop, A., Mishra, P.K., 2022. Apportioning sedimentary organic matter sources and its degradation state: Inferences based on aliphatic hydrocarbons, amino acids and $\delta^{15}N$. Environmental Research, 205, 112409.

Arndt, S., Jørgensen, B.B., LaRowe, D.E., Middelburg, J.J., Pancost, R.D., Regnier, P., 2013. Quantifying the degradation of organic matter in marine sediments: A review and synthesis. Earth-Science Reviews 123, 53–86. doi: 10.1016/j.earscirev.2013.02.008.

Ascough, P.L., Bird, M.I., Scott, A.C., Collinson, M.E., Cohen-Ofri, I., Snape, C.E., Le Manquais, K., 2010. Charcoal reflectance measurements: implications for structural characterization and assessment of diagenetic alteration. Journal of Archaeological Science 37, 1590–1599.

Ashley, K.E., Crosta, X., Etourneau, J., Campagne, P., Gilchrist, H., Ibraheem, U., Greene, S.E., Schmidt, S., Eley, Y., Massé, G., Bendle, J., 2021. Exploring the use of compound-specific carbon isotopes as a palaeoproductivity proxy off the coast of Adélie Land, East Antarctica. Biogeosciences 18, 5555–5571. doi: 10.5194/bg-18-5555-2021.

Austin, A.T., Méndez, M.S., Ballaré, C.L., 2016. Photodegradation alleviates the lignin bottleneck for carbon turnover in terrestrial ecosystems. Proceedings of the National Academy of Sciences of the United States of America 113, 4392–4397. doi: 10.1073/pnas.1516157113.

Austin, A.T., Vivanco, L., 2006. Plant litter decomposition in a semi-arid ecosystem controlled by photodegradation. Nature 442, 555–558.

Averyt, K.B., Paytan, A., 2004. A comparison of multiple proxies for export production in the equatorial Pacific. Paleoceanography, 19, PA4003, 14 pp.

Baldock, J.A., Masiello, C.A., Gélinas, Y., Hedges, J.I., 2004. Cycling and composition of organic matter in terrestrial and marine ecosystems. Marine Chemistry 92, 39–64.

Balme, B.E., 1957. Spores and pollen grains from the Mesozoic of Western Australia, Fuel Research: Physical and Chemical Survey of the National Coal Resources. C.S.I.R.O. Australia, Chatswood, pp. 1–48.

Bar-On, Y.M., Phillips, R., Milo, R., 2018. The biomass distribution on Earth. Proceedings of the National Academy of Sciences of the United States of America 115, 6506–6511. doi: 10.1073/pnas.1711842115.

Batten, D.J., 1981. Palynofacies, organic maturation and source potential for petroleum, in: Brooks, J. (ed.). Organic Maturation Studies and Fossil Fuel Exploration. Academic Press, London, pp. 201–223.

Batten, D.J., 1991. Reworking of plant microfossils and sedimentary provenance, in: Morton, A.C., Todd, S.P., Haughton, P.D.W. (eds). Developments in Sedimentary Provenance Studies, Geological Society Special Publication 57. Geological Society, London, pp. 79-90.

Batten, D.J., 1996. Chapter 26A. Palynofacies and palaeonvironmental interpretation, in: Jansonius, J., McGregor, D.C. (eds). Palynology: Principles and Applications. American Association of Stratigraphic Palynologists Foundation, Los Angeles, pp. 1011–1064.

Bechtel, A., Gratzer, R., Sachsenhofer, R.F., Gusterhuber, J., Lücke, A., Püttmann, W., 2008. Biomarker and carbon isotope variation in coal and fossil wood of Central Europe through the Cenozoic. Palaeogeography, Palaeoclimatology, Palaeoecology 262, 166–175.

Beerling, D.J., 2000. Global terrestrial productivity in the Mesozoic era, in: Hart, M.B. (ed.). Climates: Past and Present, Special Publications 181. Geological Society, London, pp. 17–32.

Behar, F., Beaumont, V., De B. Penteado, H.L., 2001. Rock-Eval 6 technology: Performances and developments. Oil & Gas Science and Technology 56, 111–134. doi: 10.2516/ogst:2001013.

Behar, F., Lewan, M.D., Lorant, F., Vandenbroucke, M., 2003. Comparison of artificial maturation of lignite in hydrous and nonhydrous conditions. Organic Geochemistry 34, 575–600.

Behar, F., Vandenbroucke, M., Teerman, S., Hatcher, P., Leblond, C., Lerat, O., 1995. Experimental simulation of gas generation from coals and a marine kerogen. Chemical Geology 126, 247–260.

Belcher, C.M., New, S.L., Santín, C., Doerr, S.H., Dewhirst, R.A., Grosvenor, M.J., Hudspith, V.A., 2018. What can charcoal reflectance tell us about energy release in wildfires and the properties of pyrogenic carbon? Frontiers in Earth Science, 6, 169, 13 pp. doi: 10.3389/feart.2018.00169.

Benner, R., Hatcher, P.G., Hedges, J.I., 1990. Early diagenesis of mangrove leaves in a tropical estuary: Bulk chemical characterization using solid-state ^{13}C NMR and elemental analyses. Geochimica et Cosmochimica Acta 54, 2003–2013.

Benninghoff, W.S., 1962. Calculation of pollen and spore density in sediments by addition of exotic pollen in known quantities. Pollen et Spores 4, 332–333.

Berenstecher, P., Vivanco, L., Pérez, L.I., Ballaré, C.L., Austin, A.T., 2020. Sunlight doubles aboveground carbon loss in a seasonally dry woodland in Patagonia. Current Biology 30, 3243–3251.

Beringer, J., Hutley, L.B., Tapper, N.J., Cernusak, L.A., 2007. Savanna fires and their impact on net ecosystem productivity in North Australia. Global Change Biology 13, 990–1004. doi: 10.1111/j.1365-2486.2007.01334.x.

Berner, R.A., 1982. Burial of organic carbon and pyrite sulfur in the modern ocean: its geochemical and environmental significance. American Journal of Science 282, 451–473. doi: 10.2475/ajs.282.4.451.

Berner, R.A., 2009. Phanerozoic atmospheric oxygen: new results using the GEOCARBSULF model. American Journal of Science 309, 603–606.

Bhattarai, H., Saikawa, E., Wan, X., Zhu, H., Ram, K., Gao, S., Kang, S., Zhang, Q., Zhang, Y., Wu, G., Wang, X., Kawamura, K., Fu, P., Cong, Z., 2019. Levoglucosan as a tracer of biomass burning: Recent progress and perspectives. Atmospheric Research 220, 20–33.

Bianchi, T.S., Cui, X., Blair, N.E., Burdige, D.J., Eglinton, T.I., Galy, V., 2018. Centers of organic carbon burial and oxidation at the land-ocean interface. Organic Geochemistry 1151, 138–155.

Bird, M.I., Ascough, P.L., 2012. Isotopes in pyrogenic carbon: A review. Organic Geochemistry 42, 1529–1539.

Bird, M.I., Wynn, J.G., Saiz, G., Wurster, C.M., McBeath, A., 2015. The pyrogenic carbon cycle. Annual Review of Earth and Planetary Sciences 43, 273–298.

Bisutti, I., Hilke, I., Raessler, M., 2004. Determination of total organic carbon—an overview of current methods. Trends in Analytical Chemistry 23, 716–726. doi: 10.1016/j.trac.2004.09.003.

Black, B.A., Lamarque, J.-F., Shields, C.A., Elkins-Tanton, L.T., Kiehl, J.T., 2014. Acid rain and ozone depletion from pulsed Siberian Traps magmatism. Geology 42, 67–70. doi: https://doi.org/10.1130/G34875.1.

Blair, N.E., Aller, R.C., 2012. The fate of terrestrial organic carbon in the marine environment. Annual Review of Marine Science 4, 401–423.

Blair, N.E., Leithold, E.L., Brackley, H., Trustrum, N., Page, M., Childress, L., 2010. Terrestrial sources and export of particulate organic carbon in the Waipaoa sedimentary system: Problems, progress and processes. Marine Geology 270, 108–118.

Blattmann, T.M., 2022. Ideas and perspectives: Emerging contours of a dynamic exogenous kerogen cycle. Biogeosciences 19, 359–373.

Blattmann, T.M., Letsch, D., Eglinton, T.I., 2018. On the geological and scientific legacy of petrogenic organic carbon. American Journal of Science 318, 861–881. doi: 10.2475/08.2018.02.

Bolton, C.T., Lawrence, K.T., Gibbs, S.J., Wilson, P.A., Cleaveland, L.C., Herbert, T.D., 2010. Glacial–interglacial productivity changes recorded by alkenones and microfossils in late Pliocene eastern equatorial Pacific and Atlantic upwelling zones. Earth and Planetary Science Letters 295, 401–411.

Bonis, N.R., Ruhl, M., Kürschner, W.M., 2010. Climate change driven black shale deposition during the end-Triassic in the western Tethys. Palaeogeography, Palaeoclimatology, Palaeoecology 290, 151–159.

Bonny, A.P., 1972. A method for determining absolute pollen frequencies in lake sediments. The New Phytologist 71, 393–405.

Bouchez, J., Beyssac, O., Galy, V., Gaillardet, J., France-Lanord, C., Maurice, L., Moreira-Turcq, P., 2010. Oxidation of petrogenic organic carbon in the Amazon floodplain as a source of atmospheric CO_2. Geology 38, 255–258. doi: 10.1130/G30608.1.

Boulter, M.C., Riddick, A., 1986. Classification and analysis of palynodebris from the Palaeocene sediments of the Forties Field. Sedimentology 33, 871–886.

Boyce, C.K., Brodribb, T.J., Feild, T.S., Zwieniecki, M.A., 2009. Angiosperm leaf vein evolution was physiologically and environmentally transformative. Proceedings of the Royal Society B 276, 1771–1776.

Boyce, C.K., Ibarra, D.E., D'Antonio, M.P., 2023. What we talk about when we talk about the long-term carbon cycle. New Phytologist 237, 1550–1557. doi: 10.1111/nph.18665.

Boyce, C.K., Zwieniecki, M.A., 2012. Leaf fossil record suggests limited influence of atmospheric CO_2 on terrestrial productivity prior to angiosperm evolution. Proceedings of the National Academy of Sciences of the United States of America 109, 10403–10408. doi: 10.1073/pnas.1203769109.

Boyce, C.K., Zwieniecki, M.A., 2019. The prospects for constraining productivity through time with the whole-plant physiology of fossils. New Phytologist 223, 40–49.

Braadbaart, F., Poole, I., 2008. Morphological, chemical and physical changes during charcoalification of wood and its relevance to archaeological contexts. Journal of Archaeological Science 35, 2434–2445.

Bradley, J.A., Hülse, D., LaRowe, D.E., Arndt, S., 2022. Transfer efficiency of organic carbon in marine sediments. Nature Communications, 13, 7297, 8 pp. doi: 10.1038/s41467-022-35112-9.

Brett, M.T., Bunn, S.E., Chandra, S., Galloway, A.W.E., Guo, F., Kainz, M.J., Kankaala, P., Lau, D.C.P., Moulton, T.P., Power, M.E., Rasmussen, J.B., Taipale, S.J., Thorp, J.H., Wehr, J.D., 2017. How important are terrestrial organic carbon inputs for secondary production in freshwater ecosystems? Freshwater Biology 62, 833–853. doi: 10.1111/fwb.12909.

Brodribb, T.J., Feild, T.S., 2010. Leaf hydraulic evolution led a surge in leaf photosynthetic capacity during early angiosperm diversification. Ecology Letters 13, 175–183. doi: 10.1111/j.1461-0248.2009.01410.x.

Brodribb, T.J., Feild, T.S., Jordan, G.J., 2007. Leaf maximum photosynthetic rate and venation are linked by hydraulics. Plant Physiology 144, 1890–1898.

Broström, A., Nielsen, A.B., Gaillard, M.-J., Hjelle, K., Mazier, F., Binney, H., Bunting, J., Fyfe, R., Meltsov, V., Poska, A., Räsänen, S., Soepboer, W., von Stedingk, H., Suutari, H., Sugita, S., 2008. Pollen productivity estimates of key European plant taxa for quantitative reconstruction of past vegetation: a review. Vegetation History and Archaeobotany 17, 461–478.

Brown, A.V., Calver, C.R., Clark, M.J., Corbett, K.D., Everard, J.L., Cumming, G., Forsyth, S.M., Goscombe, B.D., Green, D., Green, G., McClenaghan, M.P., McNeill, A.W., Pemberton, J., Seymour, D.B., Vicary, M., Woolward, I., Worthing, M., Jackman, C., 2021. Geology of Tasmania Map, Geology of Tasmania 1:500 000, 5th ed.

Burdige, D.J., 2005. Burial of terrestrial organic matter in marine sediments: A re-assessment. Global Biogeochemical Cycles, 19, GB4011, 7 pp. doi: 10.1029/2004GB002368.

Burdige, D.J., 2007. Preservation of organic matter in marine sediments: Controls, mechanisms, and an imbalance in sediment organic carbon budgets? Chemistry Reviews 107, 467–485.

Burgess, S.D., Bowring, S., Shen, S.-z., 2014. High-precision timeline for Earth's most severe extinction. Proceedings of the National Academy of Sciences of the United States of America 111, 3316–3321.

Burnham, A.K., 2017. Van Krevelen diagrams, in: Sorkhabi, R. (ed.). Encyclopedia of Petroleum Geoscience, Encyclopedia of Earth Sciences Series. Springer, Cham, pp. 1–5.

Burnham, A.K., 2019. Kinetic models of vitrinite, kerogen, and bitumen reflectance. Organic Geochemistry 131, 50–59.

Buseck, P.R., Beyssac, O., 2014. From organic matter to graphite: Graphitization. Elements 10, 421–426. doi: 10.2113/gselements.10.6.421.

Buseck, P.R., Bo-Jun, H., 1985. Conversion of carbonaceous material to graphite during metamorphism. Geochimica et Cosmochimica Acta 49, 2003–2016.

Bustin, R.M., 1988. Sedimentology and characteristics of dispersed organic matter in Tertiary Niger Delta: origin of source rocks in a deltaic environment. American Association of Petroleum Geologists Bulletin 72, 277–298.

Canadell, J.G., Le Quéré, C., Raupach, M.R., Field, C.B., Buitenhuis, E.T., Ciais, P., Conway, T.J., Gillett, N.P., Houghton, R.A., Marland, G., 2007. Contributions to accelerating atmospheric CO_2 growth from economic activity, carbon intensity, and efficiency of natural sinks. Proceedings of the National Academy of Sciences of the United States of America 47, 18866–18870. doi: 10.1073/pnas.0702737104.

Canfield, D.E., 1994. Factors influencing organic carbon preservation in marine sediments. Chemical Geology 114, 315–329.

Carr, A.D., 1999. A vitrinite reflectance kinetic model incorporating overpressure retardation. Marine and Petroleum Geology 16, 355–377.

Catalán, N., Marcé, R., Kothawala, D.N., Tranvik, L.J., 2016. Organic carbon decomposition rates controlled by water retention time across inland waters. Earth-Science Reviews 123, 53–86. doi: 10.1038/NGEO2720.

Chapin, F.S., Woodwell, G.M., Randerson, J.T., Rastetter, E.B., Lovett, G.M., Baldocchi, D.D., Clark, D.A., Harmon, M.E., Schimel, D.S., Valentini, R., Wirth, C., Aber, J.D., Cole,

J.J., Goulden, M.L., Harden, J.W., Heimann, M., Howarth, R.W., Matson, P.A., McGuire, A.D., Melillo, J.M., Mooney, H.A., Neff, J.C., Houghton, R.A., Pace, M.L., Ryan, M.G., Running, S.W., Sala, O.E., Schlesinger, W.H., Schulze, E.-D., 2006. Reconciling carbon-cycle concepts, terminology, and methods. Ecosystems 9, 1041–1050. doi: 10.1007/s10021-005-0105-7.

Chevalier, M., Davis, B.A.S., Heiri, O., Seppä, H., Chase, B.M., Gajewski, K., Lacourse, T., Telford, R.J., Finsinger, W., Guiot, J., Kühl, N., Maezumi, S.Y., Tipton, J.R., Carter, V.A., Brussel, T., Phelps, L.N., Dawson, A., Zanon, M., Vallé, F., Nolan, C., Mauri, A., Vernal, A.d., Izumi, K., Holmström, L., Marsicek, J., Goring, S., Sommer, P.S., Chaput, M., Kupriyanov, D., 2020. Pollen-based climate reconstruction techniques for late Quaternary studies. Earth-Science Reviews, 210, 103384, 33 pp. doi: 10.1016/j.earscirev.2020.103384.

Childress, L.B., Jacobsen, S.D., 2017. High-pressure high-temperature Raman spectroscopy of kerogen: Relevance to subducted organic carbon. American Mineralogist 102, 391–403. doi: 10.2138/am-2017-5719.

Clark, J.S., Lynch, J., Stocks, B.J., Goldammer, J.G., 1998. Relationships between charcoal particles in air and sediments in west-central Siberia. The Holocene 8, 19-29.

Clymo, R.S., 1984. The limits to peat bog growth. Philosophical Transactions of the Royal Society B 303, 605–654.

Cole, J.J., Caraco, N.F., 2001. Carbon in catchments: connecting terrestrial carbon losses with aquatic metabolism. Marine & Freshwater Research 52, 101–110.

Cole, J.J., Carpenter, S.R., Pace, M.L., Van de Bogert, M.C., Kitchell, J.L., Hodgson, J.R., 2006. Differential support of lake food webs by three types of terrestrial organic carbon. Ecology Letters 9, 558–568. doi: 10.1111/j.1461-0248.2006.00898.x.

Cole, J.J., Prairie, Y.T., Caraco, N.F., McDowell, W.H., Tranvik, L.J., Striegl, R.G., Duarte, C.M., Kortelainen, P., Downing, J.A., Middelburg, J.J., Melack, J., 2007. Plumbing the global carbon cycle: Integrating inland waters into the terrestrial carbon budget. Ecosystems 10, 171–184.

Collins, A., 1990. The 1–10 Spore Colour Index (SCI) scale: a universally applicable colour maturation scale, based on graded, picked palynomorphs. Mededelingen Rijks Geologische Dienst 45, 39–47.

Colwell, F.S., D'Hondt, S., 2013. Nature and extent of the deep biosphere. Reviews in Mineralogy and Geochemistry 75, 547-574.

Combaz, A., 1964. Les palynofaciès. Revue de Micropaléontologie 7, 205–218.

Combaz, A., 1980. Les kérogènes vus au microscope, in: Durand, B. (ed.). Kerogen: Insoluble Organic Matter from Sedimentary Rocks. Éditions Technip, Paris, pp. 55–111.

Cooke, R.C., Rayner, A.D.M., 1984. Ecology of Saprotrophic Fungi. Longman, New York, 415 pp.

Cooles, G.P., Mackenzie, A.S., Quigley, T.M., 1986. Calculation of petroleum masses generated and expelled from source rocks. Organic Geochemistry 10, 235–245.

Cope, M.J., 1980. Physical and chemical properties of coalified and charcoalifled phytoclasts from some British Mesozoic sediments: An organic geochemical approach to palaeobotany. Physics and Chemistry of the Earth 12, 663–677.

Craig, A.J., 1972. Pollen influx to laminated sediments: A pollen diagram from northeastern Minnesota. Ecology 53, 46–57.

Curiale, J.A., 2017. Total organic carbon (TOC), in: Sorkhabi, R. (ed.). Encyclopedia of Petroleum Geoscience, Encyclopedia of Earth Sciences Series. Springer, Cham, pp. 1–5.

Curiale, J.A., Curtis, J.B., 2016. Organic geochemical applications to the exploration for source-rock reservoirs – A review. Journal of Unconventional Oil and Gas Resources 13, 11–31.

D’Antonio, M.P., Ibarra, D.E., Boyce, C.K., 2020. Land plant evolution decreased, rather than increased, weathering rates Geology 48, 29–33. doi: 10.1130/G46776.1.

Daly, A.R., Edman, J.D., 1987. Loss of organic carbon from source rocks during thermal maturation. AAPG Bulletin, 71, Search and Discovery article 60055 (2019), 14 pp.

Day, T.A., Bliss, M.S., 2020. Solar photochemical emission of CO_2 from leaf litter: Sources and significance to C loss. Ecosystems 23, 1344–1361. doi: 10.1007/s10021-019-00473-8.

Day, T.A., Bliss, M.S., Placek, S.K., Tomes, A.R., Guénon, R., 2019. Thermal abiotic emission of CO_2 and CH_4 from leaf litter and its significance in a photodegradation assessment. Ecosphere, 10, e02745, 24 pp. doi: 10.1002/ecs2.2745.

Day, T.A., Bliss, M.S., Tomes, A.R., Ruhland, C.T., Guénon, R., 2018. Desert leaf litter decay: coupling of microbial respiration, water soluble fractions and photodegradation. Global Change Biology 24, 5454–5470.

Demars, B.O.L., 2019. Hydrological pulses and burning of dissolved organic carbon by stream respiration. Limnology and Oceanography 64, 406–421. doi: 10.1002/lno.11048.

Dettmann, M.E., 1963. Upper Mesozoic microfloras from south-eastern Australia. Proceedings of the Royal Society of Victoria 77, 1–148.

Drake, T.W., Raymond, P.A., Spencer, R.G.M., 2018. Terrestrial carbon inputs to inland waters: A current synthesis of estimates and uncertainty. Limnology and Oceanography Letters 3, 132–142.

Du, P., Walling, D.E., 2012. Using ^{210}Pb measurements to estimate sedimentation rates on river floodplains. Journal of Environmental Radioactivity 103, 59–75.

Durand, B., 1980. Sedimentary organic matter and kerogen: Definition and quantitative importance of kerogen, in: Durand, B. (ed.). Kerogen: Insoluble Organic Matter from Sedimentary Rocks. Éditions Technip, Paris, pp. 13–34.

Duringer, P., Doubinger, J., 1985. La palynologie: un outil de characterization des facies marins et continentaux a la limite Muschelkalk Supérieur–Lettenkohle. Science Géologie Bulletin, Strasbourg 38, 19–34.

Elsik, W.C., 1966. Biologic degradation of fossil pollen grains and spores. Micropaleontology 12, 515–518.

Eshet, Y., Almogi-Labin, A., 1996. Calcareous nannofossils as paleoproductivity indicators in Upper Cretaceous organic-rich sequences in Israel. Marine Micropaleontology 29, 37–61.

Etienne, D., Jouffroy-Bapicot, I., 2014. Optimal counting limit for fungal spore abundance estimation using *Sporormiella* as a case study. Vegetation History and Archaeobotany 23, 743–749.

Fall, P.L., 1987. Pollen taphonomy in a canyon stream. Quaternary Research 28, 393–406.

Fang, J., Kato, C., Runko, G.M., Nogi, Y., Hori, T., Li, J., Morono, Y., Inagaki, F., 2017. Predominance of viable spore-forming piezophilic bacteria in high-pressure enrichment cultures from ~1.5 to 2.4 km-deep coal-bearing sediments below the ocean floor. Frontiers in Microbiology, 8, 137, 10 pp. doi: 10.3389/fmicb.2017.00137.

Felix, M., 2014. A comparison of equations commonly used to calculate organic carbon content and marine palaeoproductivity from sediment data. Marine Geology 347, 1–11.

Feng, D., Pohlman, J.W., Peckmann, J., Sun, Y., Hu, Y., Roberts, H.H., Chen, D., 2021. Contribution of deep-sourced carbon from hydrocarbon seeps to sedimentary organic carbon: Evidence from radiocarbon and stable isotope geochemistry. Chemical Geology, 585, 120572. doi: 10.1016/j.chemgeo.2021.120572.

Feng, X., Simpson, A.J., Wilson, K.P., Williams, D.D., Simpson, M.J., 2008. Increased cuticular carbon sequestration and lignin oxidation in response to soil warming. Nature Geoscience 1, 836–839.

Fielding, C.R., Frank, T.D., Tevyaw, A.P., Savatic, K., Vajda, V., McLoughlin, S., Mays, C., Nicoll, R.S., Bocking, M., Crowley, J.L., 2021. Sedimentology of the continental end-Permian extinction event in the Sydney Basin, eastern Australia. Sedimentology 68, 30–62. doi: 10.1111/sed.12782.

Foereid, B., Rivero, M.J., Primo, O., Ortiz, I., 2011. Modelling photodegradation in the global carbon cycle. Soil Biology and Biochemistry 43, 1383–1386.

Foster, C.B., 1975. Permian plant microfossils from the Blair Athol Coal Measures, central Queensland, Australia. Palaeontographica Abteilung B 154, 121–171.

France-Lanord, C., Derry, L.A., 1997. Organic carbon burial forcing of the carbon cycle from Himalayan erosion. Nature 390, 65–67.

Fraser, W.T., Watson, J.S., Sephton, M.A., Lomax, B.H., Harrington, G.J., Gosling, W.D., Self, S., 2014. Changes in spore chemistry and appearance with increasing maturity. Review of Palaeobotany and Palynology 201, 41–46.

Frey, S.D., 2019. Mycorrhizal fungi as mediators of soil organic matter dynamics. Annual Review of Ecology, Evolution, and Systematics 50, 237–259. doi: 10.1146/annurev-ecolsys-110617-062331.

Friedlingstein, P., Jones, M.W., O'Sullivan, M., Andrew, R.M., Bakker, D.C.E., Hauck, J., Le Quéré, C., Peters, G.P., Peters, W., Pongratz, J., Sitch, S., Canadell, J.G., Ciais, P., Jackson, R.B., Alin, S.R., Anthoni, P., Bates, N.R., Becker, M., Bellouin, N., Bopp, L., Chau, T.T.T., Chevallier, F., Chini, L.P., Cronin, M., Currie, K.I., Decharme, B., Djeutchouang, L.M., Dou, X., Evans, W., Feely, R.A., Feng, L., Gasser, T., Gilfillan, D., Gkritzalis, T., Grassi, G., Gregor, L., Gruber, N., Gürses, Ö., Harris, I., Houghton, R.A., Hurtt, G.C., Iida, Y., Ilyina, T., Luijkx, I.T., Jain, A., Jones, S.D., Kato, E., Kennedy, D., Klein Goldewijk, K., Knauer, J., Korsbakken, J.I., Körtzinger, A., Landschützer, P., Lauvset, S.K., Lefèvre, N., Lienert, S., Liu, J., Marland, G., McGuire, P.C., Melton, J.R., Munro, D.R., Nabel, J.E.M.S., Nakaoka, S.I., Niwa, Y., Ono, T., Pierrot, D., Poulter, B., Rehder, G., Resplandy, L., Robertson, E., Rödenbeck, C., Rosan, T.M., Schwinger, J., Schwingshackl, C., Séférian, R., Sutton, A.J., Sweeney, C., Tanhua, T., Tans, P.P., Tian, H., Tilbrook, B., Tubiello, F., van der Werf, G.R., Vuichard, N., Wada, C., Wanninkhof, R., Watson, A.J., Willis, D., Wiltshire, A.J., Yuan, W., Yue, C., Yue, X., Zaehle, S., Zeng, J., 2022. Global carbon budget 2021. Earth System Science Data 14, 1917–2005. doi: 10.5194/essd-14-1917-2022.

Frieling, J., Reichart, G.-J., Middelburg, J.J., Röhl, U., Westerhold, T., Bohaty, S.M., Sluijs, A., 2018. Tropical Atlantic climate and ecosystem regime shifts during the Paleocene–Eocene Thermal Maximum. Climate of the Past 14, 39–55.

Fritz, S.A., Eronen, J.T., Schnitzler, J., Hof, C., Janis, C.M., Mulch, A., Böhning-Gaese, K., Graham, C.H., 2016. Twenty-million-year relationship between mammalian diversity and

primary productivity. Proceedings of the National Academy of Sciences of the United States of America 113, 10908–10913. doi: 10.1073/pnas.1602145113.

Galvez, M.E., Fischer, W.W., Jaccard, S.L., Eglinton, T.I., 2020. Materials and pathways of the organic carbon cycle through time. Nature Geoscience 13, 535–546. doi: 10.1038/s41561-020-0563-8.

Gastaldo, R.A., 2012. Taphonomic controls on the distribution of palynomorphs in tidally influenced coastal deltaic settings. Palaios 27, 798–810.

Geller, A., 1986. Comparison of mechanisms enhancing biodegradability of refractory lake water constituents. Limnology & Oceanography 31, 755–764. doi: 10.4319/lo.1986.31.4.0755.

Ghsoub, M., Fakhri, M., Courp, T., Khalaf, G., Buscail, R., Ludwig, W., 2020. River signature over coastal area (Eastern Mediterranean): Grain size and geochemical analyses of sediments. Regional Studies in Marine Science, 35, 101169, 15 pp. doi: 10.1016/j.rsma.2020.101169.

Glasspool, I.J., Gastaldo, R.A., 2023. A baptism by fire: fossil charcoal from eastern Euramerica reveals the earliest (Homerian) terrestrial biota evolved in a flammable world. Journal of the Geological Society, 180, jgs2022-072, 17 pp. doi: 10.1144/jgs2022-072.

Glasspool, I.J., Scott, A.C., 2010. Phanerozoic atmospheric oxygen concentrations reconstructed from sedimentary charcoal. Nature Geoscience 3, 627–630. doi: 10.1038/NGEO923.

Gliksman, D., Haenel, S., Osem, Y., Yakir, D., Zangy, E., Preisler, Y., Grünzweig, J.M., 2018. Litter decomposition in Mediterranean pine forests is enhanced by reduced canopy cover. Plant and Soil 422, 317–329. doi: 10.1007/s11104-017-3366-y.

Goldring, R., T.R., A., Marshall, J.E.A., Gabbott, S., Jenkins, C.D., 1999. Towards an integrated study of the depositional environment of the Bencliff Grit (Upper Jurassic) of Dorset, in: Underhill, J.R. (ed.). Development, Evolution and Petroleum Geology of the Wessex Basin, Special Publications 133. Geological Society, London, pp. 355–372.

Goñi, M.A., Hedges, J.I., 1990. Potential applications of cutin-derived CuO reaction products for discriminating vascular plant sources in natural environments. Geochimica et Cosmochimica Acta 54, 3073–3081.

González-Pérez, J.A., González-Vila, F.J., Almendros, G., Knicker, H., 2004. The effect of fire on soil organic matter—a review. Environment International 30, 855–870.

Goodhue, R., Clayton, G., 2010. Palynomorph Darkness Index (PDI) – a new technique for assessing thermal maturity. Palynology 34, 147–156.

Gosling, W.D., Cornelissen, H.L., McMichael, C.N.H., 2019. Reconstructing past fire temperatures from ancient charcoal material. Palaeogeography, Palaeoclimatology, Palaeoecology 520, 128–137.

Graham, L.E., Trest, M.T., Cook, M.E., 2017. Acetolysis resistance of modern Fungi: testing attributions of enigmatic Proterozoic and early Paleozoic fossils. International Journal of Plant Sciences 178, 330–339. doi: 10.1086/690280.

Gravendyck, J., Schobben, M., Bachelier, J.B., Kürschner, W.M., 2020. Macroecological patterns of the terrestrial vegetation history during the end-Triassic biotic crisis in the central European Basin: A palynological study of the Bonenburg section (NW-Germany) and its supra-regional implications. Global and Planetary Change, 194, 103286.

Graz, Y., Di-Giovanni, C., Copard, Y., Elie, M., Faure, P., Laggoun Defarge, F., Lévèque, J., Michels, R., Olivier, J.E., 2011. Occurrence of fossil organic matter in modern environments: Optical, geochemical and isotopic evidence. Applied Geochemistry 26, 1302–1314.

Graz, Y., Di-Giovanni, C., Copard, Y., Laggoun-Défarge, F., Boussafir, M., Lallier-Vergès, E., Baillif, P., Perdereau, L., Simonneau, A., 2010. Quantitative palynofacies analysis as a new tool to study transfers of fossil organic matter in recent terrestrial environments. International Journal of Coal Geology 84, 49–62.

Grünzweig, J.M., De Boeck, H.J., Rey, A., Santos, M.J., Adam, O., Bahn, M., Belnap, J., Deckmyn, G., Dekker, S.C., Flores, O., Gliksman, D., Helman, D., Hultine, K.R., Liu, L., Meron, E., Michael, Y., Sheffer, E., Throop, H.L., Tzuk, O., Yakir, D., 2022. Dryland

mechanisms could widely control ecosystem functioning in a drier and warmer world. Nature Ecology & Evolution 6, 1064–1076. doi: 10.1038/s41559-022-01779-y.

Gudasz, C., Bastviken, D., Premke, K., Steger, K., Tranvik, L.J., 2012. Constrained microbial processing of allochthonous organic carbon in boreal lake sediments. Limnology and Oceanography 57, 163–175.

Gudasz, C., Ruppenthal, M., Kalbitz, K., Cerli, C., Fiedler, S., Oelmann, Y., Andersson, A., Karlsson, J., 2017. Contributions of terrestrial organic carbon to northern lake sediments. Limnology and Oceanography Letters 2, 218–227. doi: 10.1002/lol2.10051.

Guillemette, F., von Wachenfeldt, E., Kothawala, D.N., Bastviken, D., Tranvik, L.J., 2017. Preferential sequestration of terrestrial organic matter in boreal lake sediments. Journal of Geophysical Research: Biogeosciences 122, 863–874. doi: 10.1002/2016JG003735.

Gupta, N.S., Collinson, M.E., Briggs, D.E.G., Evershed, R.P., Pancost, R.D., 2006. Reinvestigation of the occurrence of cutan in plants: implications for the leaf fossil record. Paleobiology 32, 432–449.

Gurung, K., Field, K.J., Batterman, S.A., Goddéris, Y., Donnadieu, Y., Porada, P., Taylor, L.L., Mills, B.J.W., 2022. Climate windows of opportunity for plant expansion during the Phanerozoic. Nature Communications, 13, 4530. doi: 10.1038/s41467-022-32077-7.

Gurung, K., Field, K.J., Batterman, S.A., Poulton, S.W., Mills, B.J.W., 2024. Geographic range of plants drives long-term climate change. Nature Communications, 15, 1805, 7 pp. doi: 10.1038/s41467-024-46105-1.

Haberle, S.G., Maslin, M.A., 1999. Late Quaternary vegetation and climate change in the Amazon Basin based on a 50,000 year pollen record from the Amazon Fan, ODP Site 932. Quaternary Research 51, 27–38.

Hackley, P.C., 2017. Vitrinite reflectance analysis, in: Sorkhabi, R. (ed.). Encyclopedia of Petroleum Geoscience, Encyclopedia of Earth Sciences Series. Springer, Cham, pp. 1–14.

Hage, S., Romans, B.W., Peploe, T.G.E., Poyatos-Moré, M., Ardakani, O.H., Bell, D., Englert, R.G., Kaempfe-Droguett, S.A., Nesbit, P.R., Sherstan, G., Synnott, D.P.,

Hubbard, S.M., 2022. High rates of organic carbon burial in submarine deltas maintained on geological timescales. Nature Geoscience 15, 919–924. doi: 10.1038/s41561-022-01048-4.

Hammer, Ø., Harper, D.A.T., Ryan, P.D., 2001. PAST: Paleontological statistics software package for education and data analysis. Palaeontologia Electronica, 4, 4, 9 pp.

Han, M., Feng, J., Chen, Y., Sun, L., Fu, L., Zhu, B., 2021. Mycorrhizal mycelial respiration: A substantial component of soil respired CO_2. Soil Biology and Biochemistry, 163, 108454. doi: 10.1016/j.soilbio.2021.108454.

Hardy, M.J., Wrenn, J.H., 2009. Palynomorph distribution in modern tropical deltaic and shelf sediments–Mahakam Delta, Borneo, Indonesia. Palynology 33, 19–42. doi: 10.1080/01916122.2009.9989681.

Hart, G.F., 1960. Microfloral investigations of the Lower Coal Measures (K2), Ketewaka-Mchuchuma Coalfield, Tanganyika Bulletin of the Tanganyika Geological Survey 30, 18.

Hartkopf-Fröder, C., Königshof, P., Littke, R., Schwarzbauer, J., 2015. Optical thermal maturity parameters and organic geochemical alteration at low grade diagenesis to anchimetamorphism: A review. International Journal of Coal Geology 150–151, 74–119.

Hartnett, H.E., Keil, R.G., Hedges, J.I., Devol, A.H., 1998. Influence of oxygen exposure time on organic carbon preservation in continental margin sediments. Nature 391, 572–574.

Hatcher, P.G., 1988. Dipolar-dephasing ^{13}C NMR studies of decomposed wood and coalified xylem tissue: Evidence for chemical structural changes associated with defunctionalization of lignin structural units during coalification. Energy & Fuels 2, 48–58.

Hatcher, P.G., Clifford, D.J., 1997. The organic geochemistry of coal: from plant materials to coal. Organic Geochemistry 27, 251–274. doi: https://doi.org/10.1016/S0146-6380(97)00051-X.

Head, M.J., 1992. Zygospores of the Zygnemataceae (Division Chlorophyta) and other freshwater algal spores from the uppermost Pliocene St. Erth Beds of Cornwall, southwestern England. Micropaleontology 38, 237–260.

Head, M.J., Norris, G., Mudie, P.J., 1989. Palynology and dinocyst stratigraphy of the upper Miocene and lowermost Pliocene, ODP Leg 105, Site 646, Labrador Sea, in: Srivastava, S.P., Arthur, M., Clement, B., etal. (eds). Proceedings of the Ocean Drilling Program, Scientific Results 105, pp. 423-451.

Hedges, J.I., 1988. Polymerization of humic substances in natural environments, in: Frimmel, F.H., Christman, R.F. (eds). Humic Substances and their Role in the Environment, Dahlem Workshop Reports. Wiley, Chichester, pp. 45–58.

Hedges, J.I., 1992. Global biogeochemical cycles: progress and problems. Marine Chemistry 39, 67–93.

Hedges, J.I., Hu, F.S., Devol, A.H., Hartnett, H.E., Tsamakis, E., Keil, R.G., 1999. Sedimentary organic matter preservation; a test for selective degradation under oxic conditions. American Journal of Science 299, 529–555. doi: 10.2475/ajs.299.7-9.529.

Hedges, J.I., Parker, P.L., 1976. Land-derived organic matter in surface sediments from the Gulf of Mexico. Geochimica et Cosmochimica Acta 40, 1019–1029.

Heimhofer, U., Hochuli, P.A., Herrle, J.O., Weissert, H., 2006. Contrasting origins of Early Cretaceous black shales in the Vocontian basin: Evidence from palynological and calcareous nannofossil records. Palaeogeography, Palaeoclimatology, Palaeoecology 235, 93–109.

Helgeson, H.C., Richard, L., McKenzie, W.F., Norton, D.L., Schmitt, A., 2009. A chemical and thermodynamic model of oil generation in hydrocarbon source rocks. Geochimica et Cosmochimica Acta 73, 594–695. doi: 10.1016/j.gca.2008.03.004.

Hennessee, E.L., Blakeslee, P.J., Hill, J.M., 1986. The distributions of organic carbon and sulfur in surficial sediments of the Maryland portion of Chesapeake Bay. Journal of Sedimentary Petrology 56, 674–683.

Hilton, R.G., West, A.J., 2020. Mountains, erosion and the carbon cycle. Nature Reviews Earth & Environment 1, 284–299. doi: 10.1038/s43017-020-0058-6.

Hjelle, K.L., Sugita, S., 2011. Estimating pollen productivity and relevant source area of pollen using lake sediments in Norway: How does lake size variation affect the estimates? The Holocene 22, 313–324.

Hobo, N., Makaske, B., Middelkoop, H., Wallinga, J., 2010. Reconstruction of fl oodplain sedimentation rates: a combination of methods to optimize estimates. Earth Surface Processes and Landforms 35, 1499–1515. doi: 10.1002/esp.1986.

Holmes, P., 1994. The sorting of spores and pollen by water: experimental and field evidence, in: Traverse, A. (ed.). Sedimentation of Organic Particles. Cambridge University Press, Cambridge, U.K., pp. 9–32.

Horner, T.J., Little, S.H., Conway, T.M., Farmer, J.R., Hertzberg, J.E., Janssen, D.J., Lough, A.J.M., McKay, J.L., Tessin, A., Galer, S.J.G., Jaccard, S.L., Lacan, F., Paytan, A., Wuttig, K., Members, G.P.B.P.W.G., 2021. Bioactive trace metals and their isotopes as paleoproductivity proxies: An assessment using GEOTRACES-era data. Global Biogeochemical Cycles, 35, e2020GB006814, 1–86 pp. doi: 10.1029/2020GB006814.

Hudspith, V.A., Belcher, C.M., Kelly, R., Hu, F.S., 2015. Charcoal reflectance reveals early Holocene boreal deciduous forests burned at high intensities. PLOS One, 10, e0120835, 11 pp. doi: 10.1371/journal.pone.0120835.

Hunt, J.M., 1972. Distribution of carbon in crust of Earth. AAPG Bulletin 56, 2273–2277. doi: 10.1306/819A4206-16C5-11D7-8645000102C1865D.

Hunt, J.M., 1996. Petroleum Geochemistry and Geology, 2nd ed. W. H. Freeman and Company, New York, 743 pp.

Hutton, A., Bharati, S., Robl, T., 1994. Chemical and petrographic classification of kerogen macerals. Energy and Fuels 8, 1478–1488.

Ittekot, V., 1988. Global trends in the nature of organic matter in river suspensions. Nature 332, 436–438.

Iversen, J., 1936. Sekundäres Pollen als Fehlerquelle: Eine Korrektionsmethode zur Pollenanalyse minerogener Sedimente. Danmarks geologiske Undersøgelse 2, 3–24.

Jardine, P.E., Fraser, W.T., Lomax, B.H., Sephton, M.A., Shanahan, T.M., Miller, C.S., Gosling, W.D., 2016. Pollen and spores as biological recorders of past ultraviolet irradiance. Scientific Reports, 6, 39269, 8 pp. doi: 10.1038/srep39269.

Jarvie, D.M., 1991. Total Organic Carbon (TOC) analysis in: Merrill, R.K. (ed.). Source and Migration Processes and Evaluation Techniques. American Association of Petroleum Geologists, Tulsa, pp. 113–118.

Jarvie, D.M., 2012. Shale resource systems for oil and gas: Part 1—Shale-gas resource systems, in: Breyer, J.A. (ed.). Shale Reservoirs—Giant Resources for the 21st Century, AAPG Memoirs 97. The American Association of Petroleum Geologists, Tulsa, pp. 69–87.

Jarvie, D.M., 2014. Components and processes affecting producibility and commerciality of shale resource systems. Geologica Acta 12, 307–325. doi: 10.1344/GeologicaActa2014.12.4.3.

Jetz, W., Fine, P.V.A., 2012. Global gradients in vertebrate diversity predicted by historical area-productivity dynamics and contemporary environment. PLoS Biology, 10, e1001292, 11 pp. doi: 10.1371/journal.pbio.1001292.

Jiang, H., Pan, Y., Liang, J., Yang, Y., Chen, Q., Lv, M., Pang, L., He, W., Tian, X., 2022. UV radiation doubles microbial degradation of standing litter in a subtropical forest. Journal of Ecology 110, 2156–2166. doi: 10.1111/1365-2745.13939.

Johnson, M.D., Thomas, B.W., 1884. Report on the committee on the microscopic organisms in the bowlder clays of Chicago and vicinity. Bulletin of the Chicago Academy of Sciences 1, 35–40.

Jørgensen, B.B., Wenzhöfer, F., Egger, M., Glud, R.N., 2022. Sediment oxygen consumption: Role in the global marine carbon cycle. Earth-Science Reviews, 228, 103987, 35 pp. doi: 10.1016/j.earscirev.2022.103987.

Jung, M., Ilmberger, J., Mangini, A., Emeis, K.-C., 1997. Why some Mediterranean sapropels survived burn-down (and others did not). Marine Geology 141, 51–60.

Kaiho, K., Yatsu, S., Oba, M., Gorjan, P., Casier, J.-G., Ikeda, M., 2013. A forest fire and soil erosion event during the Late Devonian mass extinction. Palaeogeography, Palaeoclimatology, Palaeoecology 392, 272–280.

Kalks, F., Noren, G., Mueller, C.W., Helfrich, M., Rethemeyer, J., Don, A., 2021. Geogenic organic carbon in terrestrial sediments and its contribution to total soil carbon. Soil 7, 347–362.

Karp, A.T., Holman, A.I., Hopper, P., Grice, K., Freeman, K.H., 2020. Fire distinguishers: Refined interpretations of polycyclic aromatic hydrocarbons for paleo-applications. Geochimica et Cosmochimica Acta 289, 93–113.

Kasin, I., Ohlson, M., 2013. An experimental study of charcoal degradation in a boreal forest. Soil Biology and Biochemistry 65, 39–49.

Katsev, S., Crowe, S.A., 2015. Organic carbon burial efficiencies in sediments: The power law of mineralization revisited. Geology 43, 607–610.

Keenan, T.F., Williams, C.A., 2018. The terrestrial carbon sink. Annual Review of Environment and Resources 43, 219–243. doi: 10.1146/annurev-environ-102017-030204.

Keiluweit, M., Nico, P.S., Kleber, M., Fendorf, S., 2016. Are oxygen limitations under recognized regulators of organic carbon turnover in upland soils? Biogeochemistry 127, 157–171.

Kieber, D.J., McDaniel, J., Mopper, K., 1989. Photochemical source of biological substrates in sea water: implications for carbon cycling. Nature 341, 637–640.

King, J.Y., Brandt, L.A., Adair, E.C., 2012. Shedding light on plant litter decomposition: advances, implications and new directions in understanding the role of photodegradation. Biogeochemistry 111, 57–81. doi: 10.1007/s10533-012-9737-9.

Kinkel, H., Baumann, K.-H., Čepek, M., 2000. Coccolithophores in the equatorial Atlantic Ocean: response to seasonal and Late Quaternary surface water variability. Marine Micropaleontology 39, 87–112.

Kirkland, D.W., 1967. Method of calculating absolute spore and pollen frequency. Oklahoma Geology Notes 27, 98–100.

Klotzbücher, T., Kaiser, K., Guggenberger, G., Gatzek, C., Kalbitz, K., 2011. A new conceptual model for the fate of lignin in decomposing plant litter. Ecology 92, 1052–1062.

Kodrans-Nsiah, M., März, C., Harding, I.C., Kasten, S., Zonneveld, K.A.F., 2009. Are the Kimmeridge Clay deposits affected by “burn-down” events? Palynological and geochemical studies on a 1 metre long section from the Upper Kimmeridge Clay Formation (Dorset, UK). Sedimentary Geology 222, 301–313.

Kolka, R., Weishampel, P., Fröberg, M., 2008. Measurement and importance of dissolved organic carbon, in: Hoover, C.M. (ed.). Field Measurements for Forest Carbon Monitoring: A Landscape-Scale Approach. Springer Science, New York, pp. 171–176.

Kuhry, P., Vitt, D.H., 1996. Fossil carbon/nitrogen ratios as a measure of peat decomposition. Ecology 77, 271–275.

Lamoureux-Var, V., Bouton, N., Espitalié, J., Benoit, Y., 2023. Chapter 2. Principles and methods, in: Baudin, F. (ed.). The Rock-Eval Method: Principles and Application, The Surface of the Lithosphere and the Biosphere. ISTE, London, pp. 11–27.

Landais, P., Michels, R., Elie, M., 1994. Are time and temperature the only constraints to the simulation of organic matter maturation? Organic Geochemistry 22, 617–630.

LaRowe, D.E., Arndt, S., Bradley, J.A., Estes, E.R., Hoarfrost, A., Lang, S.Q., Lloyd, K.G., Mahmoudi, N., Orsi, W.D., Shah Walterl, S.R., Steen, A.D., Zhao, R., 2020. The fate of organic carbon in marine sediments - New insights from recent data and analysis. Earth-Science Reviews, 204, 103146.

Lee, H., Rahn, T., Throop, H., 2012. An accounting of C-based trace gas release during abiotic plant litter degradation. Global Change Biology 18, 1185–1195. doi: 10.1111/j.1365-2486.2011.02579.x.

Lehmann, J., Gaunt, J., Rondon, M., 2006. Bio-char sequestration in terrestrial ecosystems—A review. Mitigation and Adaptation Strategies for Global Change 11, 403–427. doi: 10.1007/s11027-005-9006-5.

Lei, Y., Shen, J., Algeo, T.J., Servais, T., Feng, Q., Yu, J., 2019. Phytoplankton (acritarch) community changes during the Permian-Triassic transition in South China. Palaeogeography, Palaeoclimatology, Palaeoecology 519, 84–94.

Lenton, T.M., Daines, S.J., Mills, B.J.W., 2018. COPSE reloaded: An improved model of biogeochemical cycling over Phanerozoic time. Earth-Science Reviews 178, 1–28.

Levine, J.S., Cofer, W.R.I., Cahoon, D.R.J., Winstead, E.L., 1995. Biomass burning: a driver for global change. Environmental Science and Technology 29, 120A–125A.

Li, F.-S., Phyo, P., Jacobowitz, J., Hong, M., Weng, J.-K., 2019. The molecular structure of plant sporopollenin. Nature Plants 5, 41–46.

Li, J., Crowe, S.A., Miklesh, D., Kistner, M., Canfield, D.E., Katsev, S., 2012. Carbon mineralization and oxygen dynamics in sediments with deep oxygen penetration, Lake Superior. Limnology and Oceanography 57, 1634–1650.

Li, M., Peng, C., Wang, M., Xue, W., Zhang, K., Wang, K., Shi, G., Zhu, Q., 2017. The carbon flux of global rivers: A re-evaluation of amount and spatial patterns. Ecological Indicators 80, 40–51.

Li, Y., Zhang, H., Tu, C., Fu, C., Xue, Y., Luo, Y., 2016. Sources and fate of organic carbon and nitrogen from land to ocean: Identified by coupling stable isotopes with C/N ratio. Estuarine, Coastal and Shelf Science 181, 114–122.

Lin, D., Xi, Z., Tang, S., Lash, G.G., Li, J., Gou, Q., Zhang, K., Mei, X., Wang, K., 2024. Enrichment mechanism of organic matter and silicon in lower Cambrian shale of the Yangtze Platform. Palaeogeography, Palaeoclimatology, Palaeoecology, 648, 112282, 1–21 pp. doi: 10.1016/j.palaeo.2024.112282.

Linder, H.P., Lehmann, C.E.R., Archibald, S., Osborne, C.P., Richardson, D.M., 2018. Global grass (Poaceae) success underpinned by traits facilitating colonization, persistence and habitat transformation. Biological Reviews 93, 1125–1144. doi: 10.1111/brv.12388.

Liu, F., Peng, H., Marshall, J.E.A., Lomax, B.H., Bomfleur, B., Kent, M.S., Fraser, W.T., Jardine, P.E., 2023. Dying in the sun: Direct evidence for elevated UV-B radiation at the end-Permian mass extinction. Science Advances, 9, eabo6102.

Liu, Z., Dreybrodt, W., 2015. Significance of the carbon sink produced by H_2O–carbonate–CO_2–aquatic phototroph interaction on land. Science Bulletin 60, 182–191.

Lloret, E., Dessert, C., Pastor, L., Lajeunesse, E., Crispi, O., Gaillardet, J., Benedetti, M.F., 2013. Dynamic of particulate and dissolved organic carbon in small volcanic mountainous tropical watersheds. Chemical Geology 351, 229–244.

Loisel, J., Gallego-Sala, A.V., Amesbury, M.J., Magnan, G., Anshari, G., Beilman, D.W., Benavides, J.C., Blewett, J., Camill, P., Charman, D.J., Chawchai, S., Hedgpeth, A., Kleinen, T., Korhola, A., Large, D., Mansilla, C.A., Müller, J., van Bellen, S., West, J.B., Yu, Z., Bubier, J.L., Garneau, M., Moore, T., Sannel, A.B.K., Page, S., Väliranta, M., Bechtold, M., Brovkin, V., Cole, L.E.S., Chanton, J.P., Christensen, T.R., Davies, M.A., De Vleeschouwer, F., Finkelstein, S.A., Frolking, S., Gałka, M., Gandois, L., Girkin, N., Harris, L.I., Heinemeyer, A., Hoyt, A.M., Jones, M.C., Joos, F., Juutinen, S., Kaiser, K., Lacourse, T., Lamentowicz, M., Larmola, T., Leifeld, J., Lohila, A., Milner, A.M., Minkkinen, K., Moss, P., Naafs, B.D.A., Nichols, J., O'Donnell, J., Payne, R., Philben, M., Piilo, S., Quillet, A., Ratnayake, A.S., Roland, T.P., Sjögersten, S., Sonnentag, O., Swindles, G.T., Swinnen, W., Talbot, J., Treat, C., Valach, A.C., Wu, J., 2021. Expert assessment of future vulnerability of the global peatland carbon sink. Nature Climate Change 11, 70–77. doi: 10.1038/s41558-020-00944-0.

Lopes, G., Pereira, Z., Fernandes, P., Wicander, R., Matos, J.X., Rosa, D., Oliveira, J.T., 2014. The significance of reworked palynomorphs (middle Cambrian to Tournaisian) in the Visean Toca da Moura Complex (South Portugal). Implications for the geodynamic evolution of Ossa Morena Zone. Review of Palaeobotany and Palynology 200, 1–23.

Lorant, F., Behar, F., 2002. Late generation of methane from mature kerogens. Energy & Fuels 16, 412–427.

Lorenz, K., Lal, R., 2010. Carbon Sequestration in Forest Ecosystems. Springer, Dordrecht, 277 pp.

Lovett, G.M., Cole, J.J., Pace, M.L., 2006. Is net ecosystem production equal to ecosystem carbon accumulation? Ecosystems 9, 152–155. doi: 10.1007/s10021-005-0036-3.

Maffre, P., Godderis, Y., Pohl, A., Donnadieu, Y., Carretier, S., Le Hir, G., 2022. The complex response of continental silicate rock weathering to the colonization of the continents by vascular plants in the Devonian. American Journal of Science 322, 461–492. doi: 10.2475/03.2022.02.

Maher, L.J., 1981. Statistics for microfossil concentration measurements employing samples spiked with marker grains. Review of Palaeobotany and Palynology 32, 153–191.

Mählmann, R.F., Bozkaya, Ö., Potel, S., Le Bayon, R., Šegvić, B., Nieto, F., 2012. The pioneer work of Bernard Kübler and Martin Frey in very low-grade metamorphic terranes: paleo-geothermal potential of variation in Kübler-Index/organic matter reflectance correlations. A review. Swiss Journal of Geosciences 105, 121–152. doi: 10.1007/s00015-012-0115-3.

Mählmann, R.F., Le Bayon, R., 2016. Vitrinite and vitrinite like solid bitumen reflectance in thermal maturity studies: Correlations from diagenesis to incipient metamorphism in different geodynamic settings. International Journal of Coal Geology 157, 52–73.

Mander, L., Punyasena, S.W., 2018. Fossil Pollen and Spores in Paleoecology, in: Croft, D.A., Su, D.F., Simpson, S.W. (eds). Methods in Paleoecology: Reconstructing Cenozoic Terrestrial Environments and Ecological Communities. Springer International Publishing, Cham, pp. 215–234.

Mao, S., Buxton Eglinton, L., Whelan, J., Liu, L., 1994. Thermal evolution of sediments from Leg 139, Middle Valley, Juan de Fuca Ridge: an organic petrological study. Proceedings of the Ocean Drilling Program, Scientific Results 139, 495–508.

Marinho, O.A., Martinelli, L.A., Duarte-Neto, P.J., Mazzi, E.A., King, J.Y., 2020. Photodegradation influences litter decomposition rate in a humid tropical ecosystem, Brazil. Science of the Total Environment, 715, 136601. doi: 10.1016/j.scitotenv.2020.136601.

Marshall, J.E.A., Lakin, J., Troth, I., Wallace-Johnson, S.M., 2020. UV-B radiation was the Devonian-Carboniferous boundary terrestrial extinction kill mechanism. Science Advances, 6, eaba0768.

Marshall, J.E.A., Yule, B.L., 1999. Spore colour measurement, in: Jones, T.P., Rowe, N.P. (eds). Fossil Plants and Spores: Modern Techniques. Geological Society, London, pp. 165–168.

Martín-Closas, C., Permanyer, A., Vila, M.-J., 2005. Palynofacies distribution in a lacustrine basin. Geobios 38, 197–210.

Massicotte, P., Frenette, J.-J., 2011. Spatial connectivity in a large river system: resolving the sources and fate of dissolved organic matter. Ecological Applications 21, 2600–2617.

Mastalerz, M., Drobniak, A., Stankiewicz, A.B., 2018. Origin, properties, and implications of solid bitumen in source-rock reservoirs: A review. International Journal of Coal Geology 195, 14–36.

Mastalerz, M., Schimmelmann, A., Lis, G.P., Drobniak, A., Stankiewicz, A., 2012. Influence of maceral composition on geochemical characteristics of immature shale kerogen: Insight from density fraction analysis. International Journal of Coal Geology 103, 60–69.

Mays, C., Amores, M., Mays, A., *pre-print*. Improved absolute abundance estimates from spatial count data with simulation and microfossil case studies. PLOS One. doi: 10.48550/arXiv.2406.10921.

Mays, C., McLoughlin, S., 2022. End-Permian burnout: The role of Permian-Triassic wildfires in extinction, carbon cycling and environmental change in eastern Gondwana. Palaios 37, 292–317. doi: 10.2110/palo.2021.051.

Mays, C., McLoughlin, S., Frank, T.D., Fielding, C.R., Slater, S.M., Vajda, V., 2021. Lethal microbial blooms delayed freshwater ecosystem recovery following the end-Permian extinction. Nature Communications, 12, 5511, 11 pp. doi: 10.1038/s41467-021-25711-3.

Mays, C., Stilwell, J.D., 2013. Pollen and spore biostratigraphy of the mid-Cretaceous Tupuangi Formation, Chatham Islands, New Zealand. Review of Palaeobotany and Palynology 192, 79–102. doi: 10.1016/j.revpalbo.2012.12.008.

Mays, C., Vajda, V., Frank, T.D., Fielding, C.R., Nicoll, R.S., Tevyaw, A.P., McLoughlin, S., 2020. Refined Permian–Triassic floristic timeline reveals early collapse and delayed

recovery of south polar terrestrial ecosystems. GSA Bulletin 132, 1489–1513. doi: 10.1130/B35355.1.

McElwain, J.C., Matthaeus, W.J., Barbosa, C., Chondrogiannis, C., O'Dea, K., Jackson, B., Knetge, A.B., Kwasniewska, K., Nair, R., White, J.D., 2024. Functional traits of fossil plants. New Phytologist.

Mertens, K.N., Price, A.M., Pospelova, V., 2012. Determining the absolute abundance of dinoflagellate cysts in recent marine sediments II: Further tests of the *Lycopodium* marker-grain method. Review of Palaeobotany and Palynology 184, 74–81.

Mertens, K.N., Verhoeven, K., Verleye, T., Louwye, S., Amorim, A., Ribeiro, S., Deaf, A.S., Harding, I.C., De Schepper, S., González, C., Kodrans-Nsiah, M., De Vernal, A., Henry, M., Radi, T., Dybkjaer, K., Poulsen, N.E., Feist-Burkhardt, S., Chitolie, J., Heilmann-Clausen, C., Londeix, L., Turon, J.-L., Marret, F., Matthiessen, J., McCarthy, F.M.G., Prasad, V., Pospelova, V., Kyffin Hughes, J.E., Riding, J.B., Rochon, A., Sangiorgi, F., Welters, N., Sinclair, N., Thun, C., Soliman, A., Van Nieuwenhove, N., Vink, A., Young, M., 2009. Determining the absolute abundance of dinoflagellate cysts in recent marine sediments: The *Lycopodium* marker-grain method put to the test. Review of Palaeobotany and Palynology 157, 238–252.

Meyers, P.A., 1997. Organic geochemical proxies of paleoceanographic, paleolimnologic, and paleoclimatic processes. Organic Geochemistry 27, 213–250.

Meyers, P.A., Leenheer, M.J., Bourbonniere, R.A., 1995. Diagenesis of vascular plant organic matter components during burial in lake sediments. Aquatic Geochemistry 1, 35–52.

Middelburg, J.J., 1989. A simple rate model for organic matter decomposition in marine sediments. Geochimica et Cosmochimica Acta 53, 1577–1581. doi: 10.1016/0016-7037(89)90239-1.

Middelburg, J.J., Vlug, T., Jaco, F., van der Nat, W.A., 1993. Organic matter mineralization in marine systems. Global and Planetary Change 8, 47–58. doi: 10.1016/0921-8181(93)90062-S.

Mildenhall, D.C., 1994. Palynological Reconnaissance of Early Cretaceous to Holocene Sediments, Chatham Islands, New Zealand. Institute of Geological and Nuclear Sciences Limited, Lower Hutt, New Zealand, 204 pp.

Miller, M.F., Knepprath, N.E., Cantrill, D.J., Francis, J.E., Isbell, J.L., 2016. Highly productive polar forests from the Permian of Antarctica. Palaeogeography Palaeoclimatology Palaeoecology 441, 292–304.

Misch, D., Gross, D., Hawranek, G., Horsfield, B., Klaver, J., Mendez-Martin, F., Urai, J.L., Vranjes-Wessely, S., Sachsenhofer, R.F., Schmatz, J., Li, J., Zou, C., 2019. Solid bitumen in shales: Petrographic characteristics and implications for reservoir characterization. International Journal of Coal Geology 205, 14–31.

Modica, C.J., Lapierre, S.G., 2012. Estimation of kerogen porosity in source rocks as a function of thermal transformation: Example from the Mowry Shale in the Powder River, Basin of Wyoming. AAPG Bulletin 96, 87–108.

Moody, C.S., Worrall, F., 2017. Modeling rates of DOC degradation using DOM composition and hydroclimatic variables. Journal of Geophysical Research: Biogeosciences 122, 1175–1191. doi: 10.1002/2016JG003493.

Moorhead, D.L., Callaghan, T., 1994. Effects of increasing ultraviolet B radiation on decomposition and soil organic matter dynamics: A synthesis and modelling study. Biology and Fertility of Soils 18, 19–26.

Moss, P.T., Kershaw, A.P., Grindrod, J., 2005. Pollen transport and deposition in riverine and marine environments within the humid tropics of northeastern Australia. Review of Palaeobotany and Palynology 134, 55–69.

Mottl, O., Flantua, S.G.A., Bhatta, K.P., Felde, V.A., Giesecke, T., Goring, S., Grimm, E.C., Haberle, S., Hooghiemstra, H., Ivory, S., Kuneš, P., Wolters, S., Seddon, A.W.R., Williams, J.W., 2021. Global acceleration in rates of vegetation change over the past 18,000 years. Science 372, 860–864.

Myers, T.S., Tabor, N.J., Jacobs, L.L., Mateus, O., 2012. Estimating soil pCO_2 using paleosol carbonates: implications for the relationship between primary productivity and faunal richness in ancient terrestrial ecosystems. Paleobiology 38, 585–604.

Nelsen, M.P., DiMichele, W.A., Peters, S.E., Boyce, C.K., 2016. Delayed fungal evolution did not cause the Paleozoic peak in coal production. Proceedings of the National Academy of Sciences of the United States of America 113, 2442–2447.

Neves, R., Sullivan, H.J., 1964. Modification of fossil spore exines associated with the presence of pyrite crystals. Micropaleontology 10, 443–452.

Newman, J.W., Parker, P.L., Behrens, E.W., 1973. Organic carbon isotope ratios in Quaternary cores from the Gulf of Mexico. Geochimica et Cosmochimica Acta 37, 225–238.

Niklas, K.J., Pratt, L.M., 1980. Evidence for lignin-like constituents in early Silurian (Llandoverian) plant fossils. Science 209, 396–397. doi: 10.1126/science.209.4454.396.

Nuñez Otaño, N.B., Bianchinotti, M.V., Saparrat, M.C.N., 2021. Palaeomycology: a modern mycological view of fungal palynomorphs, in: Marret, F., O'Keefe, J., Osterloff, P., Pound, M., Shumilovskikh, L. (eds). Applications of Non-Pollen Palynomorphs: from Palaeoenvironmental Reconstructions to Biostratigraphy, Geological Society, London, Special Publications 511. The Geological Society of London, London, pp. 91–120.

Okiongbo, K.S., Aplin, A.C., Larter, S.R., 2005. Changes in Type II kerogen density as a function of maturity: Evidence from the Kimmeridge Clay Formation. Energy & Fuels 19, 2495–2499.

Ollivier, S., Jéhan, P., Olivier-Jimenez, D., Lambert, F., Boustie, J., Lohézic-Le Dévéhat, F., Le Yondre, N., 2022. New insights into the Van Krevelen diagram: Automated molecular formula determination from HRMS for a large chemical profiling of lichen extracts. Phytochemical Analysis 33, 1111–1120. doi: 10.1002/pca.3163.

Olsen, P.E., 1986. A 40-million-year lake record of early Mesozoic orbital climatic forcing. Science 234, 842–848.

Pace, M.L., Lovett, G.M., 2021. Primary production: The foundation of ecosystems, in: Weathers, K.C., Strayer, D.L., Likens, G.E. (eds). Fundamentals of Ecosystem Science, 2nd ed. Academic Press, London, pp. 29–53.

Pacton, M., Gorin, G., Fiet, N., 2009. Occurrence of photosynthetic microbial mats in a Lower Cretaceous black shale (central Italy): a shallow-water deposit. Facies 55, 401–419. doi: 10.1007/s10347-009-0178-4.

Pacton, M., Gorin, G.E., Vasconcelos, C., 2011. Amorphous organic matter—Experimental data on formation and the role of microbes. Review of Palaeobotany and Palynology 166, 253–267.

Pancotto, V.A., Sala, O.E., Robson, T.M., Caldwell, M.M., Scopel, A.L., 2005. Direct and indirect effects of solar ultraviolet-B radiation on long-term decomposition. Global Change Biology 11, 1982–1989. doi: 10.1111/j.1365-2486.2005.1027.x.

Pandey, S., Holt, K., 2018. Modern pollen distribution and its relationship to vegetation from the south-western part of the Ganges-Brahmaputra Delta, India. Palynology 42, 20–27. doi: 10.1080/01916122.2017.1298541.

Pearce, M.A., Jarvis, I., Tocher, B.A., 2009. The Cenomanian–Turonian boundary event, OAE2 and palaeoenvironmental change in epicontinental seas: New insights from the dinocyst and geochemical records. Palaeogeography, Palaeoclimatology, Palaeoecology 280, 207–234.

Pedersen, T.F., Calvert, S.E., 1990. Anoxia vs. productivity: What controls the formation of organic-carbon-rich sediments and sedimentary rocks? The American Association of Petroleum Geologists Bulletin 74, 454–466.

Pelet, R., 1983. Preservation of sedimentary organic matter, in: Bjøroy, M. (ed.). Advances in Organic Geochemistry, 1981: Proceedings of the 10th International Meeting on Organic Geochemistry, University of Bergen, Norway, 14–18 September, 1981. John Wiley & Sons, Chichester, pp. 241–250.

Perdue, E.M., Ritchie, J.D., 2003. Dissolved organic matter in freshwaters. Treatise on Geochemistry 5, 273–318. doi: 10.1016/B0-08-043751-6/05080-5.

Perrotti, A.G., Ramiadantsoa, T., O'Keefe, J., Nuñez Otaño, N., 2022. Uncertainty in coprophilous fungal spore concentration estimates. Frontiers in Ecology and Evolution 10, 7. doi: 10.3389/fevo.2022.1086109.

Peters, K.E., Magoon, L.B., Bird, K.J., Valin, Z.C., Keller, M.A., 2006. North Slope, Alaska: Source rock distribution, richness, thermal maturity, and petroleum charge. AAPG Bulletin 90, 261–292.

Petersen, H.I., 2002. A re-consideration of the "oil window" for humic coal and kerogen type III source rocks. Journal of Petroleum Geology 25, 407–432.

Petersen, H.I., Lindström, S., 2012. Synchronous wildfire activity rise and mire deforestation at the Triassic–Jurassic boundary. PLOS One, 7, e47236. doi: 10.1371/journal.pone.0047236.

Phillips, L., 1972. An application of fluorescence microscopy to the problem of derived pollen in British Pleistocene deposits. New Phytologist 71, 755–762.

Planavsky, N.J., Fakhraee, M., Bolton, E.W., Reinhard, C.T., Isson, T.T., Zhang, S., Mills, B.J.W., 2022. On carbon burial and net primary production through Earth's history. American Journal of Science 322, 413–460. doi: 10.2475/03.2022.01.

Poorter, H., Niinemets, Ü., Poorter, L., Wright, I.J., Villar, R., 2009. Causes and consequences of variation in leaf mass per area (LMA): a meta-analysis. New Phytologist 182, 565–588. doi: 10.1111/j.1469-8137.2009.02830.x.

Poorter, L., Bongers, F., 2006. Leaf traits are good predictors of plant performance across 53 rain forest species. Ecology 87, 1733–1743.

Prahl, F.G., Cowie, G.L., De Lange, G.J., Sparrow, M.A., 2003. Selective organic matter preservation in "burn-down" turbidites on the Madeira Abyssal Plain. Paleoceanography and Paleoclimatology, 18, 1052, 13 pp. doi: 10.1029/2002PA000853.

Prentice, I.C., Harrison, S.P., Bartlein, P.J., 2011. Global vegetation and terrestrial carbon cycle changes after the last ice age. New Phytologist 189, 988–998. doi: 10.1111/j.1469-8137.2010.03620.x.

Prescott, C.E., 2010. Litter decomposition: what controls it and how can we alter it to sequester more carbon in forest soils? Biogeochemistry 101, 133–149. doi: 10.1007/s10533-010-9439-0.

Price, A.M., Gurdebeke, P.R., Mertens, K.N., Pospelova, V., 2016. Determining the absolute abundance of dinoflagellate cysts in recent marine sediments III: Identifying the source of *Lycopodium* loss during palynological processing and further testing of the *Lycopodium* marker-grain method. Review of Palaeobotany and Palynology 226, 78–90.

Price, L.C., 1983. Geologic time as a parameter in organic metamorphism and vitrinite reflectance as an absolute paleogeothermometer. Journal of Petroleum Geology 6, 5–37. doi: 10.1111/j.1747-5457.1983.tb00260.x.

Price, P.B., Sowers, T., 2004. Temperature dependence of metabolic rates for microbial growth, maintenance, and survival. Proceedings of the National Academy of Sciences of the United States of America 101, 4631–4636. doi: 10.1073/pnas.0400522101.

Pross, J., Link, E., Ruf, M., Aigner, T., 2006. Delineating sequence stratigraphic patterns in deeper ramp carbonates: Quantitative palynofacies data from the Upper Jurassic (Kimmeridgian) of southwest Germany. Journal of Sedimentary Research 76, 524–538.

Radbourne, A.D., Ryves, D.B., Anderson, N.J., Scott, D.R., 2017. The historical dependency of organic carbon burial efficiency. Limnology and Oceanography 62, 1480–1497. doi: 10.1002/lno.10512.

Raiswell, R., Berner, R.A., 1987. Organic carbon losses during burial and thermal maturation of normal marine shales. Geology 15, 853–856.

Raymond, P.A., Spencer, R.G.M., 2015. Riverine DOM, in: Hansell, D.A., Carlson, C.A. (eds). Biogeochemistry of Marine Dissolved Organic Matter, 2nd ed. Elsevier, London, pp. 509–533.

Regal, R.R., Cushing, E.J., 1979. Confidence intervals for absolute pollen counts. Biometrics 35, 557–565.

Reichart, G.-J., Brinkhuis, H., 2003. Late Quaternary *Protoperidinium* cysts as indicators of paleoproductivity in the northern Arabian Sea. Marine Micropaleontology 49, 303–315.

Reid, C.M., Forsyth, S.M., Clarke, M.J., Bacon, C., 2014. The Parmeener Supergroup—Late Carboniferous to Triassic, in: Corbett, K.D., Quilty, P.G., Calver, C.R. (eds). Geological Evolution of Tasmania, Geological Society of Australia Special Publications 24. Geological Society of Australia (Tasmania Division), Hobart, pp. 363–384.

Remy, W., Taylor, T.N., Hass, H., Kerp, H., 1994. Four-hundred-million-year-old vesicular arbuscular mycorrhizae. Proceedings of the National Academy of Sciences of the United States of America 91, 11841–11843.

Repasch, M., Scheingross, J.S., Hovius, N., Lupker, M., Wittmann, H., Haghipour, N., Gröcke, D.R., Orfeo, O., Eglinton, T.I., Sachse, D., 2021. Fluvial organic carbon cycling regulated by sediment transit time and mineral protection. Nature Geoscience 14, 842–848.

Repeta, D.J., 2015. Chemical characterization and cycling of dissolved organic matter, in: Hansell, D.A., Carlson, C.A. (eds). Biogeochemistry of Marine Dissolved Organic Matter, 2nd ed. Academic Press, London, pp. 21–63.

Retallack, G.J., 2001. Soils of the Past: An Introduction to Paleopedology, 2nd ed. Blackwell Science, Oxford, U.K., 420 pp.

Retallack, G.J., Veevers, J.J., Morante, R., 1996. Global coal gap between Permian–Triassic extinction and Middle Triassic recovery of peat-forming plants. GSA Bulletin 108, 195–207.

Richter, D.D., Markewitz, D., Trumbore, S.E., Wells, C.G., 1999. Rapid accumulation and turnoverof soil carbon in a re-establishing forest. Nature 400, 56–58.

Riding, J.B., 2021. A guide to preparation protocols in palynology. Palynology 45, 1–110. doi: 10.1080/01916122.2021.1878305.

Rivas-Ubach, A., Liu, Y., Bianchi, T.S., Tolić, N., Jansson, C., Paša-Tolić, L., 2018. Moving beyond the van Krevelen diagram: A new stoichiometric approach for compound classification in organisms. Analytical Chemistry 90, 6152−6160.

Robert, P., 1988. Organic Metamorphism and Geothermal History: Microscopic Study of Organic Matter and Thermal Evolution of Sedimentary Basins. D. Reidel Publishing, Dordrecht, 311 pp.

Robinson, D., 2007. Implications of a large global root biomass for carbon sink estimates and for soil carbon dynamics. Proceedings of the Royal Society B 274.

Robl, T.L., Rimmer, S.M., Barron, L.S., 1992. Organic petrography of Mississippian and Devonian shales in east-central Kentucky. Fuel 71, 267–271.

Robl, T.L., Taulbee, D.N., Barron, L.S., Jones, W.C., 1987. Petrologic chemistry of a Devonian Type II kerogen. Energy & Fuels 1, 507–513.

Rothman, D.H., 2024. Slow closure of Earth's carbon cycle. Proceedings of the National Academy of Sciences of the United States of America, 121, e2310998121, 12 pp. doi: 10.1073/pnas.2310998121.

Royer, D.L., Donnadieu, Y., Park, J., Kowalczyk, J., Goddéris, Y., 2014. Error analysis of CO_2 and O_2 estimates from the long-term geochemical model GEOCARBSULF. American Journal of Science 314, 1259–1283. doi: 10.2475/09.2014.01.

Rozema, J., Broekman, R.A., Blokker, P., Meijkamp, B.B., de Bakker, N., van de Staaij, J., van Beem, A., Ariese, F., Kars, S.M., 2001. UV-B absorbance and UV-B absorbing compounds (para-coumaric acid) in pollen and sporopollenin: the perspective to track historic UV-B levels. Journal of Photochemistry and Photobiology B: Biology 62, 108–117.

Ruf, M., Link, E., Pross, J., Aigner, T., 2005. Integrated sequence stratigraphy: Facies, stable isotope and palynofacies analysis in a deeper epicontinental carbonate ramp (Late Jurassic, SW Germany). Sedimentary Geology 175, 391–414.

Ruhl, M., Hesselbo, S.P., Hinnov, L., Jenkyns, H.C., Xu, W., Riding, J.B., Storm, M., Minisini, D., Ullmann, C.V., Leng, M.J., 2016. Astronomical constraints on the duration of the Early Jurassic Pliensbachian Stage and global climatic fluctuations. Earth and Planetary Science Letters 455, 149–165.

Saint-Laurent, D., Lavoie, L., Drouin, A., St-Laurent, J., Ghaleb, B., 2010. Floodplain sedimentation rates, soil properties and recent flood history in southern Québec. Global and Planetary Change 70, 76–91.

Santín, C., Doerr, S.H., Preston, C.M., González-Rodríguez, G., 2015. Pyrogenic organic matter production from wildfires: a missing sink in the global carbon cycle. Global Change Biology 21, 1621–1633. doi: 10.1111/gcb.12800.

Sarkanen, K.V., Ludwig, C.H., 1971. Lignins, Occurrence, Formation, Structure and Reactions. John Wiley & Sons, New York, 916 pp.

Scheingross, J.S., Hovius, N., Dellinger, M., Hilton, R.G., Repasch, M., Sachse, D., Gröcke, D.R., Vieth-Hillebrand, A., Turowski, J.M., 2019. Preservation of organic carbon during active fluvial transport and particle abrasion. Geology 47, 958–962. doi: 10.1130/G46442.1.

Scheingross, J.S., Repasch, M.N., Hovius, N., Sachse, D., Lupker, M., Fuchs, M., Halevy, I., Gröcke, D.R., Golombek, N.Y., Haghipour, N., Eglinton, T.I., Orfeo, O., Schleicher, A.M., 2021. The fate of fluvially-deposited organic carbon during transient floodplain storage. Earth and Planetary Science Letters, 561, 116822, 13 pp.

Schlesinger, W.H., Melack, J.M., 1981. Transport of organic carbon in the world's rivers. Tellus 33, 172–187. doi: 10.3402/tellusa.v33i2.10706.

Schlünz, B., Schneider, R.R., 2000. Transport of terrestrial organic carbon to the oceans by rivers: re-estimating flux- and burial rates. International Journal of Earth Sciences 88, 599–606.

Schmidt, M.W.I., Torn, M.S., Abiven, S., Dittmar, T., Guggenberger, G., Janssens, I.A., Kleber, M., Kögel-Knabner, I., Lehmann, J., Manning, D.A.C., Nannipieri, P., Rasse, D.P., Weiner, S., Trumbore, S.E., 2011. Persistence of soil organic matter as an ecosystem property. Nature 478, 49–56. doi: 10.1038/nature10386.

Schnyder, J., Stetten, E., Baudin, F., Pruski, A.M., Martinez, P., 2017. Palynofacies reveal fresh terrestrial organic matter inputs in the terminal lobes of the Congo deep-sea fan. Deep-Sea Research Part II 142, 91–108.

Schoepfer, S.D., Shen, J., Wei, H., Tyson, R.V., Ingall, E., Algeo, T.J., 2015. Total organic carbon, organic phosphorus, and biogenic barium fluxes as proxies for paleomarine productivity. Earth-Science Reviews 149, 23–52.

Schowalter, T.T., 1979. Mechanics of secondary hydrocarbon migration and entrapment. AAPG Bulletin 63, 723–760.

Schumacher, B.A., 2002. Methods for the determination of total organic carbon (TOC) in soils and sediments. United States Environmental Protection Agency Environmental Sciences Division National Exposure Research Laboratory, Las Vegas, 23 pp.

Schwarzkopf, T.A., 1993. Model for prediction of organic carbon content in possible source rocks. Marine and Petroleum Geology 10, 478–492.

Scott, A.C., 2010. Charcoal recognition, taphonomy and uses in palaeoenvironmental analysis. Palaeogeography, Palaeoclimatology, Palaeoecology 291, 11–39. doi: https://doi.org/10.1016/j.palaeo.2009.12.012.

Scott, A.C., Glasspool, I.J., 2007. Observations and experiments on the origin and formation of inertinite group macerals. International Journal of Coal Geology 70, 53–66.

Self, S., Schmidt, A., Mather, T.A., 2014. Emplacement characteristics, time scales, and volcanic gas release rates of continental flood basalt eruptions on Earth in: Keller, G., Kerr, A.C. (eds). Volcanism, Impacts, and Mass Extinctions: Causes and Effects, GSA Special Papers 505. Geological Society of America, Boulder, pp. 319–337.

Senftle, J.T., Landis, C.R., McLaughlin, R.L., 1993. Organic petrographic approach to kerogen characterization, in: Engel, M.H., Macko, S.A. (eds). Organic Geochemistry: Principles and Applications. Plenum Press, New York, pp. 355–374.

Shen, J., Schoepfer, S.D., Feng, Q., Zhou, L., Yu, J., Song, H., Wei, H., Algeo, T.J., 2015. Marine productivity changes during the end-Permian crisis and Early Triassic recovery. Earth-Science Reviews 149, 136–162.

Shepard, F.P., 1956. Marginal sediments of Mississippi Delta. American Association of Petroleum Geologists Bulletin 40, 2537–2623.

Shi, Z., Allison, S.D., He, Y., Levine, P.A., Hoyt, A.M., Beem-Miller, J., Zhu, Q., Wieder, W.R., Trumbore, S., Randerson, J.T., 2020. The age distribution of global soil carbon inferred from radiocarbon measurements. Nature Geoscience 13, 555–559. doi: 10.1038/s41561-020-0596-z.

Silva, R.L., Mendonça Filho, J.G., Azerêdo, A.C., Duarte, L.V., 2014. Palynofacies and TOC analysis of marine and non-marine sediments across the Middle–Upper Jurassic boundary in the central-northern Lusitanian Basin (Portugal). Facies 60, 255–276.

Singh, N., Abiven, S., Torn, M.S., Schmidt, M.W.I., 2012. Fire-derived organic carbon in soil turns over on a centennial scale. Biogeosciences 9, 2847–2857. doi: 10.5194/bg-9-2847-2012.

Slatt, R.M., O'Brien, N.R., 2011. Pore types in the Barnett and Woodford gas shales: Contribution to understanding gas storage and migration pathways in fine-grained rocks. AAPG Bulletin 95, 2017–2030.

Smart, M.S., Filippelli, G., Gilhooly III, W.P., Marshall, J.E.A., Whiteside, J.H., 2023. Enhanced terrestrial nutrient release during the Devonian emergence and expansion of forests: Evidence from lacustrine phosphorus and geochemical records. GSA Bulletin 135, 1879–1898. doi: 10.1130/B36384.1.

Sobek, S., Durisch-Kaiser, E., Zurbrügg, R., Wongfun, N., Wessels, M., Pasche, N., Wehrli, B., 2009. Organic carbon burial efficiency in lake sediments controlled by oxygen exposure time and sediment source. Limnology and Oceanography 54, 2243–2254.

Spina, A., Cirilli, S., Sorci, A., Schito, A., Clayton, G., Corrado, S., Fernandes, P., Galasso, F., Montesi, G., Pereira, Z., Rashidi, M., Rettori, R., 2021. Assessing thermal maturity through a multi-proxy approach: A case study from the Permian Faraghan Formation (Zagros Basin, southwest Iran). Geosciences, 11, 484, 28 pp. doi: 10.3390/geosciences11120484.

Stanley, E.A., 1965. Use of reworked pollen and spores for determining the Pleistocene–Recent and the intra-Pleistocene boundaries. Nature 206, 289–291.

Stein, R., 1986a. Organic carbon and sedimentation rate—further evidence for anoxic deep-water conditions in the Cenomanian/Turonian Atlantic Ocean. Marine Geology 72, 199–209.

Stein, R., 1986b. Surface-water paleo-productivity as inferred from sediments deposited in oxic and anoxic deep-water environments of the Mesozoic Atlantic Ocean. Mitteilungen Geologisch-Paläontologisches Institut, Universität Hamburg 60, 55–70.

Steiner, S., Ahsan, S.A., Raina, I., Dasgupta, S., Lis, G.P., 2016. Interpreting total organic carbon TOC in source rock oil plays, Abu Dhabi International Petroleum Exhibition & Conference (November 7–10, 2016), Abu Dhabi, p. 18.

Steinthorsdottir, M., Woodward, F.I., Surlyk, F., McElwain, J.C., 2012. Deep-time evidence of a link between elevated CO_2 concentrations and perturbations in the hydrological cycle via drop in plant transpiration Geology 40, 815–818.

Stockmarr, J., 1971. Tablets with spores used in absolute pollen analysis. Pollen et Spores 13, 615–621.

Streel, M., Bless, M.J.M., 1980. Occurrence and significance of reworked palynomorphs, in: Bless, M.J.M., Bouckaert, J., Paproth, E. (eds). Pre-Permian around the Brabant Massif in Belgium, the Netherlands and Germany 32. Mededelingen Rijks Geologische Dienst, pp. 69–80.

Strömberg, C.A.E., 2011. Evolution of grasses and grassland ecosystems. Annual Review of Earth and Planetary Sciences 39, 517–544. doi: 10.1146/annurev-earth-040809-152402.

Strother, S.L., Salzmann, U., Sangiorgi, F., Bijl, P.K., Pross, J., Escutia, C., Salabarnada, A., Pound, M.J., Voss, J., Woodward, J., 2017. A new quantitative approach to identify reworking in Eocene to Miocene pollen records from offshore Antarctica using red fluorescence and digital imaging. Biogeosciences 14, 2089–2100.

Suárez-Ruiz, I., Flores, D., Graciano Mendonça Filho, J., Hackley, P.C., 2012. Review and update of the applications of organic petrology: Part 1, geological applications. International Journal of Coal Geology 99, 54–112.

Sugita, S., 2007. Theory of quantitative reconstruction of vegetation I: pollen from large sites REVEALS regional vegetation composition. Holocene 2, 229–242.

Svensen, H., Planke, S., Chevallier, L., Malthe-Sørenssen, A., Corfu, F., Jamtveit, B., 2007. Hydrothermal venting of greenhouse gases triggering Early Jurassic global warming. Earth and Planetary Science Letters 256, 554–566.

Svensen, H.H., Frolov, S., Akhmanov, G.G., Polozov, A.G., Jerram, D.A., Shiganova, O.V., Melnikov, N.V., Iyer, K., Planke, S., 2018. Sills and gas generation in the Siberian Traps. Philosophical Transactions of the Royal Society A, 376, 20170080. doi: 10.1098/rsta.2017.0080.

Sweeney, J.J., Burnham, A.K., 1990. Evaluation of a simple model of vitrinite reflectance based on chemical kinetics. AAPG Bulletin 74, 1559–1570. doi: 10.1306/0C9B251F-1710-11D7-8645000102C1865D.

Tabor, N.J., Myers, T.S., 2015. Paleosols as indicators of paleoenvironment and paleoclimate. Annual Review of Earth & Planetary Sciences 43, 333–361. doi: 10.1146/annurev-earth-060614-105355.

Tahoun, S.S., Deaf, A.S., Gentzis, T., Carvajal-Ortiz, H., 2018. Modified RGB-based kerogen maturation index (KMI): Correlation and calibration with classical thermal maturity indices. International Journal of Coal Geology 190, 70–83.

Tang, W., Llort, J., Weis, J., Perron, M.M.G., Basart, S., Li, Z., Sathyendranath, S., Jackson, T., Sanz Rodriguez, E., Proemse, B.C., Bowie, A.R., Schallenberg, C., Strutton, P.G., Matear, R., Cassar, N., 2021. Widespread phytoplankton blooms triggered by 2019–2020 Australian wildfires. Nature, 597, 370–375 pp. doi: 10.1038/s41586-021-03805-8.

Taylor, G.H., Teichmüller, M., Davis, A., Diessel, C.F.K., Littke, R., Robert, P., 1998. Organic Petrology. Borntraeger, Berlin-Stuttgart, 704 pp.

Taylor, T.N., Krings, M., Taylor, E., 2015. Fungal diversity in the fossil record, in: McLaughlin, D.J., Spatafora, J.W. (eds). The Mycota VII Part B, Systematics and Evolution, 2nd ed. Springer-Verlag, Berlin, pp. 259–278.

Theuerkauf, M., Couwenberg, J., 2021. Pollen productivity estimates strongly depend on assumed pollen dispersal II: Extending the ERV model. The Holocene 32, 1233–1250.

Theuerkauf, M., Couwenberg, J., Kuparinen, A., Liebscher, V., 2016. A matter of dispersal: REVEALSinR introduces state-of-the-art dispersal models to quantitative vegetation reconstruction. Vegetation History and Archaeobotany 25, 541–553.

Thomas, S.C., Martin, A.R., 2012. Carbon content of tree tissues: A synthesis. Forests 3, 332–352. doi: 10.3390/f3020332.

Thomsen, U., Thamdrup, B., Stahl, D.A., Canfield, D.E., 2004. Pathways of organic carbon oxidation in a deep lacustrine sediment, Lake Michigan. Limnology and Oceanography 49, 2046–2057.

Tilston, E.L., Philippa, L., Ascough, P.L., Garnett, M.H., Bird, M.I., 2016. Quantifying charcoal degradation and negative priming of soil organic matter with a ^{14}C-dead tracer. Radiocarbon 58, 905–919. doi: 10.1017/RDC.2016.45.

Tissot, B.P., Welte, D.H., 1984. Petroleum Formation and Occurrence, 2nd ed. Springer Verlag, Berlin, 699 pp.

Trager, E.A., 1924. Kerogen and its relation to the origin of oil. AAPG Bulletin 8, 301–311. doi: 10.1306/3D93266E-16B1-11D7-8645000102C1865D.

Trask, P.D., 1939. Organic content of Recent marine sediments, in: Trask, P.D. (ed.). Recent Marine Sediments. American Association of Petroleum Geologists, Tulsa, pp. 428–453.

Traverse, A., 2007. Paleopalynology, 2nd ed. Springer, Dordrecht, 813 pp.

Traverse, A., Ginsburg, R.N., 1966. Palynology of the surface sediments of Great Bahama Bank, as related to water movement and sedimentation. Marine Geology 4, 417–459. doi: 10.1016/0025-3227(66)90010-7.

Tribovillard, N., Algeo, T.J., Lyons, T., Riboulleau, A., 2006. Trace metals as paleoredox and paleoproductivity proxies: An update. Chemical Geology 232, 12–32.

Tyson, R.V., 1989. Late Jurassic palynofacies trends, Piper and Kimmeridge Clay Formations, UK onshore and northern North Sea, in: Batten, D.J., Keen, M.C. (eds).

Northwest European Micropalaeontology and Palynology. Ellis Horwood, Chichester, pp. 135–172.

Tyson, R.V., 1995. Sedimentary Organic Matter: Organic Facies and Palynofacies. Chapman & Hall, London, 615 pp.

Tyson, R.V., 2001. Sedimentation rate, dilution, preservation and total organic carbon: some results of a modelling study. Organic Geochemistry 32, 333–339.

Tyson, R.V., 2005. The “productivity versus preservation” controversy: Cause, flaws, and resolution, in: Harris, N.B. (ed.). The Deposition of Organic-Carbon-Rich Sediments: Models, Mechanisms, and Consequences 82. SEPM Society for Sedimentary Geology, Tulsa, pp. 17–33.

Vajda, V., McLoughlin, S., Mays, C., Frank, T., Fielding, C.R., Tevyaw, A., Lehsten, V., Bocking, M., Nicoll, R.S., 2020. End-Permian (252 Mya) deforestation, wildfires and flooding—an ancient biotic crisis with lessons for the present. Earth and Planetary Science Letters, 529, 115875, 13 pp. doi: 10.1016/j.epsl.2019.115875.

van Bergen, P.F., Collinson, M.E., Briggs, D.E.G., de Leeuw, J.W., Scott, A.C., Evershed, R.P., Finch, P., 1995. Resistant biomacromolecules in the fossil record. Acta Botanica Neerlandica 44, 319–342.

van de Schootbrugge, B., Gollner, S., 2013. Altered primary production during mass-extinction events, in: Bush, A.M., Pruss, S.B., Payne, J.L. (eds). Ecosystem Paleobiology and Geobiology, The Paleontological Society Papers 19. The Paleontological Society, Bethesda, pp. 87–114.

van de Schootbrugge, B., van der Weijst, C.M.H., Hollaar, T.P., Vecoli, M., Strother, P.K., Kuhlmann, N., Thein, J., Visscher, H., van Konijnenburg-van Cittert, H., Schobben, M.A.N., Sluijs, A., Lindström, S., 2020. Catastrophic soil loss associated with end-Triassic deforestation. Earth-Science Reviews, 210, 103332, 18 pp. doi: 10.1016/j.earscirev.2020.103332.

van der Velde, I.R., van der Werf, G.R., Houweling, S., Maasakkers, J.D., Borsdorff, T., Landgraf, J., Tol, P., van Kempen, T.A., van Hees, R., Hoogeveen, R., Veefkind, J.P.,

Aben, I., 2021. Vast CO_2 release from Australian fires in 2019–2020 constrained by satellite. Nature 597, 366–369. doi: 10.1038/s41586-021-03712-y.

van der Werf, G.R., Randerson, J.T., Collatz, J., Giglio, L., 2003. Carbon emissions from fires in tropical and subtropical ecosystems. Global Change Biology 9, 547–562.

van der Werf, G.R., Randerson, J.T., Giglio, L., van Leeuwen, T.T., Chen, Y., Rogers, B.M., Mu, M., van Marle, M.J.E., Morton, D.C., Collatz, G.J., Yokelson, R.J., Kasibhatla, P.S., 2017. Global fire emissions estimates during 1997–2016. Earth System Science Data 9, 697–720. doi: 10.5194/essd-9-697-2017.

van Krevelen, D.W., 1950. Graphical-statistical method for the study of structure and reaction processes of coal. Fuel 29, 269–284.

van Soelen, E.E., Kürschner, W.M., 2018. Late Permian to Early Triassic changes in acritarch assemblages and morphology in the Boreal Arctic: New data from the Finnmark Platform. Palaeogeography Palaeoclimatology Palaeoecology 505, 120–127.

van Soelen, E.E., Twitchett, R.J., Kürschner, W.M., 2018. Salinity changes and anoxia resulting from enhanced run-off during the late Permian global warming and mass extinction event. Climate of the Past 14, 441–453. doi: 10.5194/cp-14-441-2018.

Vandenbroucke, M., Bordenave, M.L., Durand, B., 1993. Transformation of organic matter with increasing burial of sediments and the formation of petroleum in source rocks, in: Bordenave, M.L. (ed.). Applied Petroleum Geochemistry. Editions Technip, Paris, pp. 101–122.

Vandenbroucke, M., Largeau, C., 2007. Kerogen origin, evolution and structure. Organic Geochemistry 38, 719–833.

Versteegh, G.J.M., Zonneveld, K.A.F., 2002. Use of selective degradation to separate preservation from productivity. Geology 30, 615–618.

Versteegh, G.J.M., Zonneveld, K.A.F., de Lange, G.J., 2010. Selective aerobic and anaerobic degradation of lipids and palynomorphs in the Eastern Mediterranean since the onset of sapropel S1 deposition. Marine Geology 278, 177–192.

Vigano, I., Röckmann, T., Holzinger, R., van Dijk, A., Keppler, F., Greule, M., Brand, W.A., Geilmann, H., van Weelden, H., 2009. The stable isotope signature of methane emitted from plant material under UV irradiation. Atmospheric Environment 43, 5637–5646.

Vigano, I., van Weelden, H., Holzinger, R., Keppler, F., McLeod, A., Röckmann, T., 2008. Effect of UV radiation and temperature on the emission of methane from plant biomass and structural components. Biogeosciences 5, 937–947.

Wagner, T., 1999. Petrology of organic matter in modern and late Quaternary deposits of the Equatorial Atlantic: climatic and oceanographic links. International Journal of Coal Geology 39, 155–184. doi: 10.1016/S0166-5162(98)00044-5.

Wagner, T., Zabel, M., Dupont, L., Holtvoeth, J., Schubert, C.J., 2003. Terrigenous signals in sediments of the low latitude Atlantic—Implications for environmental variations during the Late Quarternary: Part I: Organic carbon, in: Wefer, G., Mulitza, S., Ratmeyer, V. (eds). The South Atlantic in the Late Quaternary: Reconstruction of Material Budgets and Current Systems. Springer-Verlag, Berlin, pp. 295–322.

Wang, J., Liu, L., Wang, X., Chen, Y., 2015. The interaction between abiotic photodegradation and microbial decomposition under ultraviolet radiation. Global Change Biology 21, 2095–2104.

Wang, Q., Li, Y., Utley, J.E.P., Gardner, J., Liu, B., Hu, J., Shao, L., Wang, X., Gao, F., Liu, D., Li, H., Jiang, Z., Worden, R.H., 2023. Terrestrial dominance of organic carbon in an Early Cretaceous syn-rift lake and its correlation with depositional sequences and paleoclimate. Sedimentary Geology, 455, 106472, 25 pp. doi: 10.1016/j.sedgeo.2023.106472.

Wang, X.-C., Chen, R.F., Whelan, J., Eglinton, L., 2001. Contribution of "old" carbon from natural marine hydrocarbon seeps to sedimentary and dissolved organic carbon pools in the Gulf of Mexico. Geophysical Research Letters 28, 3313–3316.

Wardle, D.A., Nilsson, M.-C., Zackrisson, O., 2008. Fire-derived charcoal causes loss of forest humus. Science 320. doi: 10.1126/science.1154960.

Waterhouse, H.K., 1995. High-resolution palynofacies investigation of Kimmeridgian sedimentary cycles, in: House, M.R., Gale, A.S. (eds). Orbital Forcing Timescales and Cyclostratigraphy, Geological Society Special Publication 85, pp. 75–114.

Waterhouse, H.K., 1998. Palynological fluorescene in hinterland reconstruction of a cyclic shallowing-up sequence, Pliocene, Papua New Guinea. Palaeogeography, Palaeoclimatology, Palaeoecology 139, 59–82. doi: 10.1016/S0031-0182(97)00118-1.

Waterhouse, H.K., 1999. Regular terrestrially derived palynofacies cycles in irregular marine sedimentary cycles, Lower Lias, Dorset, UK. Journal of the Geological Society, London 156, 1113–1124.

Wellman, C.H., Ball, A.C., 2021. Early land plant phytodebris, in: Marret, F., O'Keefe, J., Osterloff, P., Pound, M., Shumilovskikh, L. (eds). Applications of Non-Pollen Palynomorphs: from Palaeoenvironmental Reconstructions to Biostratigraphy, Special Publications 511. Geological Society, London, pp. 309–320.

Wellman, C.H., Cascales-Miñana, B., Servais, T., 2023. Terrestrialization in the Ordovician, in: Harper, D.A.T., Lefebvre, B., Percival, I.G., Servais, T. (eds). A Global Synthesis of the Ordovician System: Part 1, Geological Society, London, Special Publications 532. Geological Society, London, pp. 171–190.

Weng, J.-K., Chapple, C., 2010. The origin and evolution of lignin biosynthesis. New Phytologist 187, 273–285. doi: 10.1111/j.1469-8137.2010.03327.x.

Westbrook, A.S., McAdam, S.A.M., 2021. Stomatal density and mechanics are critical for high productivity: insights from amphibious ferns. New Phytologist 229, 877–889. doi: 10.1111/nph.16850.

White, D., 1915. Some relations in origin between coal and petroleum. Journal of the Washington Academy of Sciences 5, 189–212.

Widmann, P., Bucher, H., Leu, M., Vennemann, T., Bagherpour, B., Schneebeli-Hermann, E., Goudemand, N., Schaltegger, U., 2020. Dynamics of the largest carbon isotope excursion during the Early Triassic biotic recovery. Frontiers in Earth Science, 8, 196. doi: 10.3389/feart.2020.00196.

Wiedemeier, D.B., Abiven, S., Hockaday, W.C., Keiluweit, M., Kleber, M., Masiello, C.A., McBeath, A.V., Nico, P.S., Pyle, L.A., Schneider, M.P.W., Smernik, R.J., Wiesenberg, G.L.B., Schmidt, M.W.I., 2015. Aromaticity and degree of aromatic condensation of char. Organic Geochemistry 78, 135–143.

Williams, C.J., Johnson, A.H., LePage, B.A., Vann, D.R., Sweda, T., 2003. Reconstruction of Tertiary Metasequoia forests. II. Structure, biomass, and productivity of Eocene floodplain forests in the Canadian Arctic. Paleobiology 29, 271–292.

Wilmshurst, J.M., McGlone, M.S., 2005. Corroded pollen and spores as indicators of changing lake sediment sources and catchment disturbance. Journal of Paleolimnology 34, 503–517.

Wolf, M., Lehndorff, E., Wiesenberg, G.L.B., Stockhausen, M., Schwark, L., Amelung, W., 2013. Towards reconstruction of past fire regimes from geochemical analysis of charcoal. Organic Geochemistry 55, 11–21.

Wood, G.D., Gabriel, A.M., Lawson, J.C., 1996. Chapter 3. Palynological techniques – processing and microscopy, in: Jansonius, J., McGregor, D.C. (eds). Palynology: Principles and Applications 1. American Association of Stratigraphic Palynologists Foundation, Dallas, pp. 29–50.

Woodwell, G.M., Whittaker, R.H., 1968. Primary production in terrestrial ecosystems. American Zoologist 8, 19–30. doi: 10.1093/icb/8.1.19.

Worrall, F., Burt, T.P., Rowson, J.G., Warburton, J., Adamson, J.K., 2009. The multi-annual carbon budget of a peat-covered catchment. Science of the Total Environment 407, 4084–4094.

Worrall, F., Evans, M.G., 2008. The carbon budget of upland peat soils, in: Bonn, A., Allott, T., Hubacek, K., Stewart, J. (eds). Drivers of Environmental Change in Uplands. Routledge, Milton Park, pp. 93–112.

Worrall, F., Reed, M., Warburton, J., Burt, T., 2003. Carbon budget for a British upland peat catchment. Science of the Total Environment 312, 133–146.

Wrenn, J.H., Beckman, S.W., 1981. Maceral and total organic carbon analyses of DVDP drill core 11, in: McGinnis, L.D. (ed.). Dry Valley Drilling Project, Antarctic Research Series 33. American Geophysical Union, Washington D.C., pp. 391–402.

Xiao, W., Cao, J., Luo, B., Wang, Y., Xiao, D., Shi, C., Hu, K., 2023. Recovering original type and abundance of organic matter in spent source rocks: A review and advances in elemental proxies AAPG Bulletin 107, 243–281. doi: 10.1306/09282221129.

Xu, M., Shang, H., 2016. Contribution of soil respiration to the global carbon equation. Journal of Plant Physiology 203, 16–28.

Yule, B., Roberts, S., Marshall, J.E.A., Milton, J.A., 1998. Quantitative spore colour measurement using colour image analysis. Organic Geochemistry 28, 139–149.

Zak, D.R., Pellitier, P.T., Argiroff, W.A., Castillo, B., James, T.Y., Nave, L.E., Averill, C., Beidler, K.V., Bhatnagar, J., Blesh, J., Classen, A.T., Craig, M., Fernandez, C.W., Gundersen, P., Johansen, R., Koide, R.T., Lilleskov, E.A., Lindahl, B.D., Nadelhoffer, K.J., Phillips, R.P., Tunlid, A., 2019. Exploring the role of ectomycorrhizal fungi in soil carbon dynamics. New Phytologist 223, 33–39.

Zhang, P., Yang, M., Jiang, Z., Zhou, K., Xu, X., Chen, H., Zhu, X., Guo, Y., Ye, H., Zhang, Y., Shao, L., Lu, J., 2023. Significant floral changes across the Permian-Triassic and Triassic-Jurassic transitions induced by widespread wildfires. Frontiers in Ecology and Evolution, 11, 1284482, 9 pp. doi: 10.3389/fevo.2023.1284482.

Zheng, B., Ciais, P., Chevallier, F., Yang, H., Canadell, J.G., Chen, Y., van der Velde, I.R., Aben, I., Chuvieco, E., Davis, S.J., Deeter, M., Hong, C., Kong, Y., Li, H., Li, H., Lin, X., He, K., Zhang, Q., 2023. Record-high CO_2 emissions from boreal fires in 2021. Science 379, 912–917.

Zonneveld, K.A.F., Versteegh, G.J.M., de Lange, G.J., 1997. Preservation of organic-walled dinoflagellate cysts in different oxygen regimes: a 10,000 year natural experiment. Marine Micropaleontology 29, 393–405.

Zonneveld, K.A.F., Versteegh, G.J.M., de Lange, G.J., 2001. Palaeoproductivity and post-depositional aerobic organic matter decay reflected by dinoflagellate cyst assemblages of the Eastern Mediterranean S1 sapropel. Marine Geology 172, 181–195.

Zwieniecki, M.A., Boyce, C.K., 2014. Evolution of a unique anatomical precision in angiosperm leaf venation lifts constraints on vascular plant ecology. Proceedings of the Royal Society B, 281, 20132829. doi: 10.1098/rspb.2013.282.

Figure captions

Figure 1. Schematic flowchart of prehistoric carbon pathways in a terrestrial carbon sink, a region with positive net terrestrial ecosystem productivity (NTEP). Sizes of carbon pathway arrows are not to relative scale. GPP = gross primary productivity (of the terrestrial ecosystem, in this case), TOC = total organic carbon, c_t = concentration of fossil terrestrial organic matter. Artist credit: Victor O. Leshyk (https://victorleshyk.com).

Figure 2. The parameters of prehistoric net terrestrial ecosystem productivity (NTEP), and terrestrial organic microfossil concentration (c_t) or terrestrial organic carbon (TrOC) as potential proxies for NTEP. Microfossil-based proxies might be used for inferring NTEP from a single catchment area; relationships between terms are expanded in Eqns 2 & 3. TOC = total organic carbon in a sediment; I = imported organic carbon from reworked basement rock (I_{POC}) or exogenous extractable hydrocarbons (I_{EOC}); Ox = oxidised carbon from photodegradation (Ox_{Ph}), wildfire (Ox_{Py}) and post-burial maturation (Ox_T) processes; E = exported organic carbon in dissolved (E_{DOC}), particulate (E_{POC}) or post-burial extractable (E_{EOC}) forms. Modern *Lycopodium* spores are utilised for estimating c_t (concentrations of microfossils per unit mass of dried sediment). Artist credit (block diagram): Victor O. Leshyk (https://victorleshyk.com).

Figure 3. Indigenous vs recycled organic microfossils from the same assemblages. All scales = 10 µm. **A**, **B**, Discrepant taxon age ranges of pollen within a mid-Cretaceous flora, Cenomanian Stage, Chatham Islands, New Zealand; **A**, mid-Cretaceous pollen, *Alisporites similis* (Balme, 1957) Dettmann, 1963, sample L25487; **B**, pollen of probable Permian age, cf. *Potonieisporites methoris* (Hart, 1960) Foster, 1975, sample L25460. **C**, **D**, Discrepant degrees of probable soil microbe damage on laevigate trilete spores (*Concavisporites-Deltoidospora* complex), Schandelah-1 core, Germany; reproduced with permission from

van de Schootbrugge *et al.* (2020, fig. 2); **C**, non-biodegraded specimen, Rhaetian Stage (Upper Triassic), sample Sch 336.80; **D**, biodegraded specimen, Hettangian Stage (Lower Jurassic), sample Sch 252.00. **E**, **F**, Preservation quality likely owing to differential physical abrasion in pollen (*Protohaploxypinus* sp. cf. *P. samoilovichii*) within an Early Triassic assemblage, Eveleigh-1 core, eastern Australia, sample S028617 (credits: M. Amores). **E**, Non-abraded specimen; **F**, abraded specimen, where the air sacs (sacci) have been severed and lost.

Figure 4. Simplified van Krevelen diagram of land plant-based (Type III) kerogens (modified from van Krevelen, 1950; Burnham, 2017). Diagram includes pre-burial O/C and H/C values of some common land plant constituents (Hatcher, 1988; Benner *et al.*, 1990; Ollivier *et al.*, 2022), and their preservation pathways (as a function of thermal maturation, measured by vitrinite reflectance, R_o).

Figure 5. Experimental maturation products from coal (Type III kerogens) with increasing temperature. Carbon mineralization products (CO_2, CO) are the primary constituents of Ox_T; methane (CH_4) is the primary contributor to E_{EOC} from Type III kerogens. Divergent trajectories are largely attributable to different initial maturities and/or compositions. All data are from confined pyrolysis (overpressurised, deoxygenated) conditions for 24–72 hours. Morwell and Mahakam (low and medium maturity, respectively) data from Behar et al. (1995); Brent coal (high maturity) data from Lorant & Behar (2002).

Figure 6. Geographic and geologic contexts for the Permian–Triassic organic microfossil assemblages. A, Map of Australia. **B**, Geological map of the Tasmania Basin (from Brown *et al.*, 2021) with location of target well core succession (Bonneys Plain-1) and approximate distributions of Permian-Triassic sedimentary strata.

Figure 7. Relationship between terrestrial organic microfossil concentrations (c_t) and total organic carbon (TOC) or terrestrial organic carbon (TrOC). A, TOC; **B,** TrOC. All samples are from Permian–Triassic non-marine strata of Bonneys Plain-1, the Tasmania Basin, Australia (see Supp. Table 1). Error bars for TOC and TrOC values indicate standard errors, error bars for c_t values indicate total error (σ_t). Terrestrial organic microfossil concentrations (c_t) and total error values (σ_t) are derived from the FOVS method (Mays *et al.*, *pre-print*); wt = weight.

Caption references

Balme, B.E., 1957. Spores and pollen grains from the Mesozoic of Western Australia, Fuel Research: Physical and Chemical Survey of the National Coal Resources. C.S.I.R.O. Australia, Chatswood, pp. 1–48.

Behar, F., Vandenbroucke, M., Teerman, S., Hatcher, P., Leblond, C., Lerat, O., 1995. Experimental simulation of gas generation from coals and a marine kerogen. Chemical Geology 126, 247–260.

Benner, R., Hatcher, P.G., Hedges, J.I., 1990. Early diagenesis of mangrove leaves in a tropical estuary: Bulk chemical characterization using solid-state ^{13}C NMR and elemental analyses. Geochimica et Cosmochimica Acta 54, 2003–2013.

Brown, A.V., Calver, C.R., Clark, M.J., Corbett, K.D., Everard, J.L., Cumming, G., Forsyth, S.M., Goscombe, B.D., Green, D., Green, G., McClenaghan, M.P., McNeill, A.W., Pemberton, J., Seymour, D.B., Vicary, M., Woolward, I., Worthing, M., Jackman, C., 2021. Geology of Tasmania Map, Geology of Tasmania 1:500 000, 5th ed.

Burnham, A.K., 2017. Van Krevelen diagrams, in: Sorkhabi, R. (ed.). Encyclopedia of Petroleum Geoscience, Encyclopedia of Earth Sciences Series. Springer, Cham, pp. 1–5.

Dettmann, M.E., 1963. Upper Mesozoic microfloras from south-eastern Australia. Proceedings of the Royal Society of Victoria 77, 1–148.

Foster, C.B., 1975. Permian plant microfossils from the Blair Athol Coal Measures, central Queensland, Australia. Palaeontographica Abteilung B 154, 121–171.

Hart, G.F., 1960. Microfloral investigations of the Lower Coal Measures (K2), Ketewaka-Mchuchuma Coalfield, Tanganyika Bulletin of the Tanganyika Geological Survey 30, 18.

Hatcher, P.G., 1988. Dipolar-dephasing ^{13}C NMR studies of decomposed wood and coalified xylem tissue: Evidence for chemical structural changes associated with defunctionalization of lignin structural units during coalification. Energy & Fuels 2, 48–58.

Lorant, F., Behar, F., 2002. Late generation of methane from mature kerogens. Energy & Fuels 16, 412–427.

Mays, C., Amores, M., Mays, A., *pre-print*. Improved absolute abundance estimates from spatial count data with simulation and microfossil case studies. PLOS One. doi: 10.48550/arXiv.2406.10921.

Ollivier, S., Jéhan, P., Olivier-Jimenez, D., Lambert, F., Boustie, J., Lohézic-Le Dévéhat, F., Le Yondre, N., 2022. New insights into the Van Krevelen diagram: Automated molecular formula determination from HRMS for a large chemical profiling of lichen extracts. Phytochemical Analysis 33, 1111–1120. doi: 10.1002/pca.3163.

van de Schootbrugge, B., van der Weijst, C.M.H., Hollaar, T.P., Vecoli, M., Strother, P.K., Kuhlmann, N., Thein, J., Visscher, H., van Konijnenburg-van Cittert, H., Schobben, M.A.N., Sluijs, A., Lindström, S., 2020. Catastrophic soil loss associated with end-Triassic deforestation. Earth-Science Reviews, 210, 103332, 18 pp. doi: 10.1016/j.earscirev.2020.103332.

van Krevelen, D.W., 1950. Graphical-statistical method for the study of structure and reaction processes of coal. Fuel 29, 269–284.

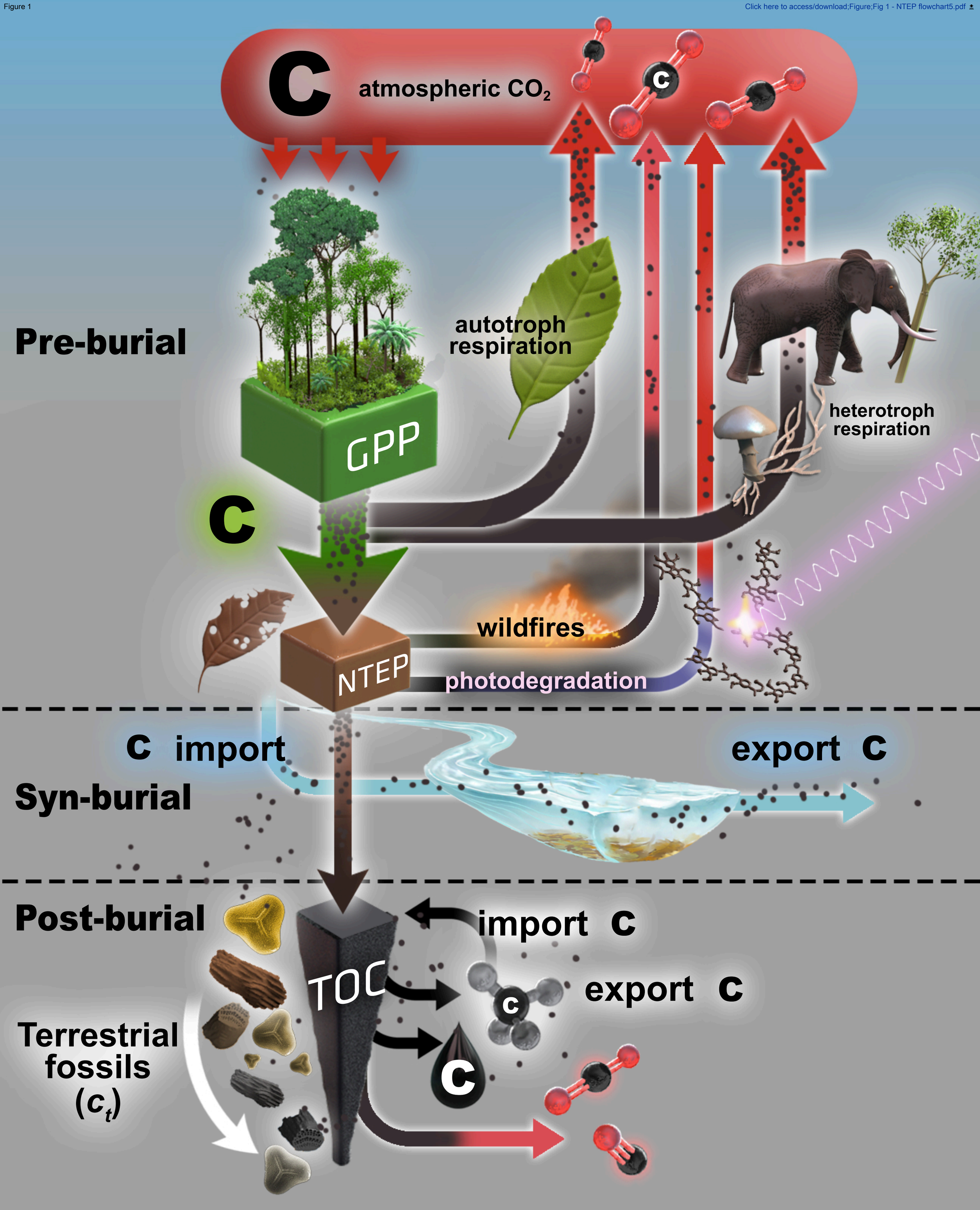

Figure 2

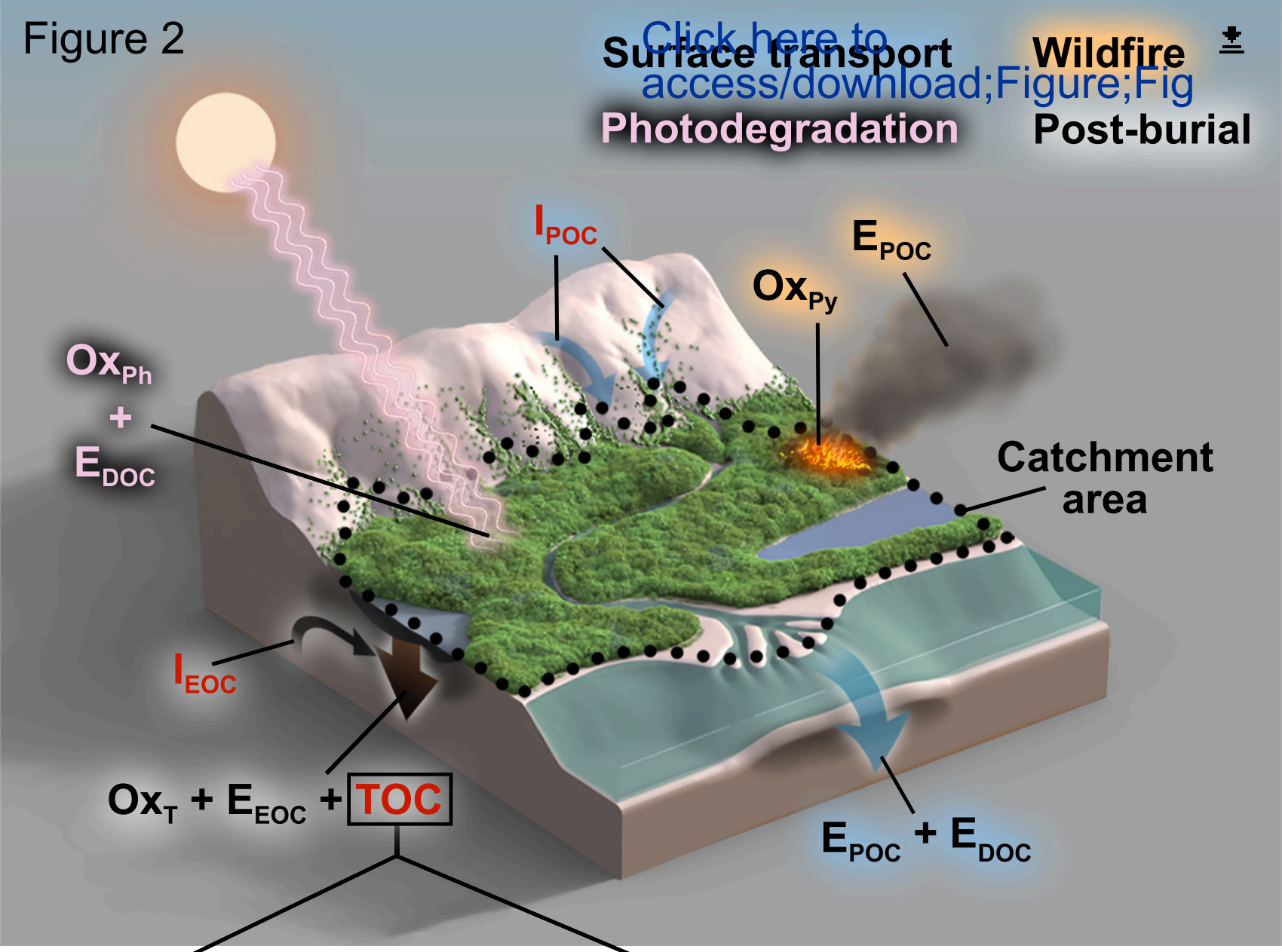

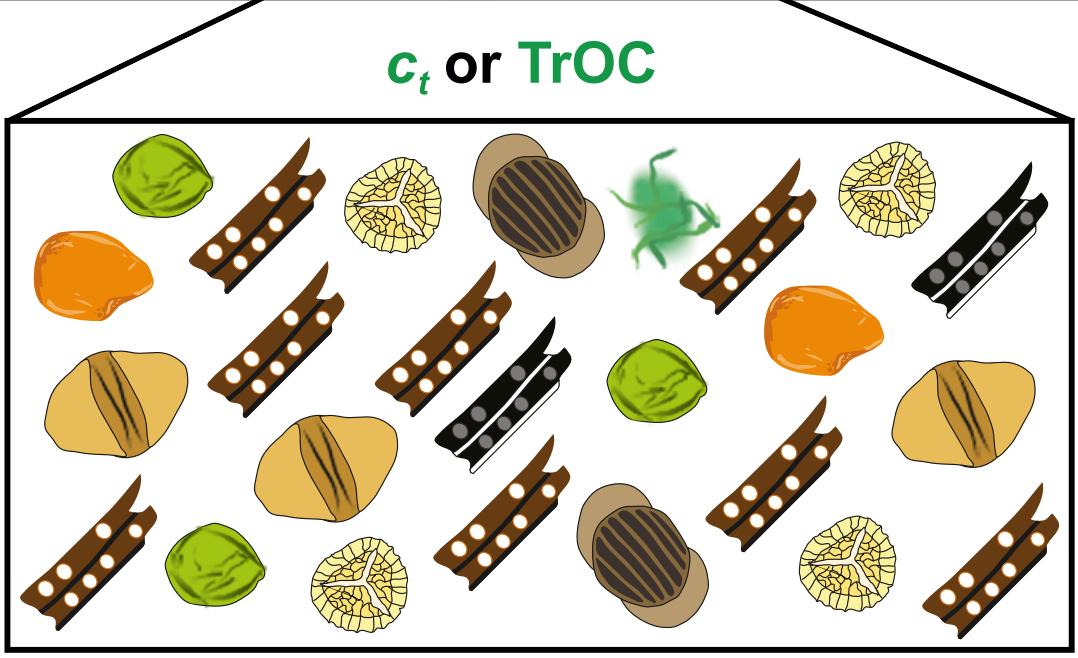

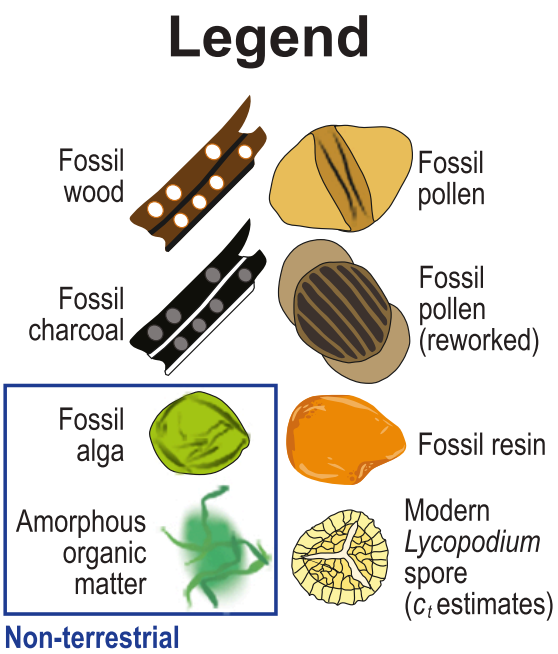

c_t or TrOC ≈ TOC – I_{EOC} – I_{POC} – non-terrestrial

Figure 3

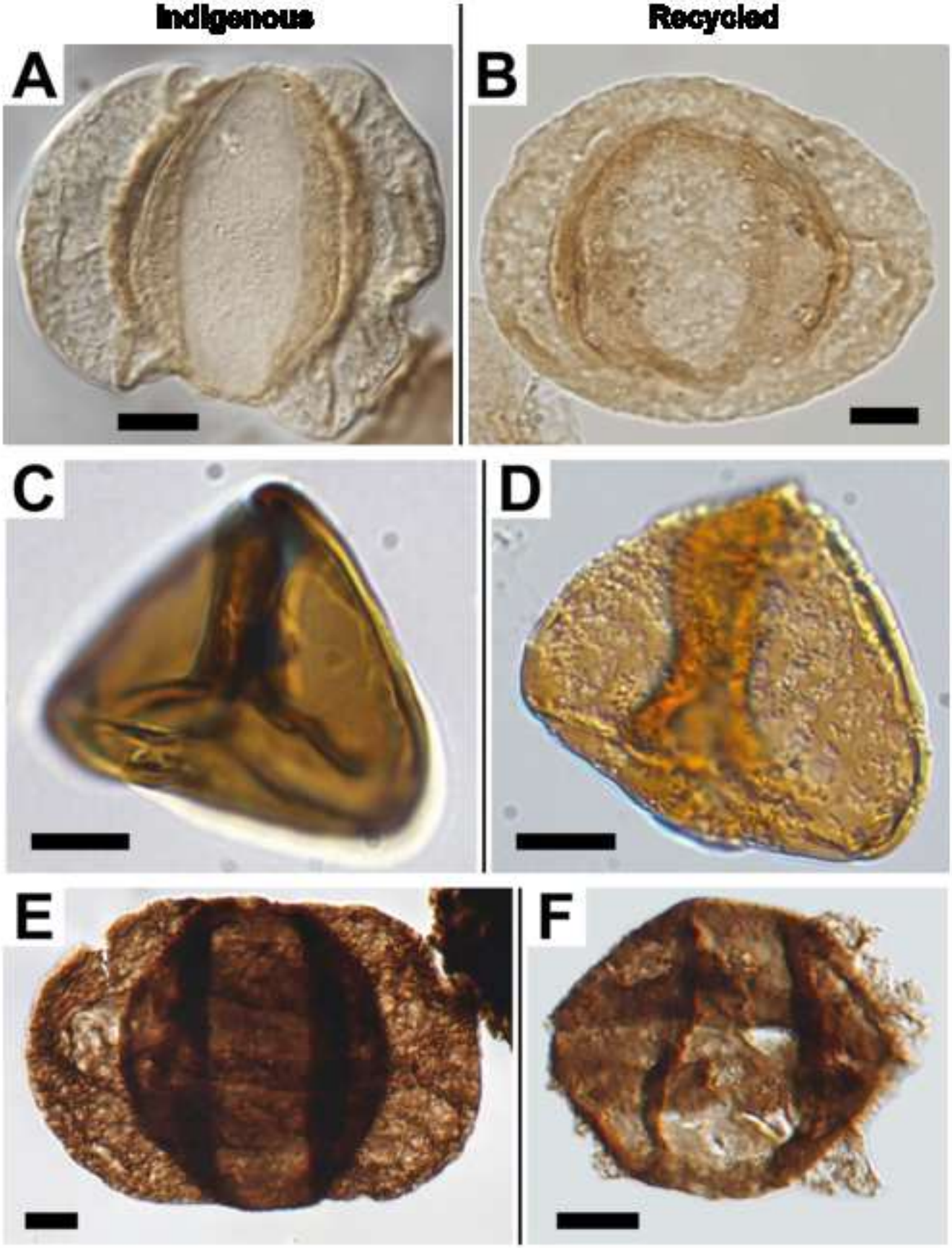

Figure 4

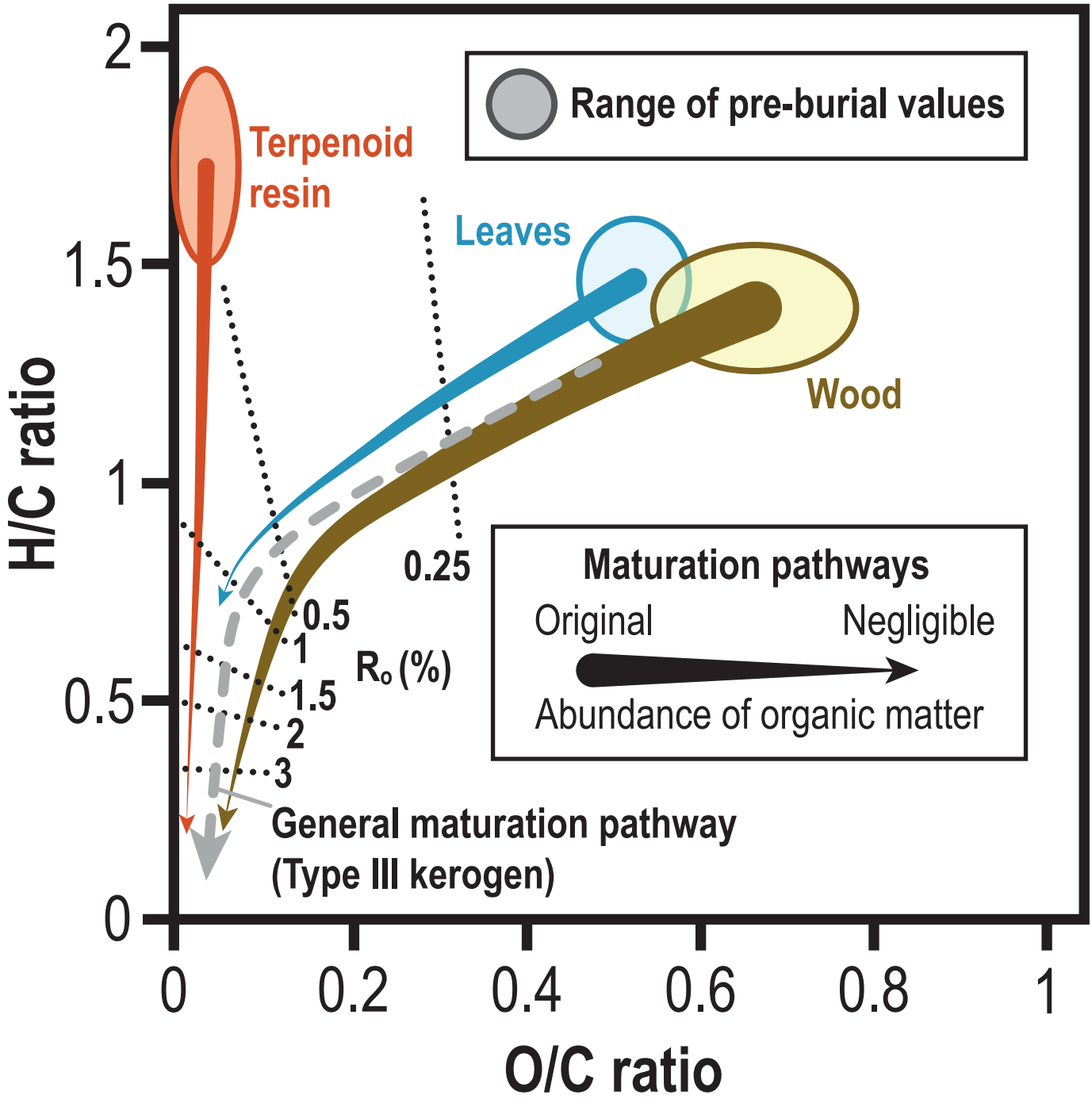

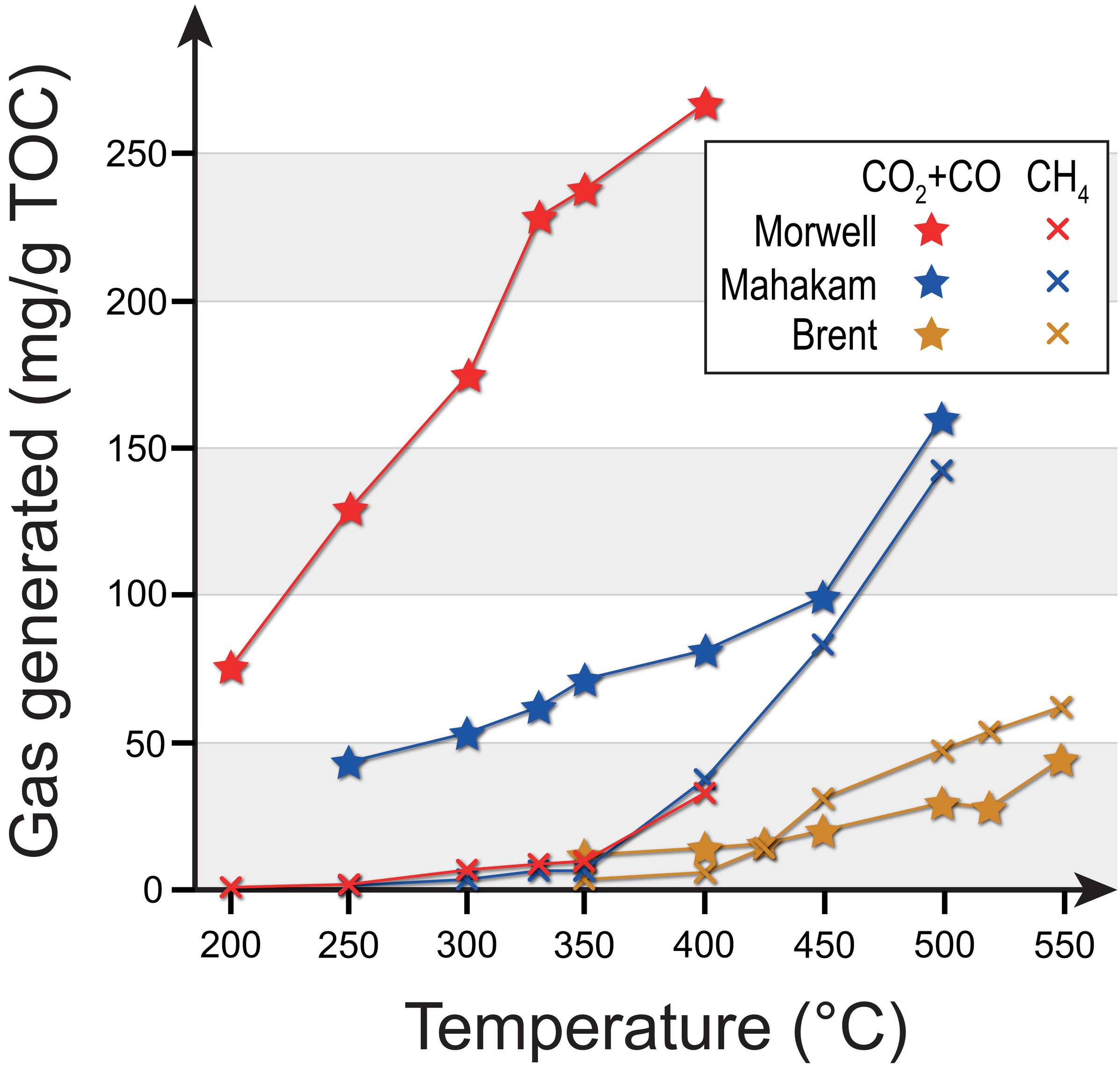

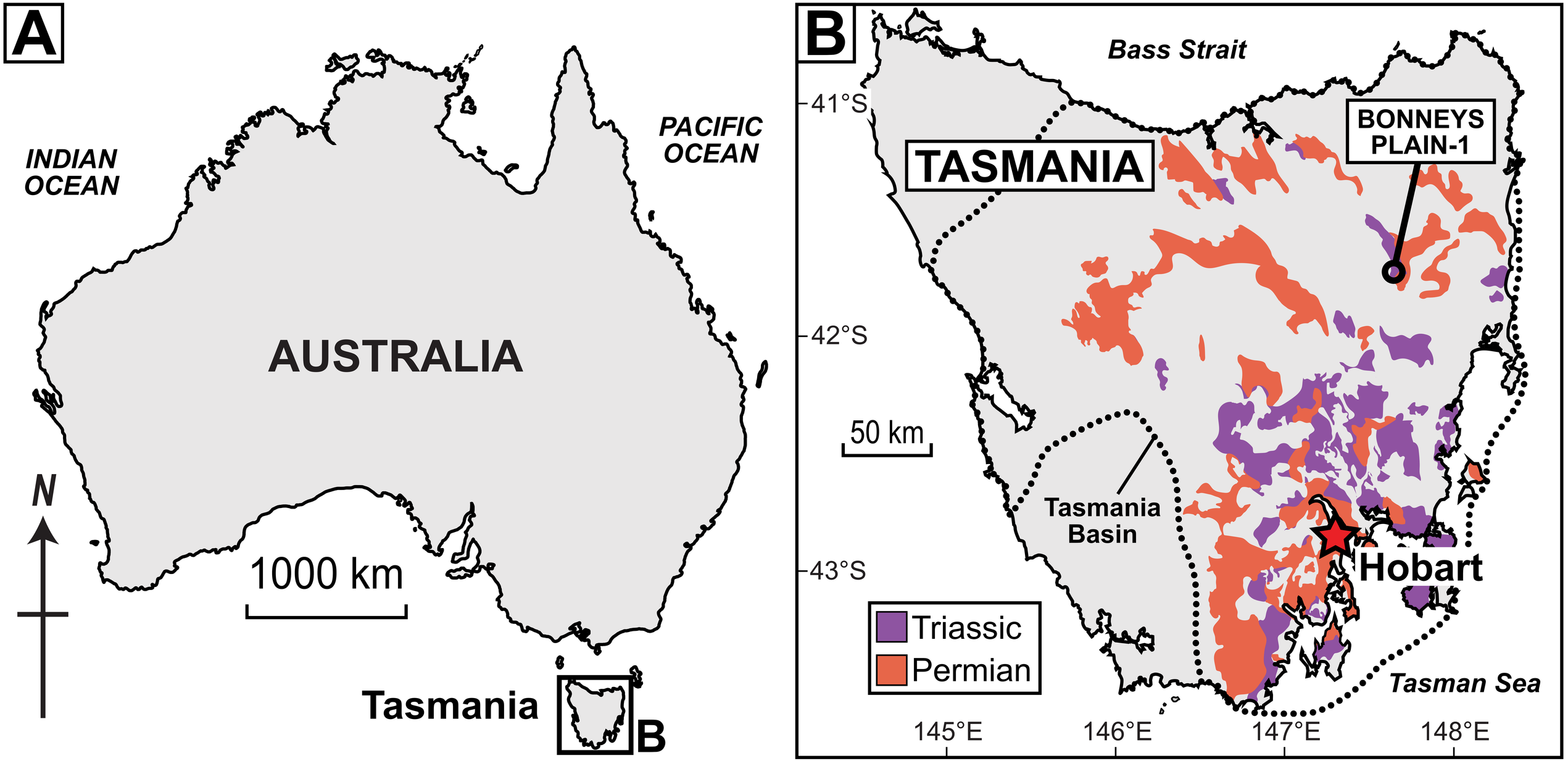

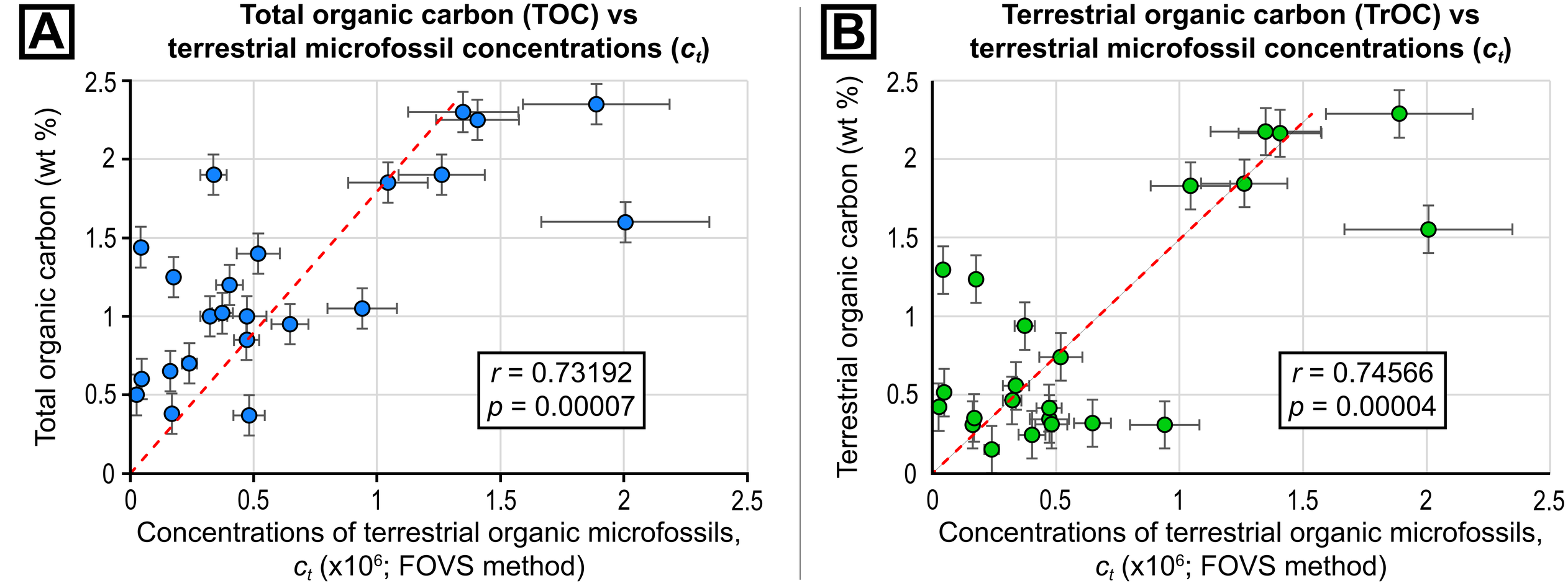

Measures of deep-time terrestrial net ecosystem productivity and carbon sink function

Chris Mays, Richard V. Tyson and Michael T. Hren

Declaration of interest statement

We, the authors (Chris Mays, Richard Tyson & Michael Hren), declare that we have no conflicts of interest, and the contents of this manuscript are not intended for publication elsewhere.

Appendix A. Sample characteristics, organic carbon (OC, including terrestrial organic carbon, TrOC), total organic microfossils concentration estimates (c) and terrestrial organic microfossil concentrations (ct) from the Permian–Triassic of the Tasmania Basin, southeastern Australia.

Sample characteristics				Exotic marker characteristics					Organic microfossils (linear method)									Terrestrial organic microfossils (FOVS method)															Organic carbon (OC)			
Inputs				Inputs				Outputs	Inputs					Outputs (terrestrial organic microfossils only)				Inputs		Calibration counts						Outputs			Full counts		Outputs						
Depth (m)	Sample reg. number	Lithofacies	$\bar{V}$: total sample mass (g)	*Lycopodium* batch #	$\bar{Y}_1$: mean *Lycopodium* spores/tablet	N_1 : no. of tablets	s_1 : sample s.d. of Y_1	s_{1P} : proportional sample s.d. of $\bar{Y}_1$	x : all organic microfossils	x_t : terrestrial microfossils	x_t / x	x_t / x (%)	n : *Lycopodium* spores	$\hat{u}$: target-to-marker ratio	σ_t : total standard error	c_t : concentration (grains/g)	x_t : terrestrial microfossils	s_3 : sample s.d. of x_t per FOV	N_{3c} : FOVs counted	$c_d(N_{3c})$: bias correction for FOVs counted	$\bar{Y}_{3n}$: mean x_t per FOV	$\bar{Y}_{3n}$: mean n per FOV	$\hat{s}_3$: unbiased population estimator for s_3	s_{3P} : proportional sample s.d. of common grains	n : *Lycopodium* spores	N_{3F} : FOVs counted	$\hat{x}_t$: extrapolated x_t count	$\hat{u}$: target-to-marker ratio	σ_t : total standard error	c_t : concentration (grains/g)	TOC mass (wt%)	σ_{TOC} : TOC standard error	σ_{TOC} / TOC : TOC standard error (% of TOC)	Terrestrial OC (TrOC) mass (wt%)
267.59	S090305	Pale grey siltstone	22.5	280521291	13761	5	448	0.0326	591	204	0.35	34.52	6	34.0	41.45	103972	288	3.7358	15	0.9823	19.20	0.12	3.8030	0.1981	40	322	6182	154.56	16.68	472644	1	0.1822	18.22	0.35
270.99	S090308	Heterolithic; grey silt/fine sandstone	22.6	280521291	13761	5	448	0.0326	1938	422	0.22	21.78	10	42.2	32.03	128477	188	2.0999	15	0.9823	12.53	0.16	2.1377	0.1706	75	471	5903	78.71	12.44	239628	0.7	0.1650	23.58	0.15
286.06	S090310	Dark grey silt/claystone; friable	22.0	280521291	13761	5	448	0.0326	2246	660	0.29	29.39	8	82.5	35.60	258019	667	7.6320	15	0.9823	44.47	0.15	7.7694	0.1747	49	331	14718	300.38	15.05	939429	1.05	0.1314	12.51	0.31
287.28	S090311	Heterolithic; grey silt/fine sandstone	18.4	280521291	13761	5	448	0.0326	547	260	0.48	47.53	6	43.3	41.32	162041	275	3.9924	15	0.9823	18.33	0.42	4.0643	0.2217	93	220	4033	43.37	11.93	162175	0.65	0.1294	19.90	0.31
290.31	S090312	Grey siltstone	18.1	50220211	18407	5	592	0.0322	1652	556	0.34	33.66	9	61.8	33.63	314128	502	6.4239	15	0.9823	33.47	0.26	6.5396	0.1954	92	350	11713	127.32	11.67	647392	0.95	0.0611	6.43	0.32
292.46	S090313	Dark grey siltstone	22.7	280521291	13761	5	448	0.0326	2268	1053	0.46	46.43	12	87.8	29.07	265975	427	4.6425	15	0.9823	28.47	0.27	4.7260	0.1660	87	325	9252	106.34	11.64	322326	1	0.0704	7.04	0.46
294.02	S090314	Silt/fine sandstone; micaceous	19.1	280521291	13761	5	448	0.0326	1789	874	0.49	48.85	9	97.1	33.54	349829	470	5.2463	15	0.9823	31.33	0.24	5.3408	0.1704	101	422	13223	130.92	10.98	471611	0.85	0.1279	15.05	0.42
295.61	S090315	Dark grey siltstone	20.0	50220211	18407	5	592	0.0322	4028	825	0.20	20.48	9	91.7	33.55	421827	141	1.9928	15	0.9823	9.40	0.11	2.0287	0.2158	68	632	5941	87.36	13.42	402031	1.2	0.1201	10.01	0.25
300.64	S090316	Heterolithic; organic-rich silt/fine sandstone	21.0	280521291	13761	5	448	0.0326	1598	469	0.29	29.35	8	58.6	35.69	192081	281	5.0634	15	0.9823	18.73	0.18	5.1546	0.2752	52	286	5358	103.03	15.65	337581	1.9	0.1235	6.50	0.56
300.88	S090317	Dark grey siltstone	20.4	280521291	13761	5	448	0.0326	3671	1941	0.53	52.87	9	215.7	33.44	727399	390	7.9373	15	0.9823	26.00	0.17	8.0801	0.3108	47	278	7228	153.79	16.71	518693	1.4	0.1103	7.88	0.74
301.18	S090318	Dark grey siltstone	15.2	280521291	13761	5	448	0.0326	792	665	0.84	83.96	6	110.8	41.03	501703	320	3.1091	15	0.9823	21.33	0.20	3.1651	0.1484	62	309	6592	106.32	13.34	481285	0.37	0.1327	35.87	0.31
301.36	S090319	Laminated grey siltstone	21.0	280521291	13761	5	448	0.0326	1661	1425	0.86	85.79	109	13.1	10.04	42834	466	3.5950	15	0.9823	31.07	2.18	3.6597	0.1178	166	76	2361	14.22	8.46	46602	0.6	0.1464	24.39	0.51
301.56	S090320	Grey siltstone	21.6	280521291	13761	5	448	0.0326	1123	947	0.84	84.33	172	5.5	8.42	17538	506	6.8292	15	0.9823	33.73	4.26	6.9521	0.2061	345	81	2732	7.92	7.71	25229	0.5	0.0149	2.98	0.42
301.81	S090321	Heterolithic; rippled silt/sandstone laminae	22.2	280521291	13761	5	448	0.0326	1533	1515	0.99	98.83	15	101.0	25.99	313032	272	2.8502	15	0.9823	18.13	0.32	2.9015	0.1600	75	234	4243	56.58	12.35	175347	1.25	0.0973	7.78	1.24
301.91	S090322	Grey silt/v-fine sandstone	16.0	280521291	13761	5	448	0.0326	611	549	0.90	89.85	54	10.2	14.34	43720	486	10.1052	15	0.9823	32.40	3.26	10.2871	0.3175	528	162	5249	9.94	9.39	42749	1.44	0.1256	8.72	1.29
301.98	S090323	Dark grey silt/fine sandstone	19.8	280521291	13761	5	448	0.0326	4673	4418	0.95	94.54	9	490.9	33.40	1705839	669	8.0339	15	0.9823	44.60	0.11	8.1785	0.1834	40	348	15521	388.02	16.57	1348370	2.3	0.1362	5.92	2.17
302.51	S090324	Heterolithic; grey silt/fine sandstone	22.8	280521291	13761	5	448	0.0326	2247	2182	0.97	97.11	9	242.4	33.43	731640	1005	10.1207	15	0.9823	67.00	0.16	10.3029	0.1538	58	362	24254	418.17	13.79	1261945	1.9	0.1019	5.36	1.85
302.64	S090325	Dark grey silt/fine sandstone	20.1	280521291	13761	5	448	0.0326	2255	2169	0.96	96.19	12	180.8	28.98	618732	914	9.9338	15	0.9823	60.93	0.15	10.1127	0.1660	82	553	33696	410.93	11.93	1406663	2.25	0.1144	5.09	2.16
302.83	S090326	Heterolithic; silt/sandstone, with cross-laminae	24.0	280521291	13761	5	448	0.0326	3666	3625	0.99	98.88	9	402.8	33.41	1154714	577	6.9165	15	0.9823	38.47	0.11	7.0410	0.1830	47	445	17118	364.21	15.40	1044132	1.85	0.1072	5.79	1.83
303.52	S090327	Heterolithic; dark grey silt/fine sandstone	20.2	280521291	13761	5	448	0.0326	2892	2807	0.97	97.06	5	561.4	44.78	1912234	664	8.9958	15	0.9823	44.27	0.08	9.1577	0.2069	39	519	22974	589.09	16.94	2006542	1.6	0.1012	6.32	1.55
305.79	S090328	Heterolithic; dark grey silt/sandstone laminae	20.4	280521291	13761	5	448	0.0326	4927	4796	0.97	97.34	9	532.9	33.40	1797325	677	7.2394	15	0.9823	45.13	0.08	7.3698	0.1633	44	546	24643	560.06	15.72	1888979	2.35	0.0735	3.13	2.29
305.95	S090329	Heterolithic; dark grey silt/fine sandstone; micaceous	16.1	280521291	13761	5	448	0.0326	1053	968	0.92	91.93	21	46.1	22.11	196993	389	4.2840	15	0.9823	25.93	0.30	4.3611	0.1682	96	323	8376	87.25	11.19	372893	1.02	0.0955	9.36	0.94
306.07	S090330	Fine/medium sandstone, with plant debris; micaceous	17.3	280521291	13761	5	448	0.0326	546	507	0.93	92.86	13	39.0	28.13	155110	574	7.8873	15	0.9823	38.27	0.91	8.0293	0.2098	221	244	9337	42.25	8.76	168032	0.38	0.0446	11.74	0.35
		Mean							**2100**	**1471**		**68.4**		**154.4**	**30.73**	**526746**	**485**	**6.0290**							**109**	**341**	**11333**	**188.7**	**12.95**	**642708**	**1.24**	**0.11**	**11.29**	**0.90**

Linear method concentrations follow Benninghoff (1962), linear method total errors are derived from Stockmarr (1971); field-of-view subsampling (FOVS) method concentrations and total errors from Mays et al. (in review). FOV = field of view; wt% = percent by weight, reg. = registration (samples registered at the Swedish Museum of Natural History); terrestrial OC mass (TrOC wt%) is the approximate mass of terrestrial particulate organic matter in the assemblage; s.d. = standard deviation. Excel version of this data table includes embedded formulae, where relevant. Parameters and formulae for both concentration methods (linear and FOVS) are provided by Mays *et al.* (*in review*). For description of terms used, see Glossary.

Appendix B: Supplementary Figure 1

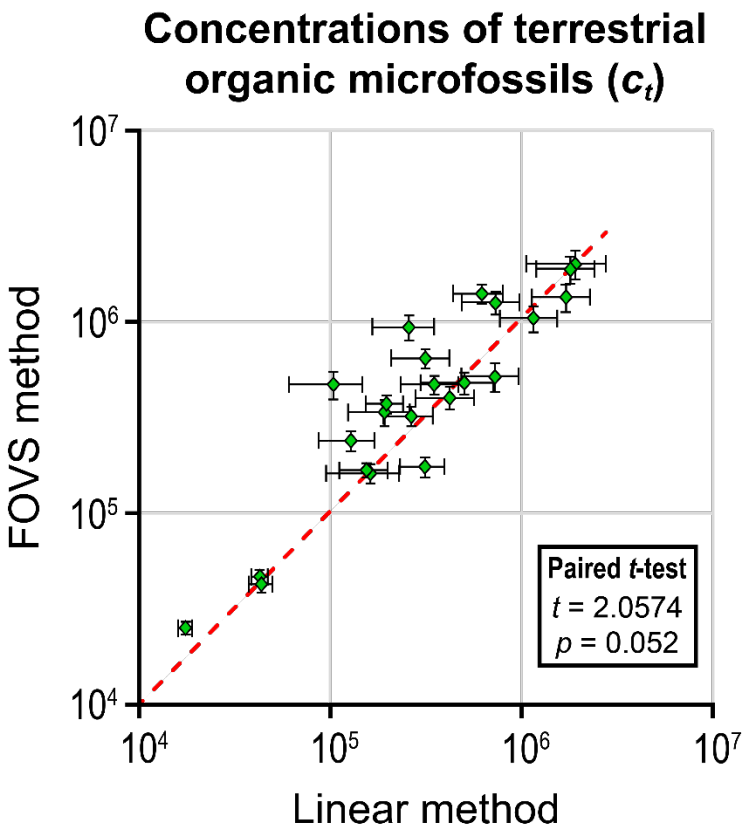

Supplementary Figure 1. Relationship between the two microfossil concentration count methods used in this study: the linear method and the field-of-view subsampling (FOVS) method. This indicates that both methods yielded similar terrestrial organic microfossil concentrations (c_t), as indicated by the non-significant difference in paired *t*-test ($p > 0.05$). However, the FOVS method consistently yielded greater precisions (= smaller error ranges). All samples are from Permian–Triassic non-marine strata of Bonneys Plain-1, the Tasmania Basin, Australia (see Appendix A). c_t are estimated using calculations by Benninghoff (1962; linear method) and Mays *et al.* (*in review*; FOVS method). Error bars represent the total error values (σ_t), using calculations by Stockmarr (1971; linear method) and Mays *et al.* (*in review*; FOVS method). Note: both x- and y-axes are logarithmically scaled.

Appendix references

Benninghoff, W.S., 1962. Calculation of pollen and spore density in sediments by addition of exotic pollen in known quantities. Pollen et Spores 4, 332–333.

Mays, C., Amores, M., Mays, A., *pre-print*. Improved absolute abundance estimates from spatial count data with simulation and microfossil case studies. PLOS One. doi: 10.48550/arXiv.2406.10921.

Stockmarr, J., 1971. Tablets with spores used in absolute pollen analysis. Pollen et Spores 13, 615–621.